CENTRO INTERNACIONAL DE ESTUDOS
DE DOUTORAMENTO E AVANZADOS
DA USC (CIEDUS)

TESE DE DOUTORAMENTO

AQUEOUS TWO-PHASE SYSTEMS FOR THE VALORIZATION OF CHEESE WHEY

Marlen González Amado

ESCOLA DE DOUTORAMENTO INTERNACIONAL

PROGRAMA DE DOUTORAMENTO EN ENXEÑARÍA QUÍMICA E AMBIENTAL

SANTIAGO DE COMPOSTELA

2019

USC
UNIVERSIDADE
DE SANTIAGO
DE COMPOSTELA

DECLARACIÓN DA AUTORA DA TESE

AQUEOUS THO-PHASE SYSTEMS FOR THE VALORIZATION OF CHEESE WHEY

Dna. Marlen González Amado

Presento a miña tese, seguindo o procedemento adecuado ao Regulamento, e declaro que:

1) A tese abarca os resultados da elaboración do meu traballo.
2) No seu caso, na tese se fai referencia ás colaboracións que tivo este traballo.
3) A tese é a versión definitiva presentada para a súa defensa e coincide coa versión enviada en formato electrónico.
4) A tese non incorre en ningún tipo de plaxio de outros autores nin de traballos presentados por min para a obtención de outros títulos.

Santiago de Compostela, 12 de Marzo de 2019

Asdo.: Marlen González Amado

USC
UNIVERSIDADE
DE SANTIAGO
DE COMPOSTELA

AUTORIZACIÓN DO DIRECTOR/TITOR DA TESE

AQUOUS TWO-PHASE SYSTEMS FOR THE VALORIZATION OF CHEESE WHEY

Dna. Ana María Soto Campos e D. Oscar Rodríguez Figueiras

INFORMAN:

Que a presente tese correspóndese co traballo realizado por Dna. Marlen González Amado baixo a dirección de Dna. Ana María Soto Campos e D. Oscar Rodríguez Figueiras, e a titorización deste último, e autorizamos a súa presentación, considerando que reúne os requisitos esixidos no Regulamento de Estudos de Doutoramento da USC, e que como directora e director-titor desta non incorre nas causas de abstención establecidas na Lei 40/2015.

Santiago de Compostela, 12 de Marzo de 2019

Ana M. Soto Campos

Oscar Rodríguez Figueiras

USC
UNIVERSIDADE
DE SANTIAGO
DE COMPOSTELA

To Michael

USC
UNIVERSIDADE
DE SANTIAGO
DE COMPOSTELA

ACKNOWLEDGEMENTS (IN SPANISH)

Quiero comenzar dándole las gracias a los profesores Alberto Arce y Ana Soto (codirectora de esta tesis) por abrirme las puertas de su laboratorio y permitirme formar parte del grupo de investigación en Procesos de Separación y Equilibrio de Fases de la Universidad de Santiago (USC), además de por compartir conmigo su amplio conocimiento. A Oscar Rodríguez, codirector y tutor de esta tesis, le agradezco el haberme introducido en el mundo de la investigación, especialmente en la recuperación de biomoléculas con sistemas de dos fases acuosas. Debo agradecerle también su ayuda y su conocimiento, pero sobre todo la confianza que depositó en mí desde el primer momento. Debo extender este agradecimiento a los profesores Eva Rodil y Héctor Rodríguez por prestarme su ayuda siempre que la he necesitado.

Parte de este trabajo se desarrolló durante una estancia de tres meses en el CICECO (Universidad de Aveiro). Esta breve experiencia me permitió crecer no solo profesionalmente, sino también personalmente. Le agradezco al profesor Joao Coutinho el haberme brindado la oportunidad de trabajar en su grupo de investigación (PATH) y a la profesora Mara Freire el abrirme las puertas de su laboratorio. Quisiera darle las gracias a Rita, Helena, Mafalda, Diana y María Joao su ayuda y paciencia durante esta etapa. A Ana Paula le agradezco el acompañarme día a día de la mano durante este tiempo ayudándome y compartiendo su conocimiento conmigo.

Cuando llegué al laboratorio Iago, María e Iría que me recibieron con los brazos abiertos, guiándome y apoyándome desde el primer momento. A Raquel quiero agradecerle su amistad, los buenos momentos, los cursos, pero sobre todo su apoyo en los momentos de flaqueza. También quiero agradecer a Carlos, Xiana, Manu, Alba, Oussama, Marta y toda la gente con la que he coincidido en el laboratorio por el buen ambiente de trabajo, no sería posible sin ellos.

El apoyo recibido durante estos cuatro años no ha sido solo por parte del trabajo. Por eso quiero darles las gracias a mis amigos Víctor, Pablo, Tatiana, Diana

y Elmar por todo su apoyo y buenos momentos. A Jara que me ha demostrado ser la mejor amiga que se puede tener, a pesar de la distancia, espero seguir compartiendo fantásticos viajes y momentos especiales contigo.

A mi familia le agradezco apoyo que me ha brindado. A mi hermana Alba, pero sobre todo a mis padres Manuel e Isabel, si he llegado hasta aquí ha sido gracias a ellos, por su apoyo incondicional, muchas gracias por estar siempre ahí. A Michael, no puedo expresar en palabras lo agradecida que estoy por tenerle siempre a mi lado de forma incondicional. Estoy deseando comenzar una nueva etapa a tu lado. Gracias por apoyarme siempre.

Finalmente me gustaría agradecer a la Xunta de Galicia el apoyo financiero mediante el proyecto de emerxentes EM 2014/023 y por el programa de consolidación y estructuración de investigación competitiva GPC2014/026). También quiero agradecer las ayudas internas de la USC por financiar mi estancia en la Universidad de Aveiro. Por último agradecer a Benigno Pereira (Queizúar S.L.) el facilitarnos las muestras de suero.

ABSTRACT

The dairy industry, of great importance in Galicia, generates in cheese production high volumes of whey, a residue with high content in organic matter that presents an environmental problem. The main objective of this thesis is the valorization of cheese whey through the recovery of high added-value compounds (lactose and proteins) using aqueous two phase systems, a mild medium for the separation of proteins and other biomolecules. Polymers (polyethylene glycols of different molecular weights and poly(ethylene glycol-ran-propylene-glycol) monobutyl ether) and salts (sodium, potassium and ammonium sulfate, and potassium tartrate) were selected as phase-forming components due to their relative low cost and green character, in addition to their compatibility with the components of cheese whey. Liquid-liquid equilibrium data for these systems were determined at several temperatures and atmospheric pressure. The measurement of physical properties (density and refractive index) was used to determine compositions of equilibrium phases. All data were adequately correlated with empirical equations to facilitate their management. These systems were used to analyze the partitioning of α-lactose, bovine serum albumin, α-lactalbumin and β-lactoglobulin between the aqueous phases. The influence of polymer molecular weight, type of salt and pH on the partitioning was analyzed. Aqueous two phase systems generated with polyethylene glycol 1500 and ammonium sulfate (298 K and pH=4) or polyethylene glycol 600 and potassium tartrate (293 K and natural pH) were found to be promising options for the separation of α-lactose and proteins. Polyethylene glycol 300 and sodium sulfate (298 K and pH ranging from 4 to 5) was found promising for proteins' fractionation. Several strategies based on these systems and ultrafiltration were designed to separate the main components of cheese whey. These strategies were assessed using first a synthetic whey formulated with the key solutes dissolved in distilled water, and later using a real cheese whey from a local cheese producer (Queizúar S.L.). The aqueous biphasic system formed with polyethylene glycol 600 and potassium tartrate allowed a very good separation of lactose and proteins. Fractionation of the proteins was not achieved. Further studies are encouraged.

RESUMEN (SPANISH)

La industria láctea, de gran importancia en Galicia, genera altos volúmenes de suero en la producción de queso. Este residuo de alto contenido en materia orgánica implica un serio problema medioambiental. El principal objetivo de esta tesis es la valorización del suero de queso mediante la recuperación de compuestos de alto valor añadido (lactosa y proteínas) utilizando sistemas de dos fases acuosas, un medio adecuado para la separación de biomoléculas. Las dos fases acuosas se generaron con polímeros (polietilenglicoles de diferentes pesos moleculares y éter monobutílico de poli(etilenglicol-ran-propilenglicol)) y sales (sulfato de sodio, potasio y amonio, y tartrato de potasio), debido a su relativo bajo coste y carácter verde, además de su compatibilidad con los componentes del suero del queso. Se determinaron los correspondientes datos de equilibrio líquido-líquido a varias temperaturas y a presión atmosférica, empleando propiedades físicas (densidad e índice de refracción) para determinar la composición de las fases en equilibrio. Todos los datos fueron adecuadamente correlacionados con ecuaciones empíricas, lo que facilita su manejo. Se utilizaron estos sistemas para analizar el reparto de α-lactosa, albúmina de suero bovino, α-lactalbúmina y β-lactoglobulina entre las dos fases acuosas. Se analizó la influencia del peso molecular del polímero, tipo de sal y pH en la distribución. Los sistemas de dos fases acuosas generados con polietilenglicol 1500 y sulfato de amonio (298 K y pH=4) o polietilenglicol 600 y tartrato de potasio (293 K y pH natural) se consideraron alternativas interesantes para la separación de la α-lactosa y las proteínas. Por otra parte, polietilenglicol 300 y sulfato de sodio (298 K y un rango de pH de 4 a 5) resultó prometedor para el fraccionamiento de proteínas. Se diseñaron varias estrategias basadas en estos sistemas y en ultrafiltración para separar los principales componentes del suero del queso. Se probaron primero con un suero sintético y posteriormente con un suero de queso proporcionado por un proveedor local (Queizúar S.L.). El sistema bifásico acuoso formado con polietilenglicol 600 y tartrato de potasio permite una muy buena separación de la lactosa y las proteínas. El fraccionamiento de proteínas no fue posible. La investigación en este tema debe continuar.

RESUMO (GALICIAN)

A industria láctea, de gran importancia en Galicia, xera altos volumes de soro na produción de queixo. Este residuo de alto contido en materia orgánica implica un serio problema ambiental. O principal obxectivo desta tese é a valorización do soro de queixo mediante a recuperación de compostos de alto valor engadido (lactosa e proteínas) utilizando sistemas de dúas fases acuosas, un medio adecuado para a separación de biomoléculas. As dúas fases acuosas xeráronse con polímeros (polietilenglicois de diferentes pesos moleculares e éter monobutílico de poli(etilenglicol- ran- propilenglicol)) e sales (sulfato de sodio, potasio e amonio, e tartarato de potasio), debido ao seu relativo baixo custo e carácter verde, ademais da súa compatibilidade cos compoñentes do soro do queixo. Determináronse os correspondentes datos de equilibrio líquido -líquido a varias temperaturas e a presión atmosférica, mediante o uso de propiedades físicas (densidade e índice de refracción) para determinar a composición das fases en equilibrio. Todos os datos foron adecuadamente correlacionados con ecuacións empíricas, o que facilita o seu manexo. Utilizáronse estes sistemas para analizar a partición de α-lactosa, albúmina de soro bovino, α-lactalbúmina y β-lactoglobulina entre as dúas fases acuosas. Analizouse a influencia do peso molecular do polímero, tipo de sal e pH na distribución. Os sistemas de dúas fases acuosas xerados con polietilenglicol 1500 e sulfato de amonio (298 K e pH=4) ou polietilenglicol 600 e tartarato de potasio (293 K e pH natural) consideráronse alternativas interesantes para a separación da α-lactosa e as proteínas. Por outra banda, polietilenglicol 300 e sulfato de sodio (298 K e un rango de pH de 4 a 5) resultou prometedor para o fraccionamento de proteínas. Deseñáronse varias estratexias baseadas nestes sistemas e na ultrafiltración para separar os principais compoñentes do soro do queixo. Probáronse primeiro cun soro sintético formulado cos solutos de interese en auga destilada, e logo cun soro de queixo proporcionado por un provedor local (Queizúar S. L.). O sistema bifásico acuoso formado con polietilenglicol 600 e tartarato de potasio permite unha moi boa separación da lactosa e as proteínas. O fraccionamento de proteínas non foi posible. A investigación neste tema debe continuar.

USC
UNIVERSIDADE
DE SANTIAGO
DE COMPOSTELA

TABLE OF CONTENTS

DECLARACIÓN DA AUTORA DA TESE *iii*

AUTORIZACIÓN DO DIRECTOR/TITOR DA TESE *v*

ACKNOWLEDGEMENTS (in Spanish) *ix*

ABSTRACT *xi*

RESUMEN (Spanish) *xii*

RESUMO (Galician) *xiii*

1. OBJECTIVE **1**

2. INTRODUCTION **5**

2.1. Cheese whey *7*

2.1.1. Products 10

2.1.1.1. Lactose 10

2.1.1.2. Proteins 11

2.1.2. Processing 12

2.2. Aqueous two phase system (ATPS) *15*

2.2.1. Types 16

2.2.1.1. Polymer-Polymer ATPS 16

2.2.1.2. Polymer-Salt ATPS 18

2.2.1.3. Other ATPS 18

2.2.2. Applications 19

2.2.3. Factors that affect partitioning in ATPS 21

2.2.4. Phase equilibrium 23

2.3. ATPS for the valorization of cheese whey *27*

3. ATPS CHARACTERIZATION **31**

3.1. Introduction *33*

3.2. Material and methods *33*

3.2.1. Chemicals 33

3.2.2. Methods 34

3.2.2.1. Physical properties 34

3.2.2.2. Solubility 37
3.2.2.3. Phase equilibrium 38
3.3. Results and discussion *39*
3.3.1. Physical properties 39
3.3.2. Solubility 48
3.3.3. Phase equilibrium 50
3.3.3.1. Binodal curve correlation 69
3.3.3.2. Tie-line data correlation 75

4. SEPARATION OF CHEESE WHEY COMPONENTS USING ATPS 81

4.1. Introduction *83*
4.2. Material and Methods *83*
4.2.1. Chemicals 83
4.2.2. Methods 85
4.3. Results and Discussion *88*
4.3.1. Biomolecules partitioning 88
4.3.1.1. Influence of solute concentration 88
4.3.1.2. Influence of the concentration of the phase-forming components 91
4.3.1.3. Screening 94
4.3.1.4. The influence of pH 102
4.3.2. Separation Strategies 107
4.3.2.1. Proteins/sugar separation 107
4.3.2.2. Proteins' fractionation 111

5. CONCLUSIONS 117

REFERENCES 123

LIST OF SYMBOLS 135

APPENDIX A: RESUMEN (SUMMARY, IN SPANISH) 139

APPENDIX B: LIST OF PUBLICATIONS 151

1. OBJECTIVE

USC
UNIVERSIDADE
DE SANTIAGO
DE COMPOSTELA

1. OBJECTIVE

Spain produces more than 400,000 tons of cheese per year, of which about 6,000 are made in Galicia. The principal residue in cheese manufacturing is a liquid substance called cheese whey, a serious environmental problem due to the high volumes produced (the production of 1 ton of cheese generates about 9 tons of whey) and its high chemical oxygen demand mainly due to the presence of lactose, proteins and fats.

These effluents with such a rich organic content could be seen not as a pollutant but a resource. The use of cheese whey as a raw material for the recovery of key components with high added value, such as proteins or lactose, means both the reduction of its environmental impact due to the decrease of the organic content, and the generation of new products improving the economy of the dairy industry.

Aqueous two-phase systems (ATPS) are a powerful tool for the separation and purification of biologically active products. Low concentration of suitable compounds produces two equilibrium phases with a high percentage of water, providing a mild medium for the recovery, for instance of proteins, that maintain their structure and prevent denaturation.

The main objective of this thesis is the valorization of cheese whey through the recovery of high added-value compounds using ATPS.

The main required step to accomplish this objective is the design of an adequate ATPS. Polymers (polyethylene glycol of different molecular weights and a random copolymer based on ethylene and propylene glycols denominated UCON) and salts (sodium, potassium and ammonium sulfates and potassium tartrate) are selected as phase-forming components due to their relative low cost and green character, in addition to their compatibility with the components of cheese whey. Phase diagrams will be determined and the influence of the temperature analyzed. To that aim, some physical properties will be measured in a range of concentration where the components form miscible mixtures. The objective is not only the use of these

properties as method of analysis of phases in equilibrium, but also the obtaining of properties, especially density, of interest in the design of these processes. To facilitate data management and comparison of systems, experimental results (binodal curves and tie-lines ends) will be correlated using different equations.

The characterization of the ATPS will allow the definition of the conditions to produce two equilibrium aqueous phases where the separation of individual solutes representative of the main components of cheese whey (lactose, bovine serum albumin, α-lactalbumin and β-lactoglobulin) will be tested. The partitioning of these key biomolecules among equilibrium phases and the effect of different parameters such as type of salt, polymer molecular weight, or pH will be evaluated. Based on these results, different separation strategies to carry out the valorization of cheese whey will be defined. Finally, the validity of these strategies will be tested firstly using a synthetic whey formulated with the key solutes dissolved in water, and later using a real cheese whey from a local cheese producer (Queizúar S.L.).

2. INTRODUCTION

USC
UNIVERSIDADE
DE SANTIAGO
DE COMPOSTELA

2. INTRODUCTION

2.1. CHEESE WHEY

The dairy sector is of key importance in the Spanish agri-food context due to its economic relevance and contribution to the development and continuity of the rural population. From all the livestock subsectors, dairy is second in importance only to the porcine subsector [1]. The dairy industry is divided into several production sectors according to the kind of product that it is produced: milk, cheese, butter, milk powder, condensate, etc. All these processes have in common the generation of specific contaminants in their wastewaters. Cheese production effluents are among the largest sources of organic contamination in this industry [2].

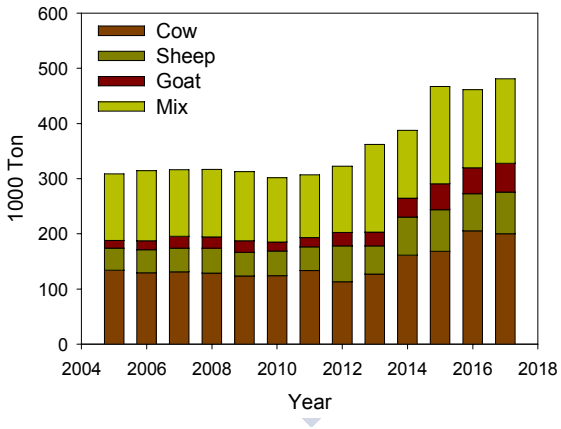

Figure 2.1. Evolution in cheese production in Spain in terms of the milk type [3]

Spain produces cheese all around the country. The evolution of cheese production in Spain from 2005 to 2016 is shown in Figure 2.1 [3]. The numbers presented in this Figure show the relevance of this industrial sector that in recent years has produced more than $4 \cdot 10^5$ Ton/year. In this Figure, cheese production is also presented in terms of milk source. Four types of cheese are commonly produced in Spain: cow, sheep, goat and mixture (three types of milk are mixed in different proportion). Despite the fact that the production of goat cheese has been increasing

during recent years, this type of cheese has the lowest production, whilst the highest production corresponds to cow and mixture (mainly produced with cow milk) cheeses.

The principal residue in the cheese making is a liquid substance, whey, obtained by separating the coagulum from milk, cream, or skim milk. Whey may also be obtained by direct acidification of milk (casein manufacture). However, more than 90 % of whey originates from cheese production. Thus, cheese whey can be found in different effluents from this industry. Cheese whey results from cheese production, second cheese whey is a result of the cottage cheese production, and cheese whey wastewater is washing water with different fractions of cheese whey and/or second cheese whey [2].

In spite of its nutritional value, cheese whey is an effluent with strong organic and saline content. It represents a significant environmental problem due to its physicochemical properties (see Table 2.1), the high volumes produced (the production of 1 kg of cheese generates 9 kg of whey), and its high organic matter content mainly due to the presence of lactose (0.18-60 kg/m^3), proteins (1.4-33.5 kg/m^3) and fats (0.08-10.58 kg/m^3), that lead to a chemical oxygen demand of about 60000-80000 ppm [2, 4].

Table 2.1. Cheese whey physicochemical properties

Minerals	0.46-10 %
Total Suspended Solids	0.1-22 kg/m^3
pH	3.3-9.0
Phosphorus	0.006-0.5 kg/m^3
Total Kjeldahl Nitrogen	0.01-1.7 kg/m^3
Organic Load	0.6-102 kg/m^3

The evolution in the production of whey coming from the cheese and casein manufacturing in Spain since 2005 is shown in Figure 2.2 [3]. This whey can be found in different states: liquid, concentrate or powder and blocks, but most

frequently in a liquid state. The amount of whey resulting from the production of cheese is high, causing a serious problem.

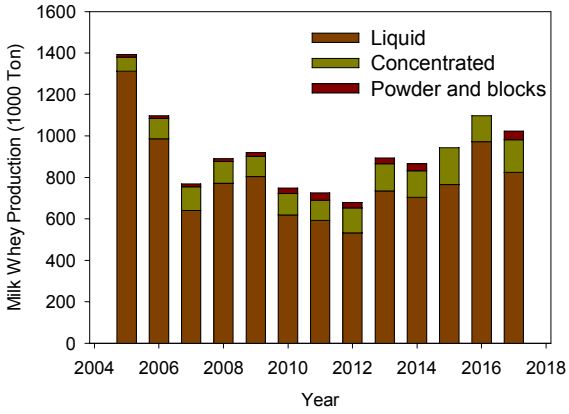

Figure 2.2. Evolution in milk whey production in Spain* [3]

Whey holds the 55 % of milk nutrients, being the most abundant: lactose (4.5-5 %), soluble proteins (0.6-0.8 %), lipids (0.4-0.5 %) and mineral salts (8-10 % of dried extract) due to the NaCl addition during cheese production. These effluents with such a rich organic content could be seen not as a pollutant but a resource. The use of this residue as raw material for the extraction of valuable compounds means both the reduction of its environmental impact due to the decrease of the organic content, and the production of a byproduct that improves the economy of the process [4].

For cheese whey valorization three different options can be considered. Cheese whey processing can be carried out to recover, from the effluents, the valuable compounds like proteins and lactose. The second method relies on the application of biological treatments such as hydrolysis and controlled fermentation processes to obtain high added-value compounds: glucose, peptides, organic acids, single cell proteins and oils, biopolymers and bacteriocins. The third choice is the application

* Data for power and block whey are confidential for 2015 and 2016

of physicochemical treatments such as coagulation, flocculation, ozonation, etc. In some cases the combination of methods can be an alternative, for instance the use of whey permeate obtained from ultrafiltration as a fermentation medium [2, 5].

2.1.1. Products

2.1.1.1. Lactose

Lactose can be obtained from whey or milk permeates by crystallization and is available in various grades of purity: crude lactose (95-98 %), edible and refined edible grade (99-99.5 %) and pharmaceutical grade (99.5-99.9 %) [4, 6].

Lactose is used in the food industry for sweetness reduction, aroma fortification, improved color of baked products and improved shelf life. In the pharmaceutical industry, lactose is used as a carrier for tablets or dry powder inhalers, and as filling agent in capsules [6]. The generation of derivatives from lactose can be an interesting tool to increase its value. Biogas, polyhydroxyalkanoates (PHAs), lactic acid and single cell proteins are some of the products obtained from lactose fermentation [4, 5].

PHAs are polyesters synthesized through the action of aerobic bacteria from macromolecules. Their mechanical, physical and chemical properties are comparable to the petroleum-derived plastics. However, these biodegradable plastics are ahead in terms of biodegradability, resistance to ultraviolet radiation, oxygen impermeability and biocompatibility. There are three routes for the transformation of lactose to PHAs: a) direct conversion, b) hydrolysis of lactose and conversion of glucose and galactose to PHAs, and c) lactose fermentation to lactic acid and then conversion of lactic acid to PHAs [5].

Acetic, propionic, lactic, lactobionic, citric, gluconic and itaconic acids can be obtained from lactose/whey fermentation, lactic acid being the most relevant from an economic point of view. Besides its application as a biodegradable plastic

component, it is frequently employed in the food industry as preservative or acidulant [5].

2.1.1.2. Proteins

The major proteins presents in whey are: β-lactoglobulin (β-LG) (50 % wt), α-lactalbumin (α-LA) (20 % wt), bovine serum albumin (BSA) (10 % wt) and immunoglobulin (IG) (10 % wt). Besides these, whey also contains numerous minor proteins, called low abundance proteins, such as lactoferrin (LF), lactoperoxidase (LP), proteose peptone (OPN), lysozyme (LZ). The concentration of whey proteins depends on the type of whey (acid when is produced by direct acidification of milk or sweet if is produced from cheese), the source of milk (bovine, caprine or ovine) and the stage of lactation, the period of the year, the type of feed, and the process quality. The principal characteristics of whey proteins, such as the molecular weight or the isoelectric point (pI), pH value at which the net charge is zero, are summarized in Table 2.2 [5, 7-9].

Table 2.2. Characteristics of whey proteins

Protein	Molecular weight (kg/mol)	Concentration (g/L)	Number of amino acids	Isoelectric point
ß-LG	18	3.2	162	5.4
α-LA	14	1.2	123	4.4
BSA	66	0.4	582	5.1
IG	150	0.7	†	5-8
LF	77	0.1	700	7.9
LP	78	0.03	612	9.6

Proteins have important biological properties. For example, *β*-LG and IG modulate human immune responses, *α*-LA and BSA have anti-carcinogenic activity, LF has properties as an antimicrobial and antiviral agent but it also helps in immune

† Variable values

system modulation, LP is also antimicrobial, antiviral and anti-carcinogenic. Their individual supply is of high interest, especially for people who need to tailor their diet to improve health, and converts them into products of high added value.

2.1.2. Processing

The processing of whey streams can be carried out to simply reduce the water content to obtain dairy solids of interest in food formulations or, more interestingly, to separate components of added value. Figure 2.3 shows a flow diagram for the obtaining of different whey products.

Dry whey is the product of the water removal present in the whey. This step is necessary to reduce storage and transportation costs and produce an ingredient to be used as a food additive. Whey powder is produced either by drying fresh whey from the rennet casein or cheese manufacture, or from cottage cheese, casein or fresh cultured cheese. Demineralized whey powder is the product of removal of the monovalent ions (for instance by means of ion exchange chromatography or electrodialysis). These ions have negative sensorial properties, while divalent ions contribute to the healthy image of the product. Ultrafiltration (UF) is generally used to remove lactose and minerals while the proteins are concentrated. The product thus obtained is called whey protein concentrate (WPC) and contains about 50-85 % proteins on a dry basis. Additional Microfiltration (MF) or UF processes allow the production of a whey protein isolate (WPI) with a content of about 90-98 % of proteins and very small amounts of lactose and fat [5, 6].

Differences in molecular weight, concentration or pI are the main properties of the proteins that are used to carry out their separation. Processes proposed for commercial-scale production of whey protein fractions fall into four main categories: membrane filtration, selective precipitation, selective adsorption and selective elution [7].

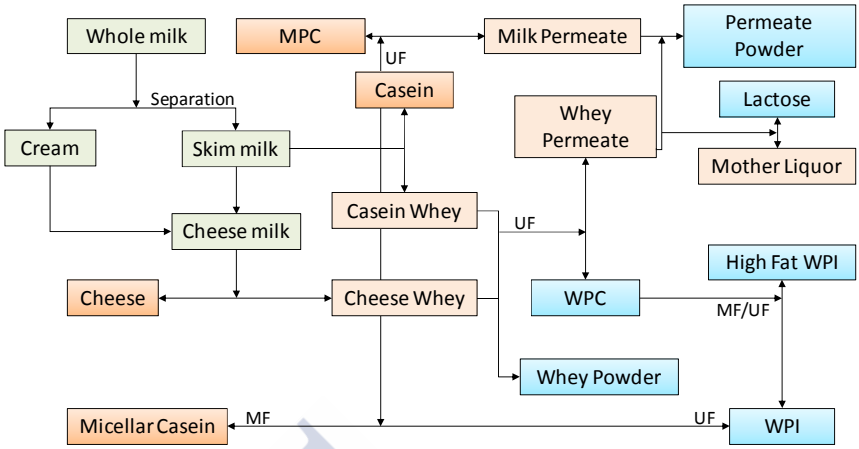

Figure 2.3. Flow diagram for the whey protein production (adapted from [6])

Membrane filtration was originally used only to produce a whey protein concentrate. The fractionation of proteins with these techniques was only possible if they drastically differed in molecular weight, charge or size. Nowadays, the separation of proteins with similar molecular weight is possible with an adequate adjustment of the solution pH and ionic strength. UF, MF, nanofiltration (NF) and reverse osmosis (RO) are some techniques currently used to recover and purify proteins from cheese whey. Table 2.3 shows the range of pressure and main characteristics of these filtration processes. The drawbacks these technologies have include limitations related to poor selectivity, fouling and lifetime of the membranes. Moreover, from an economic point of view, these processes are frequently very expensive due to the need of high pressures [2, 5, 6].

Selective precipitation involves adjusting the pH and temperature to promote insolubility. Proteins are typically least soluble at a pH near the pI or in low ionic strength solutions, and are most likely to aggregate under these conditions. For example β-LG precipitates rapidly and selectively at high temperature (70-120 °C) and pH 8, whereas α-LA precipitates and aggregates better at low pH (3.5-5.5) and moderate temperature (50-65 °C) with long reaction times [5]. This adjustment of the conditions usually requires precipitants. The main difficulty of this method lies in the choice of a selective precipitant for a target protein. Major disadvantages of

these precipitants are their usually low biodegradability and high cost. Moreover, many other factors have to be considered such as the means of adding the precipitant, the environment in which precipitation occurs, the separation after the operation, and the recovery of the targeted protein. The minimization of losses of either precipitant or protein is also a key issue.

Table 2.3. Membranes used in diary industry [2, 6, 10]

Type	Pore size (μm)	Molecular weight cut off (kDa)	Pressure and principle	Compounds in retentate	Range of protein retention (%)
MF	0.2-1.4	>200	Low pressure, driven membrane process	Separation of protein, bacteria and other particles	28-85
UF	0.001-0.05	1-200	Medium pressure, pressure driven process to overcome the viscosity	Casein micelles, fat globules, colloidal minerals, bacteria and somatic cells	56-81
NF	0.5-2	300-1000	Medium to high pressure, mass transfer phenomena and electrostatic interactions	Separate monovalents salt and water	87-100
RO	No pores	0.1	High pressure	Based on the principle of solubility	94-96

Selective adsorption consists of the adhesion of a single purified protein to a surface, simultaneously producing a treated whey solution with low concentration in that protein. Adsorption mechanisms can be physical, chemical or electrostatic. In selective elution all the proteins in a mixture are trapped simultaneously onto the adsorbent, rinsed free of contaminants, and then eluted one by one to obtain different purified proteins [5]. These methods are the basis for chromatographic techniques in which separation is achieved mainly thanks to differences between the adsorption

affinities of the sample components for the surface of an active solid. For instance, ion exchange chromatography can operate under two conditions: selective adsorption of whey proteins, or selective elution from ion exchange resin [6, 11]. On a large scale, high operational costs are associated to the pressure drop required for a given flow rate and frequent chromatographic medium replacement.

A relatively recent technique for whey protein purification is magnetic fishing. It involves the use of magnetic particles (hydrophobic ligand, biopolymers, etc.) that have affinity to the desired component. The target protein binds to these particles forming a complex which is easily and rapidly removed from the sample with an appropriate magnetic separator [11]. The use of aqueous two-phase systems has also recently been proposed for whey protein fractionation. This process, as in the case of magnetic fishing, has not yet been scaled-up to the industrial level. Gaining greater knowledge of the fundamentals and the optimization of the conditions for the process are required steps, and research on these systems is encouraged.

2.2. AQUEOUS TWO PHASE SYSTEM (ATPS)

A microbiologist, Martinus Willem Beijerinck, was the first to observe (1896) an aqueous two-phase system (ATPS). He found that the mixture of agar, gelatin and water in a certain concentration range separated into two aqueous phases, the top enriched in gelatin and the bottom being an agar rich phase [12]. In 1947, Dobry and Boyer-Kawenoki [13] tested the miscibility between 14 polymers with high molecular weight dissolved in 13 solvents. The results of the experiments showed that incompatibility, leading to two-phase systems, was the normal situation.

In 1950 a successful application for ATPS as an extraction media in biotechnology was found when Albertsson proposed their use for the separation of biomolecules [14]. ATPS are suitable for biotechnological applications due to the high percentage of water present in both equilibrium phases, providing a mild medium for the recovery of proteins that maintain their structure and prevent

denaturation. Moreover, this separation technique is also useful for the separation of viruses, cellular organelles, antibiotics and whole cells [14].

2.2.1. Types

ATPS are obtained when mixing two aqueous solutions of suitable components, under certain concentration and temperature conditions. Both components have to be soluble in water, but at some specific conditions the system separates into two coexisting immiscible aqueous phases when the equilibrium is reached. One phase is enriched in one of the components, while the other phase is enriched in the other. These constituents are usually two polymers (e.g. polyethylene glycol and dextran) or a polymer and a salt (e.g. polypropylene glycol and sodium phosphate) [15, 16]. In the last several years, new types of ATPS systems have been identified: ionic liquid/salt, alcohol/salt and micellar [17, 18].

A special case of polymer-based ATPS are those formed by thermo-separating polymers. Thermo-separating polymers drastically change their solubility in water with temperature, splitting into two immiscible phases when incubated above their lower critical solution temperature (LCST) [19]. Random ethylene glycol and propylene glycol copolymers (EOPO) are a typical example of thermo-separating polymer which has been successfully applied for recovery of biomolecules with polymer recycling [20]. By heating the system above the cloud point, a two-phase system is quickly formed, where the bottom phase is enriched in polymer (between 40 and 80 %wt polymer) and the top phase contains almost pure water. When introducing these EOPO copolymers into the conventional polymer/polymer and polymer/salt ATPS, a large amount of hybrid ATPS can be generated [21-25].

2.2.1.1. Polymer-Polymer ATPS

Several polymers can be used to obtain polymer–polymer ATPS. Moreover, for each polymer, different molecular weights can be selected thus obtaining ATPS with different properties and capabilities to separate biomolecules. Some examples, previously described in literature, are summarized in Table 2.4.

Table 2.4. Common polymer-polymer ATPS [26]

Polymer 1	Polymer 2
Polypropylene Glycol (PPG)	Methoxypolyethylene Glycol
	Polyethylene Glycol (PEG)
	Polyvinyl Alcohol (PVA)
	Polyvinylpyrrolidone (PVP)
	Hydroxypropyl Dextran
	Dextran
	Hydroxypropyl Starch (PES)
	Maltodextrin
Polyethylene Glycol (PEG)	Polyvinyl Alcohol (PVA)
	Polyvinylpyrrolidone (PVP)
	Dextran
	Ficoll
	Pullulan
Polyvinyl Alcohol (PVA)	Methylcellulose
	Hydroxypropyl Dextran
	Dextran
Methylcellulose	Hydroxypropyl Dextran
	Dextran
Ethylhydroxyethylcellulose	Dextran
	Hydroxypropyl Starch (PES)
Hydroxypropyl Dextran	Dextran
Ficoll	Dextran

The most studied systems are the combination of polyethylene glycols (PEG) of high molecular weight and dextran. This is due to their stable physical or chemical structure and non-toxic properties for biological materials. However, this kind of ATPS presents several problems: high viscosity of the dextran rich phase, high cost of dextran which means it is too expensive to scale-up the process, and the difficulty of recovery and cyclic utilization of polymers [17]. Nevertheless, when the

cost of the product of interest is considerable and compensates the cost of the phase-forming polymers, the use of these systems is an option to consider [27].

2.2.1.2. Polymer-Salt ATPS

Common polymer-salt ATPS are shown in Table 2.5. The most studied are formed by polyethylene glycol (PEG) and inorganic salts like sulfates (ammonium, sodium or magnesium), phosphates (potassium) or carbonates (sodium). The main advantages of the use of these types of systems are: the low cost of the phase-forming chemicals, the far-reaching knowledge accumulated including wide characterization, and their stability on the basis of phase formation [27].

Table 2.5. Common polymer-salt ATPS [15]

Polymer	Salt
PEG 600	Ammonium sulfate
	Potassium phosphate
PEG 1000	Ammonium sulfate
	Sodium sulfate
	Magnesium sulfate
	Potassium phosphate
	Sodium Carbonate
PEG 8000	Ammonium sulfate
	Sodium sulfate
	Magnesium sulfate
	Sodium carbonate

2.2.1.3. Other ATPS

The relevance given in the last decades to ionic liquids (ILs) has led to development of new ATPS systems formed by a chaotropic and a kosmotropic salt. ILs are salts with low melting or glass transition temperatures (lower than 100 ºC). Due to their ionic nature, they present special and interesting features such as their negligible volatility and, in most cases, non-flammability. Additionally, the

polarities and affinities of these salts as phase-forming agents in ATPS systems, can be designed with the proper selection of the cations and anions. Only ILs miscible with water near room temperature can be considered for the formation of IL-salt ATPS. Thus, the most studied systems involve imidazolium cations with halide or sulfate anions [28].

The alcohol-salt ATPS are systems based on aliphatic alcohols and salts as phase-forming components. In equilibrium conditions, the top phase is enriched in alcohol whilst the bottom phase is rich in salt [18]. The alcohols commonly used to generate these biphasic systems are: ethanol, 1-propanol or 2-propanol, and they appear combined with different salts such as ammonium sulfate, potassium phosphate or sodium citrate [29, 30].

In ATPS micellar systems, an aqueous surfactant solution, under appropriate conditions, spontaneously separates into two predominantly aqueous, yet immiscible, liquid phases. The equilibrium phases have different physicochemical environments, one micelle-rich phase (with larger and more abundant micelles) and another micelle-poor phase. These different domains are the basis of an effective separation and make ATPS micellar systems a convenient and potentially useful method for the separation, purification and concentration of different biomaterials [12]. Most studied systems involve the use of Triton X-Series of nonionic surfactants (alkylaryl polyether alcohols). Some examples are Triton X-100 combined with sodium citrate [31] or with sorbitol [32], or Triton X-114 combined with different ionic liquids (imidazolium, phosphonium and quaternary ammonium) [33].

2.2.2. Applications

Since ATPS are mainly composed of water, they are a biocompatible media for cells, cell organelles and biologically active substances. In this context, they can be used as an analytical tool or as a separation technique. In the first case, they are used for the primary recovery and partial purification of a variety of biological products (see Table 2.6). In the second case, ATPS have proved useful for biomolecule

extraction in biotechnological processes. The basis of separation in ATPS is the selective distribution of substances between the two immiscible phases.

Table 2.6. Examples of biomolecules recovery with ATPS

Biological Product	Reference
Proteins	[34, 35]
Genetic material	[36, 37]
Low molecular weight products	[38]
Cells and cell organelles	[39, 40]

Separation processes with ATPS involve two operations: equilibration and phase separation. Equilibration is rapid, involving the mixing of the phase-forming components with the material subjected to partitioning in water. Mass transfer occurs between the phases in an attempt to reach equilibrium. The aqueous phases are then mechanically separated from each other (settling). The phase separation under gravity is a relatively slow process, varying between a few minutes and a few hours, due to the rather low difference in the densities of the two phases, their viscosity and the time required for the small droplets to aggregate into larger ones [26, 41]. By substituting centrifugal for gravitational force in the settler (centrifuges), operation times are reduced.

ATPS show promising features in biotechnological processes: simple technology, continuous operation, possible recovery and recycling of the phase-forming components, low energy requirements, relatively low operation times (quick partition equilibrium), low cost, easy to scale up, and process integration capability [14, 18, 41]. However, they have revealed limitations at the industrial level, which is why current applications have been developed only at the laboratory level or small scale. These limitations are mainly associated, according to some authors [42, 43], with the absence of thermodynamic or empirical models that allow the prediction of the ATPS and solutes behavior when the formulation, the conditions or the system change.

2.2.3. Factors that affect partitioning in ATPS

The selective distribution of biomolecules between the equilibrium phases in an ATPS is governed by the properties of the phase-forming components and the material subjected to partitioning, as well as the interaction between them [41]. Regarding the most common ATPS, polymer-salt, the environmental conditions influencing biomolecule partitioning include: the type of salt and its concentration; polymer characteristics: type, molecular weight and concentration; the presence of polymer derivatives; hydrophobic or affinity types; temperature; and gravity. Also of influence are the structural properties of the biomolecule including its size, structure, net charge, hydrophobicity and other surface properties [26].

For the study of solute partitioning in polymer-salt ATPS, in order to achieve a desirable separation, it is necessary to keep in mind that the system parameters and the solute properties are directly related. In this way the molecular weight and size of polymers, the concentration of polymer, ionic strength, pH, and the use of additional salts to increase the hydrophobic resolution of the system, are the principal system parameters. While the hydrophobicity, surface charge, concentration, size and bioaffinity are the most important solute properties [44].

Molecular weight or size

Since the solutes to be partitioned in an ATPS have a defined size, they are subject to steric effects imposed by the phase-forming constituents of the system. These steric effects are typically related to the available volume for the solutes to be fractionated toward a particular phase. This is generally known as the free volume effect.

When a polymer is one of the phase-forming components, the free volume available in the polymer-rich phase is limited due to the considerable length and molecular weight of this compound. This effect is enlarged with the increase of the tie-line length (TLL) because the polymer concentration increases [18].

For salt-polymer ATPS, the maximum biomolecule concentration in the polymer-rich phase is determined mainly by a steric exclusion effect of the polymer, and in the salt-rich phase by a salting-out effect. True partitioning behavior only occurs at relatively low biomolecule concentration. When the concentration of the biomolecule exceeds relatively low values, precipitation at the interface can be observed. This precipitated biomolecule is in equilibrium with the two liquid phases with different concentration of the solubilized solute [44].

Hydrophobicity

Hydrophobic interactions likely play the main role in the fractionation of biomolecules in most ATPS. Two effects are involved in these interactions: the phase hydrophobicity effect, directly related to the chemical identity of the system constituents as well as their concentration, and the salting-out effect.

The two equilibrium phases in an ATPS are obviously hydrophilic, although the phase rich in polymer is usually more hydrophobic. This favors the partition of amphipathic and less hydrophilic solutes toward that particular phase. In polymer-salt systems the phase hydrophobicity may be manipulated varying TLL (increasing the TLL an intrinsic reduction of the water content is achieved, hence the system becomes more hydrophobic as less water is available), the polymer molecular weight (when the polymer molecular weight increases, the hydrophobicity also increases), and by the addition of an adequate salt [18, 44]. A salting-out effect is observed in systems with at least one highly ionic phase. In these cases, since the amount of water needed to dissolve the salts in the systems is high, the solutes to be partitioned are only partially hydrated, so partitioning toward the less hydrophilic phase is favored under such circumstances [18].

Salt addition

The addition of salts to the ATPS results in an increase in the hydrophobic difference due to generation of an electrical potential difference between two phases. This increase in the hydrophobicity is related to the decrease of the amount of bound

water in order to keep the final composition of the systems constant, and also because of the ion solvation. However, the addition of high neutral salt concentration may cause denaturation of biomolecules [18].

pH

The influence of pH on electrochemical interactions is fundamental, and the solubility of the biomolecule is intimately related to the superficial charge interaction with the ions presented in the system. Therefore, the pH of the system may be manipulated in order to promote selective separation. An adequate initial pH is a decisive factor to achieve the required separation. This value should be greater than the pI or pK_a of the target compound in order to generate electrochemical affinity between the negatively charged product and the polymer, which has a positive dipolar momentum [27, 44]. As salt solubility constrains the pH conditions, buffers can be required.

Bioaffinity

The recovery and purification of biomolecules can be dramatically increased by using modified ATPS with biospecific ligands that favor selective partitioning. One method is based on the attachment of a ligand, able to create binding affinity with the target solutes to the phase-forming polymer. Another method simply relies on the addition of free ligands to the system to modify the partitioning without the modification of the phase-forming components.

2.2.4. Phase equilibrium

An ATPS comprises the liquid-liquid equilibrium of two aqueous phases at constant temperature and pressure. The graphical representation of phase equilibria is a useful tool that allows a quick visualization of all the information contained in the data. Each ATPS generated with specific phase-forming components under certain conditions of pressure, temperature and pH is represented by a unique phase diagram. It contains information about the components and concentrations in the top

and bottom phases, and the ratio of phase volumes. So the phase diagram delineates the working area for a particular ATPS [41].

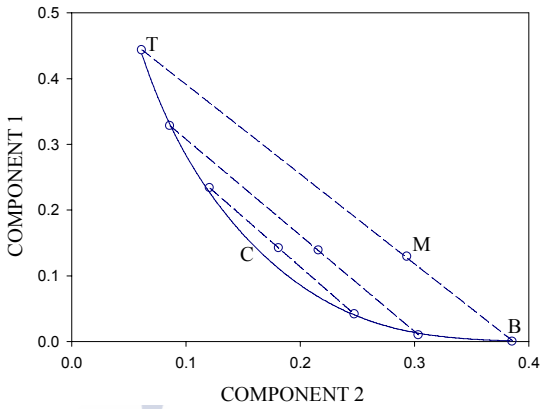

Figure 2.4. ATPS phase diagram

Liquid-liquid equilibrium of ternary mixtures is usually represented by triangular diagrams. Nevertheless in the case of ATPS, due to the high water content, the phase diagram is usually illustrated using a rectangular representation where the solvent concentration is omitted. In the case of polymer-salt ATPS, the X-axis generally represents the concentration of salt while the Y-axis represents the concentration of polymer. An example of this rectangular phase diagram for a system formed by two general compounds is shown in Figure 2.4. The curve that connects the points T-C-B in this figure is called the binodal curve, and separates the left area that is an homogenous region with only one phase present, from the right area that is an heterogeneous region where two phases are in equilibrium. For the heterogeneous region, a mixture of two components whose composition is given by point M will be separated in two equilibrium phases of compositions T and B that represent the final concentration of components in equilibrium phases. The lines that connect these two points of the binodal curve are denominated tie-lines. All points in the tie-line will have identical composition in the equilibrium phases, but the phase mass and volume will be different. In this figure, the critical point (C) of the binodal

curve is also represented. At this point the composition and the volume of both phases are equal [15, 41, 45].

Two parameters are frequently used to characterize the tie-lines: the tie-line length (TLL) and the tie-line slope (STL). The TLL corresponds to the distance between points T and B (see Equation 2.1) and it has the same units as the component concentration. The STL gives an idea of the components distribution and can be calculated as shown in Equation 2.2.

$$\mathrm{TLL} = \sqrt{(\mathrm{X_T} - \mathrm{X_B})^2 + (\mathrm{Y_T} - \mathrm{Y_B})^2} \qquad 2.1$$

$$\mathrm{STL} = \frac{Y_T - Y_B}{X_T - X_B} \qquad 2.2$$

where X and Y represent the concentration for components 1 and 2, and the subscript T and B indicate top and bottom phases, respectively [28].

The partitioning of soluble molecules occurs between the two phases in equilibrium of an ATPS, top and bottom, and it is characterized by the term partition coefficient (K) which is the ratio of the concentration of the solute in the top phase (C_T) to the bottom phase (C_B):

$$K = \frac{C_T}{C_B} \qquad 2.3$$

The partition coefficient depends on the properties of the phases and the biomolecule, and also temperature, but it is independent of the solute concentration and volume ratio of the phases [41]. Partition coefficients are used to evaluate the extension of the separation process. A K greater than 1 means that the solute will be recovered in the top phase, on the contrary, if the partition coefficient is lower than 1 the solute will be recovered in the bottom phase. K values close to unity indicate that the partition between the equilibrium phases is similar, so separation is not effective.

Solute partition in a given ATPS is a consequence of several interactions between the molecule and each phase of the biphasic system. These interactions can involve different forces such as electrostatic, hydrophobic/hydrophilic, van der

Waals, hydrogen bonds and also conformational effects. In this way, Albertsson [14] described the partition coefficient of a given biomolecule as a sum of different contributions:

$$Ln\ K = Ln\ K^0 + Ln\ K_{elec} + Ln\ K_{hyfob} + Ln\ K_{biosp} + Ln\ K_{size} + Ln\ K_{conf} \qquad 2.4$$

where the subscripts: $elec$, $hyfob$, $biosp$, $size$ and $conf$ refer to the electrochemical, hydrophobic, biospecific, size and conformational contributions to the partition coefficient, respectively. These contributions are the result of the biomolecule structural properties and the environmental conditions. The term K^0 corresponds to the other parameters that are not included in the contributions indicated above. Taking this into account, Diamond and Hsu [26] expressed the partition coefficient as:

$$Ln\ K = Ln\ K_{environment} + Ln\ K_{structure} \qquad 2.5$$

The environmental conditions influencing biomolecule partitioning were discussed in section 2.2.3. As a consequence, the recovery and the purification parameters of a given biomolecule can be optimized manipulating those environmental conditions. The physical and chemical parameters of the systems which can be manipulated include: the type and molecular weight of the polymer, the nature and concentration of added salts, the difference between the concentrations of the phase-forming components, pH of the system, and the addition of molecules able to generate biospecific affinity [46].

Selectivity is another key thermodynamic parameter in order to decide the suitability of an ATPS for a given separation. It refers to the ability of the system to concentrate one component in one of the phases in preference to another, and it is calculated as the quotient of the partition coefficients of components to be separated:

$$S = \frac{K_{S1}}{K_{S2}} \qquad 2.6$$

where S is the selectivity and K_{S1} and K_{S2} are the partition coefficients of the solutes (1 and 2) to be separated. When selectivity is higher, the separation of the two solutes is greater [18].

Another parameter very important regarding the efficiency of the separation is the recovery yield (Y_T). It is calculated at the phase where the target is partitioned preferentially, and it is expressed relative to the initial amount of the compound of interest in the sample loaded to the ATPS, according to Equation 2.7 [18]:

$$Y_T(\%) = \frac{C_t \cdot V_t}{C_i \cdot V_i} \text{x } 100 \qquad 2.7$$

where C is the concentration, V is the volume and the subscripts t and i represent the solute in the partitioned phase and in the stock solution added to the system, respectively.

2.3. ATPS FOR THE VALORIZATION OF CHEESE WHEY

The main proteins present in cheese whey are β-LG, α-LA and BSA. Consequently, all the work on cheese whey revalorization using ATPS found in the Literature up to now [47-52], focuses on the separation of these proteins. Table 2.7 contains a summary of these studies where polymers and salts were used as phase-forming agents.

Chen [49] focused his efforts on the separation of α-LA and β-LG from cheddar cheese whey. In his work, firstly the influence of the system parameters on the partitioning behavior was studied using a synthetic mixture of pure proteins. The results showed that the systems formulated at 23 ºC with a polymer of low molecular mass (PEG 1000), high salt (20 % wt of potassium phosphate) and low polymer (12 % wt) concentrations, neutral pH, and with the addition of neutral salts (0.6 M of NaCl), led to the best separations. Secondly, this ATPS was applied to cheddar cheese whey. As expected, the purities of α-LA and β-LG obtained were lower than the purities obtained for the synthetic mixture. β-LG was recovered in the bottom phase contaminated with 11 % wt of α-LA, whilst this second protein was mainly recovered in the top phase with a purity of 91 % wt.

Table 2.7. Cheese whey proteins partitioning in ATPS

Polymer	Salt		
	$(NH_4)_2SO_4$	KPB‡	NaCB§
PEG 6000		α-LA/β-LG[49]	
PEG 4000		α-LA/β-LG[49]	
PEG 3400		α-LA/β-LG/BSA[50]	α-LA/β-LG/BSA[52]
PEG 200		α-LA/β-LG[53]	
PEG 1500	α-LA/β-LG[47]	α-LA/β-LG[48], [49] α-LA/β-LG/BSA[50]	α-LA/β-LG/BSA[52]
PEG 1000		α-LA/β-LG[49] α-LA/β-LG/BSA[50]	α-LA/β-LG/BSA[52]
PEG 900	α-LA/β-LG[47]		
PEG 600	α-LA/β-LG[47]		
UCON		α-LA/β-LG[51]	

Alves *et al.* [48] studied the partitioning of *α*-LA and *β*-LG from WPI using PEG 1500 and potassium phosphate. The aim of the research was the analysis of the influence of the PEG concentration in the separation. They found that concentrations of about 14 % wt of PEG and 18 % wt of salt (values similar to those proposed by Chen [49]) at 25 ºC allowed the best separation. ATPS formulated with these concentrations led to partition coefficients of 0.031 for *α*-LA and 8 for *β*-LG. A high value of selectivity (318) was found, demonstrating the feasibility of using this ATPS to carry out the target separation. Zhang *et al.* [51] also employed WPI as a raw material to carry out the separation of these proteins. These authors formulated the ATPS with UCON (40 % wt) and potassium phosphate (15.5 % wt) at pH 4 and 23 ºC. The system allowed the protein fractionation. *α*-LA was recovered in the top phase and *β*-LG in the bottom phase with extraction rates of 98 % and 96 %, respectively. The authors do not present information about the purities obtained.

‡ Potassium phosphate buffer.

§ Sodium citrate buffer.

Rodrigues *et al*. [47] focused their work on WPC. They designed the adequate ATPS using a synthetic mixture of α-LA and β-LG, and concluded that PEG 900 with concentrations between 14-16 % wt and about 14 % wt of ammonium sulfate at pH 7 allowed the best separation. Working with WPC, β-LG was recovered in the bottom phase without the detection of any other protein. However, α-LA could only be recovered in the top phase contaminated with BSA.

Alcântara *et al*. [53] studied the partitioning of α-LA and β-LG from fresh whey using a system composed of PEG 2000 (13 % wt) and potassium phosphate (13 % wt) with the addition of 0.35 M of NaCl at pH 6.7 and 25 ºC. The extraction yield for β-LG in bottom phase was 97.3 % and for the α-LA in top phase was 81.1 %. This fractionation was performed in a three stage cross-flow extraction system.

Sivakumar *et al.* [54] studied the recovery of α-LA present in cheese whey prepared from pasteurized milk. To carry out the recovery, they used an ATPS formulated with tri sodium citrate and polyethylene glycol. The effect of the PEG molecular mass in the partitioning behavior of α-LA and β-LG was evaluated. In agreement with the work of Chen [49], the lowest molecular mass of the polymer allowed a better separation of both proteins. So, using PEG 1000 and tri sodium citrate, a maximum partition coefficient of 16.67 was achieved for α-La at the system conditions of 28 % wt PEG and 14 % wt salt at pH 8 and 40 °C, whereas the partition coefficient of β-LG was 0.27. In this work, equilibrium conditions (polymer and salt concentrations in the ATPS) were also identified

Just a very recent work [55] was found in Literature that aims to separate proteins and lactose present in whey (basket cheese). The system employed at 25 ºC was composed of 0.1 % wt PEG 4000 and 34.7 % wt ammonium sulfate. Under these conditions the proteins showed more affinity for the top phase with a partition coefficient value of 31.5, whilst the lactose moved towards the bottom phase with a partition coefficient value of 0.92. The recovery yields were 93 % and 72.3 % for proteins and lactose, respectively.

ATPS were also employed to separate other compounds of cheese whey. The system formulated with PEG 6000 and potassium phosphate at pH 7 was used to carry out the separation of proteins and fat, but also to concentrate the proteins in the top phase [56]. Regarding the recovery of α-1 antitrypsin present in the milk whey, Capezio *et al.* [50] used ATPS formulated with potassium phosphate and PEG 1500 at pH 6.3 and 8 ºC, and Boaglio *et al.* [52] employed PEG 1450 with sodium citrate at pH 5.2 and 20 ºC. In both cases, recoveries of the protein greater than 80 % were achieved.

Practically none of the above mentioned manuscripts, except the work carried out by Sivakumar *et al.* [54], consider the liquid-liquid equilibrium involved in the separation. Polymer and salt concentrations in equilibrium phases are not determined, the influence of TLL and STL on the biomolecules separation is not considered, and the optimization of the conditions of the system is basically a trial and error method. This work is intended to carry out a more complete study considering the fundamentals of the separation, the equilibria involved. Moreover, the absence of works focusing on the separation of lactose, even when it is the most abundant nutrient of cheese whey, is noticeable. This work will also focus on the separation of this disaccharide.

3. ATPS characterization

All the results presented in this chapter have been published in:

- M. González-Amado, E. Rodil, A. Arce, A. Soto, O. Rodríguez, The effect of temperature on polyethylene glycol (4000 or 8000)-(sodium or ammonium sulfate) Aqueous Two Phase Systems, *Fluid Phase Equlibr*., 428 (2016) 95-101.
- X. Rico-Castro, M. González-Amado, A. Soto, O. Rodríguez, Aqueous two-phase systems with thermo-sensitive EOPO co-polymer (UCON) and sulfate salts: Effect of temperature and cation, *J. Chem. Thermodyn*., 108 (2017) 136-142.
- M. González-Amado, E. Rodil, A. Arce, A. Soto, O. Rodríguez, Polyethylene glycol (1500 or 600)-potassium tartrate aqueous two phase systems, *Fluid Phase Equlibr*., 470 (2018) 120-125.

USC
UNIVERSIDADE
DE SANTIAGO
DE COMPOSTELA

3. ATPS CHARACTERIZATION

3.1. INTRODUCTION

In order to separate and valorize cheese whey components by means of aqueous biphasic systems, the main required step is the design of an adequate ATPS. This development stage involves the correct selection of parameters such as phase-forming components, TLL, pH and phase volume ratio for the particular product or products to be recovered [18].

In this work, polymers and salts are selected as phase-forming components due to their relative low cost and green character, in addition to their compatibility with the components of cheese whey. As the first and a highly important action, in this chapter the initial characterization of the ATPS through the determination of the liquid-liquid equilibrium involved will be carried out. The binodal curve and tie-lines ends, consequently TLL, comprise the most important system properties. The influence of the temperature on these parameters will also be considered. Moreover, as the determination of physical properties (density and refractive index) will be used as a method of analysis, these properties for aqueous solutions of polymers and salts will be determined. Knowledge of these properties, especially density, is of high interest for the design of processes where these phase-forming components are involved.

3.2. MATERIAL AND METHODS

3.2.1. Chemicals

Polyethylene glycols: PEG 1500 (BioUltra 1500), PEG 4000 (Bio Ultra 4000), PEG 8000 (PhEur 8000) were obtained from Sigma, whilst PEG 600 (synthesis grade) was purchased from Merck. Solid polymers (PEG 1500, 4000 and 8000) were dried for at least 24 h at 40 ºC in order to eliminate adsorbed water. Stock solutions with appropriate concentration were prepared in distilled water for all polymers.

Poly (ethylene glycol-ran-propylene-glycol) monobutyl ether, known as UCON (commercial name used by Dow Chemical), was purchased from Sigma. This chemical is a random copolymer composed of 50 % wt ethylene glycol and 50 % wt propylene glycol with an average molecular mass of 3900.

Sodium sulfate (Na_2SO_4, ACS Reagent, ≥99.0 %, anhydrous, granular), ammonium sulfate ($(NH_4)_2SO_4$, for molecular biology, ≥99.0 %) and potassium sulfate (K_2SO_4 ACS Reagent, ≥99.4 %) were obtained from Sigma. These salts were dried for at least 24 h at 140 ºC in order to eliminate adsorbed water. The organic salt potassium tartrate dibasic hemihydrate ($C_4H_4K_2O_6 \cdot 0.5H_2O$) was also purchased from Sigma and dried for at least 24 h at 60 ºC in order to eliminate adsorbed water.

Distilled water was used in the preparation of all stock solutions and dilutions needed.

3.2.2. Methods

3.2.2.1. Physical properties

To obtain a reliable and precise method of composition analysis, physical properties were used in this work. In the case of salt + water binary mixtures calibration curves were obtained by measuring, at 298.15 K and atmospheric pressure, the density of aqueous samples ranging from 0 to 10 wt % of salt. In the case of polymer + salt + water systems, two properties (density and refractive index) were required. Homogeneous ternary mixtures with total compositions ranging from 0 to 10 wt % (polymer + salt) were used for calibration curves also determined at 298.15 K and atmospheric pressure. At least two measurements for each physical property were carried out, ensuring that the results obtained were replicated within the expected uncertainty.

All weighting was carried out on a Mettler Toledo balance model XPE205 (Figure 3.1), with precision of 0.01 mg. In the case of the salt potassium tartrate, the

water content of the salt was considered to calculate the final water content of the mixture.

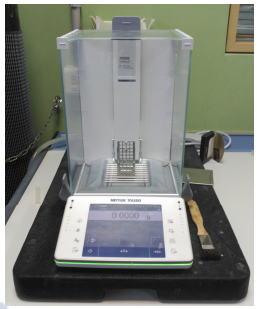

Figure 3.1. Analytical balance

Density was measured using an Anton Paar DSA-48 densimeter with internal control of temperature and automatic correction of the viscosity influence on the density (Figure 3.2). The precision on density measurement is 10^{-4} g/cm^3. This instrument is based on a glass cell (Duran 50) consisting of a U-shaped oscillator inserted into a glass cover. The U-tube is electronically excited and oscillates at a characteristic frequency that depends on the density of the filled sample. Calibration was carried out with air and water.

Figure 3.2. Densimeter

For the density measurement, 2 mL of sample were slowly injected with a syringe into the measurement cell to ensure that air bubbles, which prevent apparatus stabilization and suitable property measurement, were not generated.

Refractive indices were measured with an ATAGO RX-5000 refractometer (Figure 3.3), with a precision of 10^{-5}, which has a digital thermometer incorporated with a precision of 0.1 °C. The instrument consists of a prism of sapphire, located in the bottom of a deposit of stainless steel of conical form, protected by an acrylic cover. To measure the refractive index a collimated light strikes the prism surface and the liquid sample. Calibration was carried out with water.

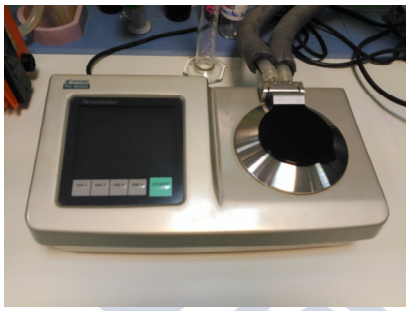

Figure 3.3. Refractometer

The temperature was maintained at the desired value using a thermostatic bath, a Julabo F 12–ED (Figure 3.4) with a precision of 0.1 °C. For the refractive index measurement, approximately two drops of sample are placed on the prism screen allowing the liquid to spread across the entire surface of the prism without air bubbles or dry spots.

Figure 3.4. Thermostatic bath

3.2.2.2. Solubility

Salt solubilities at several temperatures were measured, for some cases of particular interest or when data were not available in Literature, using a glass solubility cell (Figure 3.5) thermostated with a Julabo F 12–ED (Figure 3.4). Water and salt in excess were added into the solubility cell and the solution was agitated with a magnetic stirrer for 5 h and allowed to settle for 24 h. Preliminary tests showed that times for agitation and sedimentation were sufficient to attain equilibrium and achieve a good separation of the phases. The excess salt deposited in the bottom of the cell and a sample from the supernatant phase were withdrawn for composition analysis. The liquid sample was appropriately diluted for compositional analysis using a density calibration curve prepared in the range of compositions explained in section 3.2.2.1. At least two samples of the liquid phase were analyzed, ensuring that the compositions obtained from density measurement were replicated within the expected uncertainty.

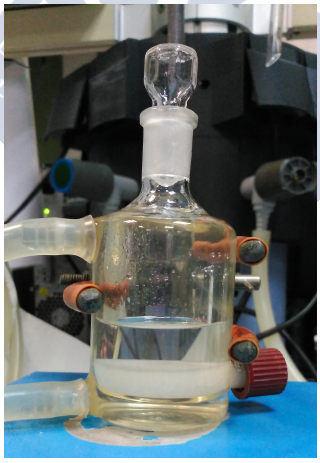

Figure 3.5. Solubility cell

3.2.2.3. Phase equilibrium

Tie-lines were determined experimentally at 278.15, 293.15 and 308.15 K using jacketed liquid-liquid equilibrium cells made of glass (Figure 3.6). The cell jacket was connected to a thermostatic bath Julabo F 12–ED for temperature control.

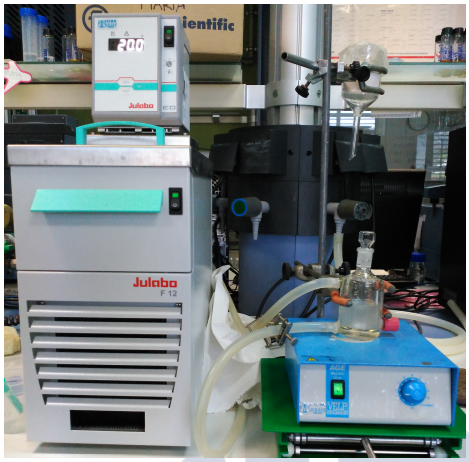

Figure 3.6. Experimental set-up for tie-lines determination

Suitable amounts of each stock solution (polymer and salt) and distilled water were added to the equilibrium cell to obtain mixtures of different compositions in the heterogeneous region of the phase diagram. The system was agitated 30 min using a magnetic stirrer, and then allowed to settle during 24 h until the two equilibrium phases were completely clear and separated. Preliminary tests showed that times for agitation and sedimentation were sufficient to attain equilibrium and achieve a good separation of the phases. Then, samples from the top and bottom phases were taken with plastic syringes and diluted appropriately for compositional analysis using density and refractive index calibration curves. At least two samples of equilibrium phases were measured, ensuring that the compositions obtained from density and refractive index measurements were replicated within the expected uncertainty.

3.3. RESULTS AND DISCUSSION

3.3.1. Physical properties

The densities and refractive indices, at 298.15 K and atmospheric pressure, of aqueous solutions of the salts used in this work (sodium, potassium and ammonium sulfate, and potassium tartrate) are shown in Table 3.1.

Table 3.1. Density and refractive index of salt + water binary mixtures at 298.15 k and 0.1 MPa

Composition (mass fraction)	Density ($g \cdot cm^{-3}$)	Refractive index	Composition (mass fraction)	Density ($g \cdot cm^{-3}$)	Refractive index
Sodium Sulfate			Ammonium Sulfate		
0.0005	0.9976	1.33258	0.0005	0.9974	1.33259
0.0011	0.9981	1.33266	0.0011	0.9977	1.33268
0.0053	1.0020	1.33331	0.0053	1.0003	1.33337
0.0108	1.0069	1.33414	0.0104	1.0033	1.33425
0.0214	1.0165	1.33570	0.0208	1.0094	1.33594
0.0420	1.0351	1.33875	0.0412	1.0212	1.33921
0.0719	1.0626	1.34307	0.0712	1.0384	1.34393
0.0994	1.0885	1.34535	0.1007	1.0553	1.34856
Potassium Sulfate			Potassium tartrate		
0.0005	0.9974	1.33257	0.0013	0.9979	1.33268
0.0009	0.9978	1.33262	0.0068	1.0015	1.33345
0.0050	1.0011	1.33310	0.0137	1.0060	1.33443
0.0098	1.0049	1.33368	0.0271	1.0148	1.33634
0.0196	1.0127	1.33487	0.0536	1.0323	1.34008
0.0401	1.0293	1.33731	0.0795	1.0497	1.34377
0.0704	1.0542	1.34086	0.1038	1.0665	1.34730
0.0986	1.0779	1.34418	0.1277	1.0832	1.35081

$u(w)$=0.0002. $u(P)$=5 kPa. For density measurements: $u(T)$ = 0.1 K, $u(\rho)$ = 0.0001 g/cm^3. For refractive index measurements: $u(T)$ = 0.05 K, $u(n_D)$= 0.00004.

As densities of aqueous solutions of sodium sulfate and potassium tartrate are used for compositional analysis in the measurements of solubilities, those experimental data were fitted to polynomial expansions up to order 2 by least-squares:

$$z = a + b \cdot w_S + c \cdot w_S^2 \qquad 3.1$$

where Z is density and w_S are the mass fractions of salt, and *a, b,* and *c* are fitting parameters. Correlation parameters and average arithmetic relative deviations (AARD) of the fits are shown in Table 3.2. Experimental, correlated and comparative data found in Literature [57-59] are shown in Figure 3.7.

Table 3.2. Fitting of the density data of salt aqueous solutions to Equation 3.1

Fitting parameters			AARD*
a	b	c	
Sodium sulfate aqueous solution			
0.9970	0.9166	-	0.0002
Potassium tartrate aqueous solution			
-2.1876	2.8644	-0.6718	0.0005

* Average arithmetic relative deviation, $AARD = (\sum|(Exptl - Calc)/Exptl|)/N$

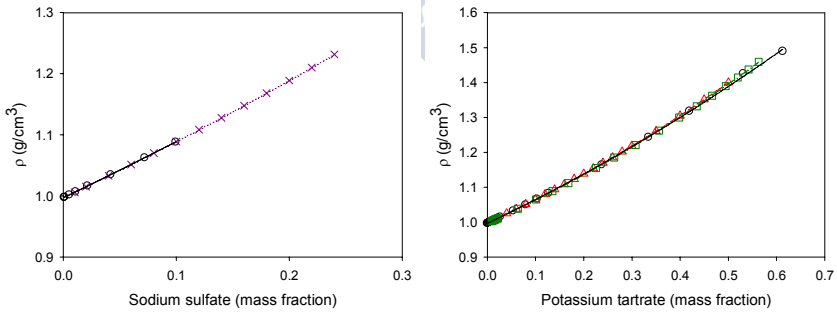

Figure 3.7. Density of potassium tartrate aqueous solution: —o— this work, ···x··· [57] , -·-□-·- [58], --Δ-- [59] (293.15 K)

The densities and refractive indices, at 298.15 K and atmospheric pressure, of aqueous solutions of the polymers used in this work (PEG 600, 1500, 4000, 8000, and UCON) are shown in Table 3.3.

Table 3.3. Density and refractive index of polymer + water binary mixtures at 298.15 k and 0.1 MPa

Composition (mass fraction)	Density ($g \cdot cm^{-3}$)	Refractive index	Composition (mass fraction)	Density ($g \cdot cm^{-3}$)	Refractive index
PEG 600			PEG 1500		
0.0010	0.9972	1.33263	0.0010	0.9972	1.33276
0.0053	0.9979	1.33318	0.0054	0.9977	1.33321
0.0107	0.9987	1.33388	0.0107	0.9987	1.33392
0.0214	1.0004	1.33525	0.0215	1.0028	1.33531
0.0426	1.0038	1.33801	0.0430	1.0040	1.33819
0.0636	1.0072	1.34079	0.0638	1.0074	1.34099
0.0842	1.0106	1.34354	0.0842	1.0109	1.34378
0.1029	1.0136	1.34603	0.1054	1.0143	1.34667
PEG 4000			PEG 8000		
0.0010	0.9972	1.33262	0.0005	0.9972	1.33256
0.0057	0.9980	1.33325	0.0010	0.9973	1.33263
0.0112	0.9989	1.33399	0.0048	0.9979	1.33314
0.0221	1.0007	1.33544	0.0101	0.9988	1.33386
0.0430	1.0041	1.33828	0.0234	1.0009	1.33564
0.0710	1.0088	1.34211	0.0406	1.0038	1.33789
0.0860	1.0113	1.34421	0.0702	1.0087	1.34201
1.0000	1.0148	1.34702	0.0989	1.0136	1.34602
UCON					
0.0005	0.9971	1.33282			
0.0010	0.9970	1.33263			
0.0050	0.9975	1.33316			
0.0100	0.9980	1.33387			
0.0184	0.9987	1.33464			
0.0394	1.0016	1.33782			
0.0994	1.0090	1.34615			

$u(w)$=0.0002. $u(P)$=5 kPa. For density measurements: $u(T)$ = 0.1 K, $u(\rho)$ = 0.0001 g/cm^3. For refractive index measurements: $u(T)$ = 0.05 K, $u(n_D)$= 0.00004.

The densities and refractive indices, at 298.15 K and atmospheric pressure, of polymer + salt + water ternary systems are shown in Table 3.4 to Table 3.7.

Table 3.4. Density and refractive index of polymer + sodium sulfate + water ternary mixtures at 298.15 k and 0.1 MPa

Polymer composition (mass fraction)	Salt composition (mass fraction)	Density (g·cm^{-3})	Refractive index
PEG 4000 + Sodium Sulfate + Water			
0.0121	0.0538	1.0179	1.34152
0.0197	0.0864	1.0797	1.34802
0.0254	0.0405	1.038	1.34204
0.0392	0.0272	1.0283	1.34197
0.0419	0.0655	1.0640	1.34807
0.0509	0.0137	1.0179	1.34152
0.0627	0.0445	1.0481	1.34799
0.0843	0.0227	1.0319	1.34758
PEG 8000 + Sodium Sulfate + Water			
0.0140	0.0629	1.0558	1.34359
0.0219	0.0810	1.0748	1.34754
0.0291	0.0312	1.0301	1.34121
0.0386	0.0413	1.0404	1.34389
0.0386	0.0616	1.0596	1.34700
0.0545	0.0109	1.0158	1.34157
0.0630	0.0245	1.0446	1.34735
0.0827	0.0216	1.0306	1.34723
UCON + Sodium Sulfate + Water			
0.0036	0.0592	1.0510	1.34170
0.0129	0.0501	1.0438	1.34172
0.0242	0.0350	1.0316	1.34111
0.0254	0.0460	1.0416	1.34286
0.0351	0.0240	1.0229	1.34098
0.0501	0.0125	1.0145	1.34138
0.0671	0.0386	1.0403	1.34777
0.0775	0.0220	1.0266	1.34672

$u(w)$=0.0002. $u(P)$=5 kPa. For density measurements: $u(T)$ = 0.1 K, $u(\rho)$ = 0.0001 g/cm^3. For refractive index measurements: $u(T)$ = 0.05 K, $u(n_D)$= 0.00004.

Table 3.5. Density and refractive index of polymer + ammonium sulfate + water ternary mixtures at 298.15 k and 0.1 MPa

Polymer composition (mass fraction)	Salt composition (mass fraction)	Density (g·cm^{-3})	Refractive index
PEG 1500 + Ammonium Sulfate + Water			
0.0127	0.0533	1.0303	1.34285
0.0204	0.0930	1.0544	1.35061
0.0253	0.0428	1.0263	1.34288
0.0390	0.0294	1.0208	1.34259
0.0421	0.0710	1.0454	1.34985
0.0523	0.0148	1.0144	1.34215
0.0624	0.0469	1.0349	1.34930
0.0837	0.0235	1.0248	1.34780
PEG 4000 + Ammonium Sulfate + Water			
0.0123	0.0563	1.0322	1.34336
0.0209	0.0917	1.0541	1.35018
0.0247	0.0429	1.0265	1.34294
0.0395	0.0285	1.0205	1.34430
0.0412	0.0702	1.0405	1.34958
0.0505	0.0141	1.0138	1.34171
0.0637	0.0472	1.0355	1.34904
0.0841	0.0239	1.0252	1.34807
PEG 8000 + Ammonium Sulfate + Water			
0.0199	0.0897	1.0525	1.34960
0.0258	0.0566	1.0345	1.34521
0.0298	0.0230	1.0156	1.34032
0.0403	0.0287	1.0208	1.34266
0.0419	0.0670	1.0432	1.34907
0.0426	0.0447	1.0304	1.34562
0.0640	0.0451	1.0343	1.34881
0.0849	0.0228	1.0248	1.34810

Table 3.5. Continuation

Polymer composition (mass fraction)	Salt composition (mass fraction)	Density ($g \cdot cm^{-3}$)	Refractive index
UCON + Ammonium Sulfate + Water			
0.0083	0.0751	1.0408	1.34545
0.0101	0.0575	1.0310	1.34306
0.0239	0.0430	1.0245	1.34269
0.0317	0.0640	1.0374	1.34655
0.0361	0.0288	1.0179	1.34215
0.0466	0.0146	1.0112	1.34132
0.0596	0.0482	1.0320	1.34858
0.0752	0.0248	1.0206	1.34705

u(w)=0.0002. *u(P)*=5 kPa. For density measurements: $u(T)$ = 0.1 K, $u(\rho)$ = 0.0001 g/cm^3. For refractive index measurements: $u(T)$ = 0.05 K, $u(n_D)$= 0.00004.

Table 3.6. Density and refractive index of UCON + potassium sulfate + water ternary mixtures at 298.15 k and 0.1 MPa

Polymer composition (mass fraction)	Salt composition (mass fraction)	Density ($g \cdot cm^{-3}$)	Refractive index
0.0107	0.0475	1.0368	1.33948
0.0111	0.0645	1.0507	1.34183
0.0247	0.0355	1.0290	1.34015
0.0344	0.0232	1.0202	1.34006
0.0401	0.0582	1.0493	1.34527
0.0439	0.0118	1.0123	1.34000
0.0586	0.0406	1.0373	1.34582
0.0801	0.0197	1.0230	1.34625

u(w)=0.0002. *u(P)*=5 kPa. For density measurements: $u(T)$ = 0.1 K, $u(\rho)$ = 0.0001 g/cm^3. For refractive index measurements: $u(T)$ = 0.05 K, $u(n_D)$= 0.00004.

Table 3.7. Density and refractive index of polymer + potassium tartrate + water ternary mixtures at 298.15 k and 0.1 MPa

Polymer composition (mass fraction)	Salt composition (mass fraction)	Density ($g \cdot cm^{-3}$)	Refractive index
PEG 600 + Potassium tartrate + Water			
0.0124	0.0641	1.0414	1.34329
0.0202	0.1049	1.0706	1.35026
0.0248	0.0495	1.0336	1.34281
0.0375	0.0330	1.0247	1.34213
0.0421	0.0830	1.0567	1.34934
0.0504	0.0169	1.0162	1.34152
0.0617	0.0539	1.0427	1.34844
0.0831	0.0272	1.0284	1.34740
PEG 1500 + Potassium tartrate + Water			
0.0124	0.0641	1.0411	1.34323
0.0202	0.1036	1.0697	1.35014
0.0249	0.0480	1.0327	1.34287
0.0377	0.0324	1.0245	1.34219
0.0408	0.0784	1.0559	1.34929
0.0507	0.0162	1.0159	1.34161
0.0619	0.0530	1.0423	1.34855
0.0828	0.0266	1.0282	1.34756

u(w)=0.0002. *u(P)*=5 kPa. For density measurements: $u(T)$ = 0.1 K, $u(\rho)$ = 0.0001 g/cm^3. For refractive index measurements: $u(T)$ = 0.05 K, $u(n_D)$= 0.00004.

Experimental data were fitted to polynomial expansions up to order 2 by least-squares:

$$z = a + b \cdot w_P + c \cdot w_S + d \cdot w_P^2 + e \cdot w_S^2 + f \cdot w_P \cdot w_S \qquad 3.2$$

where Z is the physical property (density or refractive index), w_P and w_S are the mass fractions of polymer and salt, respectively, and *a, b, c, d, e* and *f* are fitting

parameters. Correlation parameters and average arithmetic relative deviations (AARD) of the fits are shown in Table 3.8 and Table 3.9 respectively.

Table 3.8. Fitting of the density data of the ternary systems to Equation 3.2

Fitting Parameters						AARD*
a	b	c	d	e	f	
PEG 4000 + Sodium Sulfate + Water						
0.9971	$8.973 \cdot 10^{-3}$	$1.528 \cdot 10^{-3}$	$2.190 \cdot 10^{-5}$	$1.894 \cdot 10^{-5}$	$1.277 \cdot 10^{-5}$	0.0001
PEG 8000 + Sodium Sulfate + Water						
0.9970	$9.060 \cdot 10^{-3}$	$1.808 \cdot 10^{-3}$	$-3.418 \cdot 10^{-6}$	$3.241 \cdot 10^{-7}$	$9.562 \cdot 10^{-5}$	0.001
UCON + Sodium Sulfate + Water						
0.9969	0.9139	0.1206	-	-	-	0.0002
UCON + Potassium Sulfate + Water						
0.9968	0.8171	0.1234	-	-	-	0.0002
PEG 1500 + Ammonium Sulfate + Water						
0.9973	0.5787	0.1632	-	-	-	0.0002
PEG 4000 + Ammonium Sulfate + Water						
0.9970	$6.009 \cdot 10^{-3}$	$1.570 \cdot 10^{-3}$	-	-	-	0.001
PEG 8000 + Ammonium Sulfate + Water						
0.9971	$5.914 \cdot 10^{-3}$	$1.628 \cdot 10^{-3}$	$-1.402 \cdot 10^{-5}$	$3.660 \cdot 10^{-6}$	$8.271 \cdot 10^{-6}$	0.00004
UCON + Ammonium Sulfate + Water						
0.9970	0.5766	0.1196	-	-	-	0.0005
PEG 600 + Potassium Tartrate + Water						
0.9970	0.6655	0.1584	-	-	-	0.00001
PEG 1500 + Potassium Tartrate + Water						
0.9971	0.6662	0.1627	-	-	-	0.00001

* Average arithmetic relative deviation, $AARD = (\sum|(Exptl - Calc)/Exptl|)/N$

Table 3.9. Fitting of the refractive index data of the ternary systems to Equation 3.2

Fitting Parameters						AARD*
a	b	c	d	e	f	
PEG 4000 + Sodium Sulfate + Water						
1.33249	$1.60205 \cdot 10^{-3}$	$1.27211 \cdot 10^{-3}$	$-2.45362 \cdot 10^{-5}$	$1.30337 \cdot 10^{-5}$	$1.81954 \cdot 10^{-5}$	0.0001
PEG 8000 + Sodium Sulfate + Water						
1.33246	$1.64323 \cdot 10^{-3}$	$1.36100 \cdot 10^{-3}$	$-3.26668 \cdot 10^{-5}$	$1.64412 \cdot 10^{-6}$	$3.31153 \cdot 10^{-5}$	0.0002
UCON + Sodium Sulfate + Water						
1.33248	0.168037	0.129612	-0.368377	$8.32911 \cdot 10^{-2}$	$9.98049 \cdot 10^{-2}$	0.0001
UCON + Potassium Sulfate + Water						
1.33244	0.120246	0.139296	-	-	-	0.0002
PEG 1500 + Ammonium Sulfate + Water						
1.33263	0.161683	0.134631	-	-	-	0.0002
PEG 4000 + Ammonium Sulfate + Water						
1.33229	$1.75243 \cdot 10^{-3}$	$1.21736 \cdot 10^{-3}$	-	-	-	0.0006
PEG 8000 + Ammonium Sulfate + Water						
1.33251	$1.65215 \cdot 10^{-3}$	$1.33095 \cdot 10^{-3}$	$-6.37422 \cdot 10^{-6}$	$4.22663 \cdot 10^{-6}$	$7.34704 \cdot 10^{-6}$	0.00002
UCON + Ammonium Sulfate + Water						
1.33252	0.16480	0.12937	$-7.28588 \cdot 10^{-2}$	$9.37889 \cdot 10^{-2}$	$2.70138 \cdot 10^{-2}$	0.0002
PEG 600 + Potassium Tartrate + Water						
1.33248	0.142621	0.131442	-	-	-	0.000001
PEG 1500 + Potassium Tartrate + Water						
1.33247	0.143401	0.135037				0.000002

* Average arithmetic relative deviation, $AARD = (\sum|(Exptl - Calc)/Exptl|)/N$

3.3.2. Solubility

The formulation of an ATPS requires salt solubility higher than the critical concentration needed for phase splitting into two immiscible phases. For many salts, this is not possible because the low temperatures needed for the application cause salt precipitation.

In order to check whether the solubility of sodium sulfate in water was too low to produce phase splitting in a concentration range of practical interest, solubility measurements at atmospheric pressure and 278.15, 283.15 and 293.15 K were carried out (see Table 3.10). Results obtained are presented in Figure 3.8a together with available data from literature [60-62]. Our data, in excellent agreement with those previously published, show that solubility of sodium sulfate is low and drastically decreases with decreasing temperature (5.88 % wt at 278.15 K). Such a low solubility of the salt prevents the use of ATPS with sodium sulfate at low temperatures (salt solubility is lower than the critical composition needed for ATPS formation). Thus, in this work, studies about ATPS containing sodium sulfate will not be carried out at 278.15 K.

Table 3.10. Sodium sulfate solubility as a function of temperature

Temperature (K)	Solubility (wt)
278.15	0.059
283.15	0.082
293.15	0.156

Solubility of potassium tartrate was measured from 278.15 to 323.15 K (see Table 3.11) and the results are shown in Figure 3.8b. As expected, solubility of the salt increases with increasing temperature and this increase is more pronounced at elevated temperatures. It is important to note that high solubility (>57 % wt) is obtained even at low temperatures.

Table 3.11. Potassium tartrate solubility as a function of temperature

Temperature (K)	Solubility (wt)
278.15	0.575
283.15	0.578
288.15	0.582
293.15	0.585
298.15	0.589
303.15	0.595
308.15	0,599
313.15	0.603
318.15	0.608
323.15	0.613

Comparison of solubility curves in Figure 3.8 shows that potassium tartrate presents a significantly higher solubility than sodium sulfate. This fact allows the use of this tartrate salt to form ATPS at very low temperatures. As another advantage of potassium tartrate, in the range of temperatures studied, the solubility increases with temperature, whereas for sodium sulfate at approximately 310 K solubility goes down likely due to the change in the hydration of the molecule.

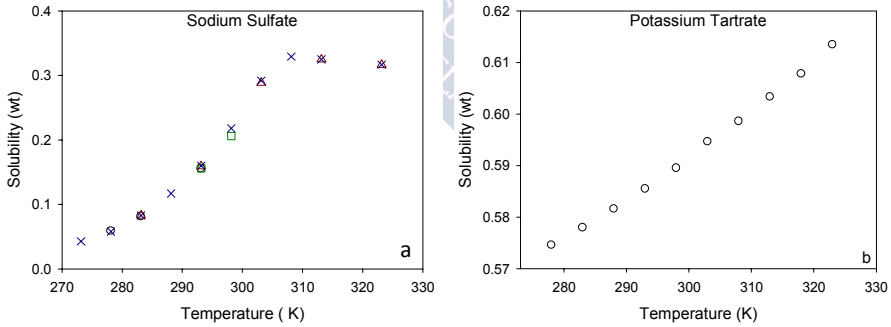

Figure 3.8. Solubility as function of temperature. This work (o); Okorafor (Δ) [61]; Brenner (□) [60]; Ullmann's (×) [62]

3.3.3. Phase equilibrium

Liquid-liquid equilibrium data for ATPS formed with sodium sulfate and PEG 4000, PEG 8000 and UCON at 293.15 K and 308.15 K and atmospheric pressure are presented in Table 3.12 to Table 3.14 and Figure 3.9 to Figure 3.11.

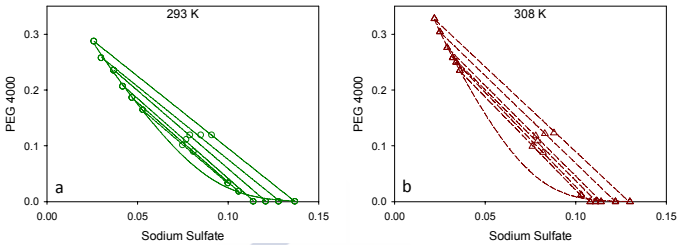

Figure 3.9. Binodal curve and tie-lines for PEG 4000/Sodium sulfate ATPS at (a) —□— 293.15 K and (b) ---Δ--- 308.15 K

Table 3.12. Experimental composition (mass fraction) of the equilibrium phases, together with the corresponding TLL and STL for PEG 4000/Sodium sulfate ATPS at 293.15 and 308.15 K and 0.1 MPa

Feed		Top Phase		Bottom Phase		TLL	STL
PEG	Salt	PEG	Salt	PEG	Salt		
			293.15 K				
0.119	0.091	0.287	0.026	0.000	0.137	0.31	-2.58
0.119	0.085	0.257	0.030	0.000	0.128	0.27	-2.64
0.119	0.079	0.235	0.037	0.000	0.121	0.25	-2.79
0.111	0.077	0.206	0.042	0.000	0.114	0.22	-2.88
0.089	0.081	0.186	0.047	0.018	0.106	0.12	-2.85
0.101	0.075	0.164	0.053	0.033	0.100	0.14	-2.81
			308.15 K				
0.123	0.088	0.328	0.022	0.000	0.130	0.34	-3.05
0.122	0.083	0.304	0.025	0.000	0.122	0.32	-3.13
0.118	0.078	0.276	0.029	0.000	0.114	0.28	-3.24
0.109	0.079	0.258	0.032	0.000	0.111	0.27	-3.28
0.088	0.082	0.250	0.034	0.000	0.108	0.26	-3.34
0.099	0.076	0.235	0.036	0.012	0.103	0.23	-3.34

$u(w_i^{feed}) < 0.001$; $u(w_i^{top\ phase}) = 0.002$; $u(w_i^{bottom\ phase}) = 0.001$; $u(P) = 5$ kPa; $u(T) = 0.05$ K.

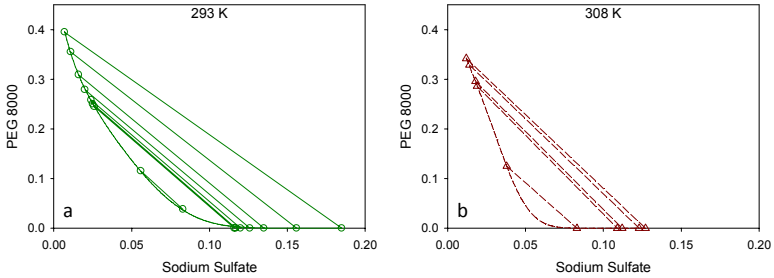

Figure 3.10. Binodal curve and tie-lines for PEG 8000/Sodium sulfate ATPS at (a)—□— 293.15 K and (b) ---Δ--- 308.15 K

Table 3.13. Experimental composition (mass fraction) of the equilibrium phases, together with the corresponding TLL and STL for PEG 8000/Sodium sulfate ATPS at 293.15 and 308.15 K and 0.1 MPa

Top Phase		Bottom Phase		TLL	STL
PEG	Salt	PEG	Salt		
		293.15 K			
0.395	0.007	0.000	0.185	0.43	-2.23
0.355	0.011	0.000	0.156	0.38	-2.41
0.309	0.016	0.000	0.135	0.33	-2.59
0.279	0.020	0.000	0.126	0.30	-2.63
0.258	0.024	0.000	0.120	0.27	-2.70
0.250	0.025	0.000	0.117	0.27	-2.73
0.245	0.026	0.000	0.116	0.26	-2.72
0.115	0.056	0.038	0.083	0.08	-2.85
		308.15 K			
0.342	0.012	0.000	0.127	0.36	-2.97
0.329	0.014	0.000	0.123	0.35	-3.01
0.296	0.018	0.000	0.112	0.31	-3.17
0.286	0.019	0.000	0.109	0.30	-3.16
0.125	0.038	0.000	0.083	0.13	-2.82

$u(w_i)$ = 0.003; $u(P)$ = 5 kPa; $u(T)$ = 0.05 K.

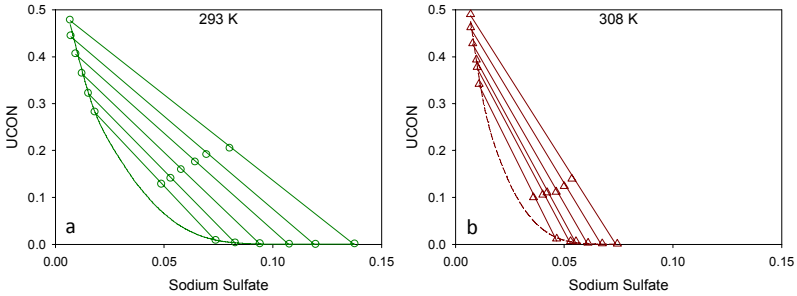

Figure 3.11. Binodal curve and tie-lines for UCON/Sodium sulfate ATPS at (a) —□— 293.15 K and (b) ---Δ--- 308.15 K

Table 3.14. Experimental composition (mass fraction) of the equilibrium phases, together with the corresponding TLL and STL for UCON/Sodium sulfate ATPS at 293.15 and 308.15 K and 0.1 MPa

Feed		Top Phase		Bottom Phase		TLL	STL
UCON	Salt	UCON	Salt	UCON	Salt		
			293.15 K				
0.205	0.080	0.476	0.007	0.002	0.138	0.49	-3.64
0.191	0.070	0.442	0.008	0.003	0.119	0.45	-3.93
0.176	0.064	0.404	0.010	0.003	0.107	0.41	-4.11
0.159	0.058	0.363	0.012	0.005	0.094	0.37	-4.41
0.141	0.053	0.321	0.015	0.007	0.082	0.32	-4.69
0.128	0.049	0.282	0.018	0.012	0.073	0.28	-4.90
			308.15 K				
0.140	0.054	0.488	0.007	0.005	0.074	0.49	-7.29
0.124	0.050	0.463	0.007	0.006	0.067	0.46	-7.26
0.112	0.046	0.427	0.008	0.006	0.061	0.42	-8.07
0.110	0.042	0.009	0.055	0.394	0.010	0.39	-8.52
0.106	0.040	0.010	0.052	0.378	0.010	0.37	-8.72
0.100	0.036	0.015	0.046	0.340	0.011	0.33	-9.35

$u(w_i^{UCON}) = 0.002$; $u(w_i^{Salt}) = 0.001$; $u(P) = 5$ kPa; $u(T) = 0.05$ K.

According to the results shown in section 3.3.2, systems containing sodium sulfate were not studied at 278.15 K due to that low temperature causes the

precipitation of the salt. Surprisingly, the system was found published in the literature [63]. We believe that data there presented cannot been confident.

The phase diagram for PEG 4000 + sodium sulfate + water ATPS has been determined by Taboada *et al.* at 298.15 K [64] and by Carvalho *et al*. from 278.15 to 318.15 K [65] (see Figure 3.12a). Data determined by these authors at 308.15 K are in good agreement with ours. For PEG 8000 + sodium sulfate + water ATPS, Rodríguez *et al.* [42] determined the phase diagram at 296.15 K, while Snyder *et al.* [63] reported data at 298.15 K (see Figure 3.12b). Regarding the data comparison, there are some small differences in the working temperatures between previously published data and ours, but these differences are not expected to be relevant on the phase diagrams. There is good agreement with data from [42] in the top phase and the slope of the tie-lines, but there are differences for the bottom phase compositions. In reference [42], compositions were obtained combining the binodal curve by cloud-point method with salt analysis by flame atomic absorption spectroscopy. The use of a visual method and different method of analysis are likely the reasons for the differences. There is good agreement with data from [63] for the bottom phase, but there are important differences in the top phase. Phase compositions were obtained by analysis of the equilibrium phases using HPLC, while in this work the analysis was carried out by measurement of physical properties.

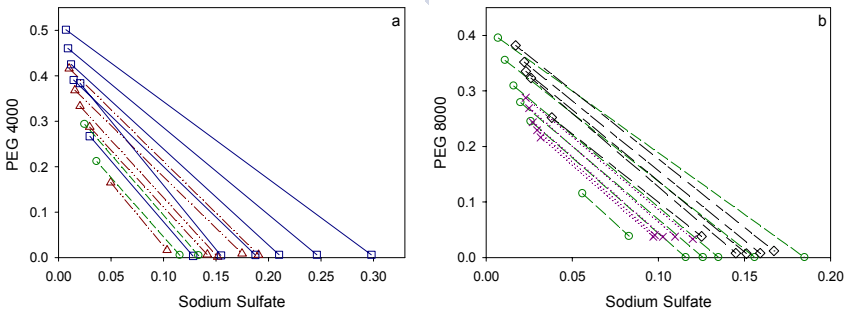

Figure 3.12. PEG/Sodium sulfate ATPS. Comparison of experimental and bibliographic data. This work (--o--), Taboada *et al*. [64] (—□—), Carvalho *et al*. [65] (···Δ···), Rodríguez *et al*. [42] (···×···), Snyder *et al*. [63] (-—◇-—)

Data obtained in this work for the system with UCON and sodium sulfate at 298.15 K are in good agreement with the data reported by Silvério *et al.* [66] at 296.15 K. Results obtained in this work increase the composition range covered in the phase diagram determined by those authors (Figure 3.13).

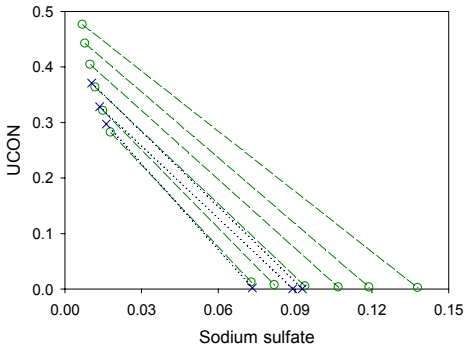

Figure 3.13. UCON/Sodium sulfate ATPS. Comparison of experimental and bibliographic data. This work (--o--), Silvério *et al*. [66] (···×···)

The phase diagrams obtained (see Figure 3.9 to Figure 3.11) present a large heterogeneous region. Comparison of these phase diagrams shows up that, in general, temperature increases the TLL (size of the heterogeneous region). Moreover, the STL significantly increases (more negative slope) when increasing the temperature. This means that changing the temperature affects the equilibrium compositions: increases the polymer content in the top phase and reduces the salt content in the bottom phase. For systems formulated with UCON, a phase inversion was found at the highest temperature. In general the top phase is enriched in polymer whilst the bottom phase is enriched in salt. In this case, since the temperature effect is to increase the polymer composition in polymer-rich phase while reducing the salt concentration in the salt-rich phase, at some temperature the density of the salt-rich phase becomes smaller than that of polymer-rich phase. In order to calculate STL, in this work T always refers to the polymer-rich phase (in general in the top) and B always refers to the salt-rich phase (generally in the bottom). This phase inversion produces an important increase in the STL thus calculated.

The influence of the PEG molecular weight on STL is small. However, TLL increases with PEG molecular mass, because a salting-out effect is produced and contents of polymer in the top phase and salt in the bottom phase increase. UCON has a molecular mass close to PEG 4000. However, both TLL and STL have higher values with UCON than with any PEG. This is due to the interactions caused by the mixing of polymers that allow a higher content of polymer in the phase enriched in this compound.

Liquid-liquid equilibrium data for ATPS formed with ammonium sulfate and PEG 1500 were determined at 298.15 K and atmospheric pressure. These data are presented in Table 3.15 and Figure 3.14. Systems with ammonium sulfate and PEG 4000, PEG 8000 and UCON were determined at 278, 15 K, 293.15 K and 308.15 K and atmospheric pressure. Data are presented in Table 3.16 to Table 3.18 and Figure 3.15 to Figure 3.17

The phase diagram for PEG 4000 + ammonium sulfate + water ATPS was found in Literature [67] only at 298.15 K. There is a small difference in the working temperature between previously published data and our data at 293.15 K, but these differences are not expected to be relevant on the phase diagrams. Comparing with our data at 293.15 K, there are certain differences in the vicinity of the critical region and also in the slope of tie-lines. The authors combined a titration method for ammonium sulfate with drying (evaporation) of water (gravimetric method) for the analysis of phase compositions. The direct analytical method used in this work is supposed to be more accurate than the determination of compositions by evaporation.

Equilibrium data for the systems PEG 8000 + ammonium sulfate + water and UCON + ammonium sulfate + water were also found in Literature [42, 63] but only at 298.15 K. Data show a good agreement with our results (at 293.15 K) which also increase the composition range studied in the phase diagram.

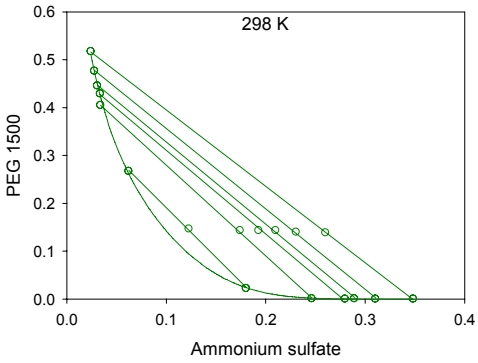

Figure 3.14. Binodal curve and tie-lines for PEG 1500/Ammonium sulfate ATPS at 298.15 K

Table 3.15. Experimental composition (mass fraction) of the equilibrium phases, together with the corresponding TLL and STL for PEG 1500/Ammonium sulfate ATPS at 298.15 K and 0.1 MPa

Feed		Top Phase		Bottom Phase		TLL	STL
PEG	Salt	PEG	Salt	PEG	Salt		
0.138	0.260	0.517	0.024	0.000	0.348	0.61	-1.60
0.140	0.231	0.476	0.028	0.000	0.311	0.55	-1.68
0.143	0.210	0.446	0.031	0.001	0.289	0.52	-1.72
0.143	0.193	0.428	0.034	0.000	0.280	0.49	-1.75
0.143	0.174	0.404	0.034	0.000	0.246	0.46	-1.90
0.146	0.123	0.267	0.062	0.022	0.181	0.27	-2.07

$u(w_{PEG}^{Top})$ =0.01; $u(w_{PEG}^{Bot})$ =0.0003; $u(w_{Salt}^{Top})$ =0.003; $u(w_{Salt}^{Bot})$ =0.002; $u(P)$ = 5 kPa; $u(T)$ = 0.05 K.

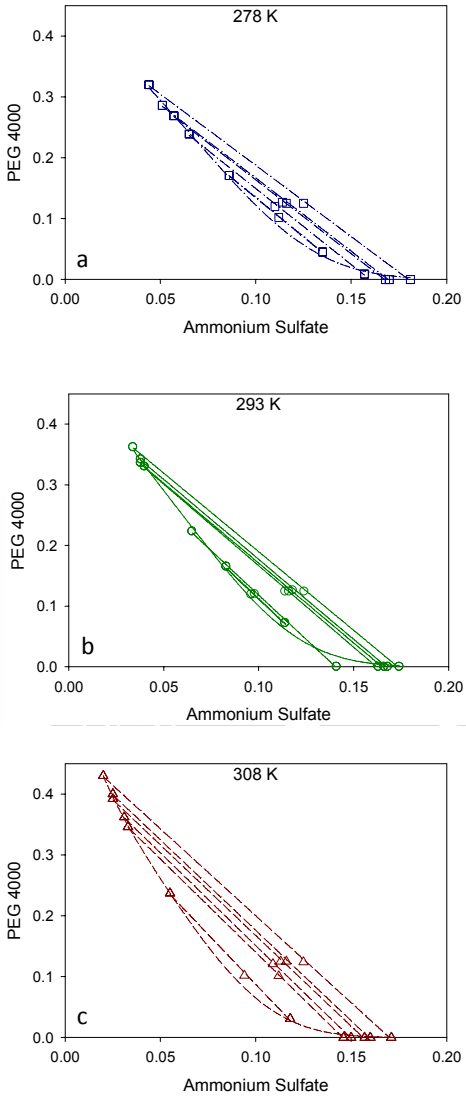

Figure 3.15. Binodal curve and tie-lines for PEG 4000/Ammonium sulfate ATPS at (a) -•-□-•- 278.15, (b) —□— 293.15 and (c) ---Δ--- 308.15 K

Table 3.16. Experimental composition (mass fraction) of the equilibrium phases, together with the corresponding TLL and STL for PEG 4000/Ammonium sulfate ATPS at 278.15, 293.15 and 308.15 K and 0.1 MPa

Feed		Top Phase		Bottom Phase		TLL	STL
PEG	Salt	PEG	Salt	PEG	Salt		
			278.15 K				
0.125	0.125	0.320	0.044	0.000	0.181	0.35	-2.35
0.125	0.116	0.286	0.051	0.000	0.170	0.31	-2.40
0.127	0.114	0.269	0.057	0.000	0.168	0.29	-2.42
0.120	0.110	0.239	0.065	0.009	0.157	0.25	-2.49
0.102	0.112	0.171	0.086	0.045	0.135	0.14	-2.57
			293.15 K				
0.124	0.124	0.362	0.034	0.000	0.174	0.39	-2.58
0.126	0.118	0.342	0.038	0.000	0.168	0.36	-2.64
0.124	0.116	0.336	0.038	0.000	0.166	0.36	-2.64
0.124	0.114	0.330	0.040	0.000	0.163	0.35	-2.68
0.120	0.098	0.223	0.065	0.000	0.141	0.35	-2.94
0.119	0.096	0.165	0.083	0.072	0.114	0.10	-2.92
			308.15 K				
0.124	0.125	0.430	0.020	0.000	0.171	0.46	-2.85
0.125	0.116	0.400	0.025	0.000	0.160	0.42	-2.96
0.125	0.113	0.392	0.025	0.000	0.157	0.41	-2.98
0.121	0.109	0.362	0.031	0.000	0.150	0.38	-3.06
0.101	0.112	0.346	0.033	0.000	0.146	0.26	-3.08
0.102	0.094	0.237	0.055	0.031	0.118	0.21	-3.28

$u(w_i^{feed}) < 0.001$; $u(w_i^{top\ phase}) = 0.01$; $u(w_i^{bottom\ phase}) = 0.001$; $u(P) = 5$ kPa; $u(T) = 0.05$ K.

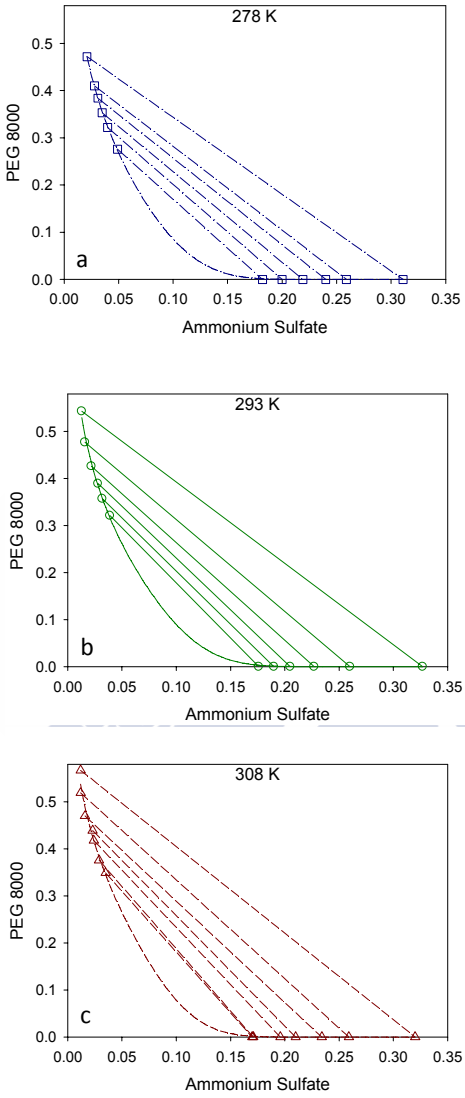

Figure 3.16. Binodal curve and tie-lines for PEG 8000/Ammonium sulfate ATPS at (a) -•-□-•- 278.15, (b) —□— 293.15 and (c) ---Δ--- 308.15 K

Table 3.17. Experimental composition (mass fraction) of the equilibrium phases, together with the corresponding TLL and STL for PEG 8000/Ammonium sulfate ATPS at 278.15, 293.15 and 308.15K and 0.1 MPa

Top Phase		Bottom Phase		TLL	STL
PEG	Salt	PEG	Salt		
		278.15 K			
0.472	0.021	0.000	0.311	0.55	-1.63
0.410	0.028	0.000	0.259	0.47	-1.77
0.384	0.031	0.000	0.240	0.44	-1.84
0.353	0.035	0.000	0.219	0.40	-1.91
0.322	0.040	0.000	0.200	0.36	-2.01
0.276	0.049	0.000	0.182	0.31	-2.07
		293.15 K			
0.543	0.013	0.000	0.327	0.63	-1.73
0.477	0.016	0.000	0.260	0.54	-1.96
0.426	0.022	0.000	0.227	0.47	-2.08
0.389	0.028	0.000	0.205	0.43	-2.19
0.357	0.032	0.000	0.190	0.39	-2.26
0.321	0.039	0.000	0.176	0.35	-2.33
		308.15 K			
0.567	0.012	0.000	0.320	0.64	-1.85
0.519	0.012	0.000	0.259	0.57	-2.10
0.470	0.016	0.000	0.234	0.52	-2.16
0.439	0.023	0.000	0.210	0.48	-2.35
0.418	0.024	0.000	0.196	0.45	-2.43
0.376	0.029	0.000	0.171	0.40	-2.63
0.349	0.035	0.000	0.170	0.37	-2.59

$u(w_i) = 0.001$; $u(P) = 5$ kPa; $u(T) = 0.05$ K.

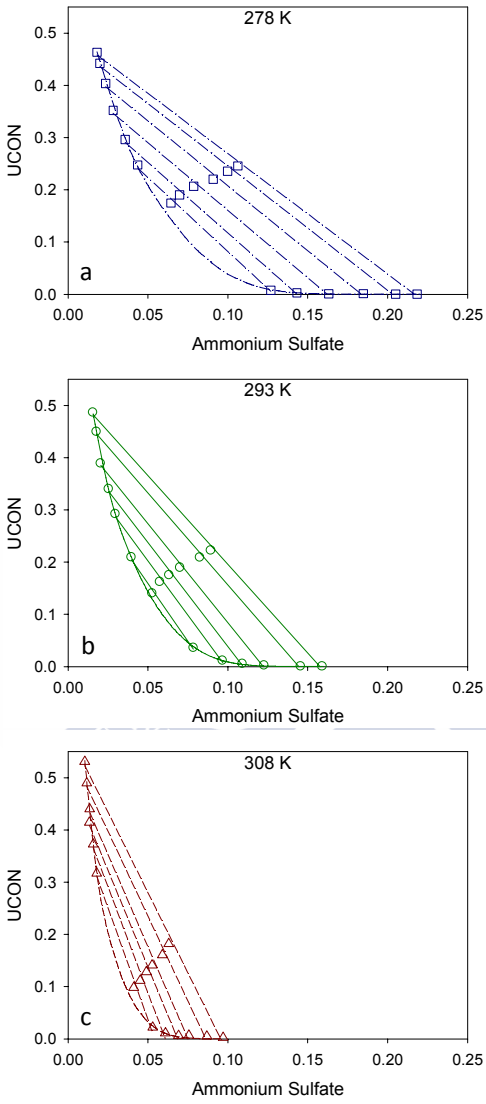

Figure 3.17. Binodal curve and tie-lines for UCON/Ammonium sulfate ATPS at (a) -•-□-•- 278.15, (b) —□— 293.15 and (c) ---Δ--- 308.15 K

Table 3.18. Experimental composition (mass fraction) of the equilibrium phases, together with the corresponding TLL and STL for UCON/Ammonium sulfate ATPS at 278.15, 293.15 and 308.15K and 0.1 MPa

Feed		Top Phase		Bottom Phase		TLL	STL
UCON	Salt	UCON	Salt	UCON	Salt		
			278.15 K				
0.246	0.106	0.463	0.018	<0.001	0.218	0.50	-2.31
0.236	0.100	0.442	0.020	<0.001	0.205	0.48	-2.38
0.220	0.091	0.403	0.023	0.001	0.185	0.43	-2.48
0.207	0.079	0.352	0.028	0.001	0.163	0.38	-2.59
0.190	0.070	0.296	0.036	0.003	0.143	0.31	-2.70
0.175	0.064	0.247	0.044	0.008	0.127	0.25	-2.83
			293.15 K				
0.222	0.089	0.486	0.016	<0.001	0.159	0.51	-3.39
0.209	0.083	0.450	0.018	<0.001	0.146	0.47	-3.51
0.189	0.070	0.389	0.020	0.002	0.123	0.40	-3.78
0.175	0.063	0.340	0.026	0.005	0.109	0.34	-3.99
0.162	0.058	0.291	0.030	0.011	0.097	0.29	-4.16
0.140	0.053	0.209	0.040	0.036	0.078	0.18	-4.41
			308.15 K				
0.182	0.063	0.002	0.097	0.530	0.010	0.54	-6.14
0.160	0.059	0.005	0.087	0.489	0.012	0.49	-6.49
0.141	0.053	0.007	0.076	0.440	0.013	0.44	-7.05
0.128	0.049	0.006	0.069	0.414	0.013	0.41	-7.41
0.111	0.045	0.011	0.061	0.372	0.016	0.36	-8.10
0.098	0.041	0.022	0.053	0.317	0.018	0.30	-8.55

$u(w_i^{UCON}) = 0.004$; $u(w_i^{Salt}) = 0.003$; $u(P) = 5$ kPa; $u(T) = 0.05$ K.

As in the case of ATPS with sodium sulfate, temperature also affects both TLL and STL when the cation is exchanged by ammonium. Increasing temperature produces an increase of both parameters. The average slope of the tie-lines increases (in absolute value) more than 10 % for each temperature interval. As it was previously explained, this means that increasing the temperature increases the polymer content in the top phase and reduces the salt content in the bottom phase. Similarly to systems with $NaSO_4$, when the phase-forming agent is UCON, the influence of temperature on TLL is not evident and a phase inversion in the system at 308.15 K appears producing an important increase in the STL. There is an increase of TLL and a slight decrease (absolute value) of STL with PEG molecular mass. TLL for the systems with UCON are significantly higher than for the systems with PEG, being more pronounced at the highest temperature. Interestingly, for a given polymer and temperature of work, the STL is more negative for the systems with sodium than the systems with ammonium.

Liquid-liquid equilibrium data for ATPS formed with potassium sulfate and UCON at 293.15 K and 308.15 K and atmospheric pressure are presented in Table 3.19 and Figure 3.18. Comparison of data presented in Table 3.14, Table 3.18 and Table 3.19, does not show an evident effect of the different cations in the phase diagrams of ATPS generated with sulfate salts and UCON. The discussion will be established in the next section once the data had been correlated.

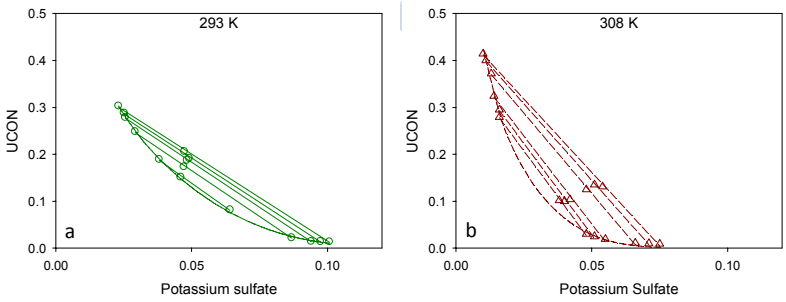

Figure 3.18. Binodal curve and tie-lines for UCON/Potassium sulfate ATPS at (a) —□— 293.15 and (b) ---Δ--- 308.15 K

Table 3.19. Experimental composition (mass fraction) of the equilibrium phases, together with the corresponding TLL and STL for UCON/Potassium sulfate ATPS at 293.15 and 308.15K and 0.1 MPa

Feed		Top Phase		Bottom Phase		TLL	STL
UCON	Salt	UCON	Salt	UCON	Salt		
293.15 K							
0.206	0.047	0.301	0.023	0.014	0.101	0.30	-3.69
0.192	0.049	0.287	0.025	0.014	0.097	0.28	-3.76
0.187	0.048	0.277	0.026	0.014	0.094	0.27	-3.84
0.173	0.047	0.247	0.029	0.022	0.087	0.23	-3.89
0.151	0.046	0.188	0.038	0.081	0.064	0.11	-4.0
308.15 K							
0.131	0.054	0.414	0.010	0.009	0.075	0.49	-7.29
0.135	0.051	0.400	0.011	0.010	0.071	0.46	-7.67
0.125	0.048	0.372	0.013	0.011	0.066	0.42	-8.07
0.104	0.042	0.019	0.055	0.324	0.014	0.39	-8.52
0.100	0.040	0.025	0.051	0.295	0.016	0.37	-8.72
0.102	0.038	0.030	0.048	0.279	0.016	0.33	-9.35

$u(w_i^{UCON}) = 0.008$; $u(w_i^{Salt}) = 0.001$; $u(P) = 5$ kPa; $u(T) = 0.05$ K.

Liquid-liquid equilibrium data for ATPS formed with potassium tartrate and PEG 600 and PEG 1500 at 278.15 K, 293.15K and 308.15K and atmospheric pressure are presented in Table 3.20 and Table 3.21 and Figure 3.19 and Figure 3.20. When the systems are generated with this organic salt, as in the previous cases, temperature increases TLL and STL. However, the molecular weight of polymer increases both TLL and slightly STL.

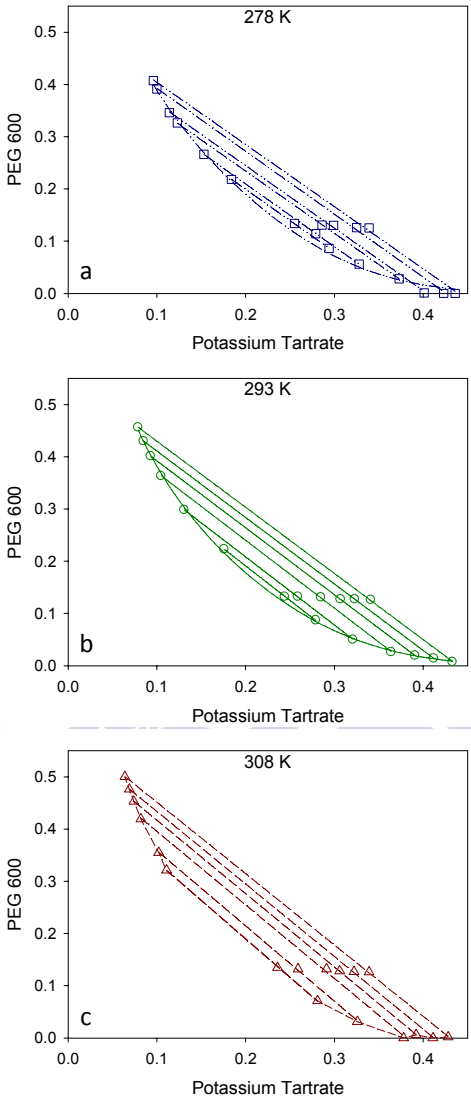

Figure 3.19. Binodal curve and tie-lines for PEG 600/Potassium tartrate ATPS at (a) -•-□-•- 278.15, (b) —□— 293.15 and (c) ---Δ--- 308.15 K

Table 3.20. Experimental composition (mass fraction) of the equilibrium phases, together with the corresponding TLL and STL for PEG 600/Potassium tartrate ATPS at 278.15, 293.15 and 308.15K and 0.1 MPa

Feed		Top Phase		Bottom Phase		TLL	STL
PEG	Salt	PEG	Salt	PEG	Salt		
			278.15 K				
0.125	0.339	0.407	0.096	0.000	0.436	0.53	-1.19
0.126	0.325	0.391	0.100	0.000	0.423	0.51	-1.20
0.130	0.299	0.346	0.114	0.001	0.401	0.45	-1.20
0.131	0.286	0.326	0.123	0.028	0.373	0.39	-1.19
0.114	0.279	0.266	0.153	0.056	0.328	0.27	-1.20
0.134	0.255	0.218	0.184	0.086	0.294	0.17	-1.19
			293.15 K				
0.126	0.341	0.456	0.079	0.007	0.433	0.57	-1.26
0.127	0.323	0.430	0.085	0.014	0.412	0.53	-1.27
0.127	0.307	0.401	0.093	0.019	0.391	0.48	-1.28
0.131	0.285	0.363	0.105	0.026	0.364	0.43	-1.30
0.132	0.259	0.298	0.131	0.050	0.321	0.31	-1.31
0.132	0.244	0.223	0.176	0.087	0.279	0.17	-1.32
			308.15 K				
0.126	0.339	0.500	0.064	0.002	0.428	0.62	-1.36
0.127	0.322	0.476	0.069	0.000	0.411	0.58	-1.39
0.128	0.306	0.453	0.074	0.006	0.392	0.55	-1.40
0.132	0.291	0.419	0.082	0.000	0.378	0.51	-1.41
0.132	0.259	0.355	0.102	0.031	0.326	0.40	-1.44
0.135	0.236	0.321	0.111	0.071	0.281	0.30	-1.47

$u(w_{PEG}^{Top}) = 0.003$; $u(w_{PEG}^{Bot}) = 0.001$; $u(w_{Salt}^{Top}) = 0.001$; $u(w_{Salt}^{Bot}) = 0.002$; $u(P) = 5$ kPa; $u(T) = 0.05$ K.

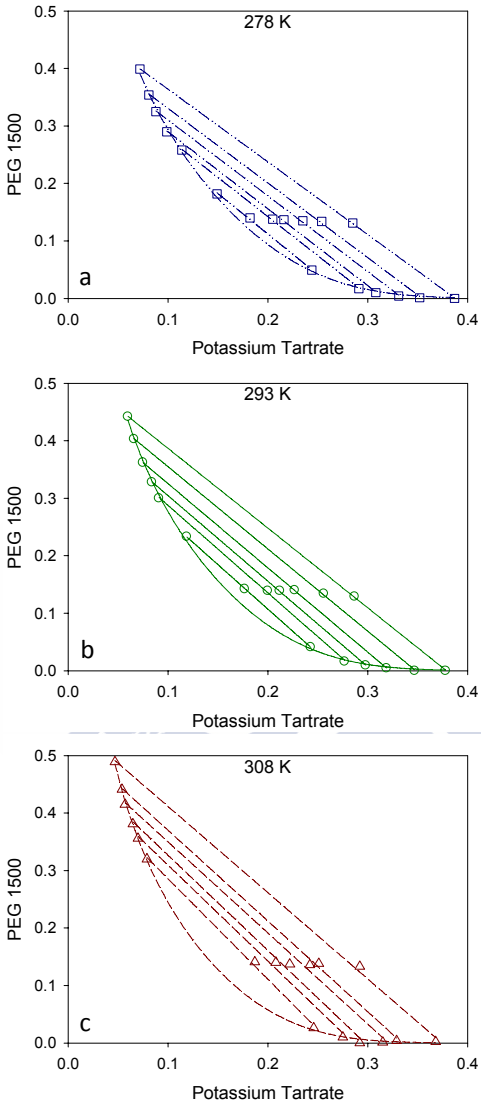

Figure 3.20. Binodal curve and tie-lines for PEG 1500/Potassium tartrate ATPS at (a) -•-□-•- 278.15, (b) —□— 293.15 and (c) ---Δ--- 308.15 K

Table 3.21. Experimental composition (mass fraction) of the equilibrium phases, together with the corresponding TLL and STL for PEG 1500/Potassium tartrate ATPS at 278.15, 293.15 and 308.15K and 0.1 MPa

Feed		Top Phase		Bottom Phase		TLL	STL
PEG	Salt	PEG	Salt	PEG	Salt		
			278.15 K				
0.131	0.285	0.399	0.072	0.000	0.387	0.51	-1.27
0.134	0.254	0.354	0.081	0.001	0.352	0.45	-1.30
0.135	0.235	0.325	0.088	0.004	0.331	0.40	-1.32
0.137	0.216	0.290	0.099	0.010	0.308	0.35	-1.34
0.138	0.205	0.258	0.114	0.017	0.291	0.30	-1.36
0.140	0.182	0.182	0.149	0.049	0.244	0.16	-1.40
			293.15 K				
0.129	0.287	0.442	0.060	0.000	0.378	0.54	-1.39
0.134	0.256	0.403	0.066	0.000	0.347	0.49	-1.43
0.140	0.227	0.362	0.075	0.004	0.319	0.43	-1.47
0.139	0.212	0.328	0.084	0.009	0.298	0.38	-1.49
0.139	0.200	0.300	0.091	0.016	0.277	0.34	-1.52
0.142	0.177	0.233	0.119	0.041	0.243	0.23	-1.55
			308.15 K				
0.133	0.133	0.292	0.489	0.047	0.002	0.58	-1.50
0.138	0.138	0.251	0.441	0.054	0.004	0.52	-1.58
0.136	0.136	0.242	0.415	0.057	0.001	0.49	-1.58
0.137	0.137	0.222	0.381	0.065	0.000	0.44	-1.66
0.140	0.140	0.208	0.356	0.070	0.010	0.40	-1.67
0.141	0.141	0.187	0.320	0.079	0.026	0.33	-1.74

$u(w_{PEG}^{Top}) = 0.003$; $u(w_{PEG}^{Bot}) = 0.002$; $u(w_{Salt}^{Top}) = 0.001$; $u(w_{Salt}^{Bot}) = 0.004$; $u(P) = 5$ kPa; $u(T) = 0.05$ K.

3.3.3.1. Binodal curve correlation

For a given ATPS, the binodal curve is defined by the end points of the tie-lines. The experimental data obtained in this work were fitted to the empirical equation suggested by Merchuk and co-workers [68]:

$$w_p = a \cdot exp[b \cdot (w_s)^{0.5} - c \cdot (w_s)^3] \qquad 3.3$$

where w_p and w_s are the polymer and salt compositions in mass fraction, respectively, and a, b and c are fitting parameters obtained by nonlinear regression.

The experimental data obtained can also be fitted with the equation suggested by Guan and co-workers [69]:

$$Ln\left(V^* \cdot w_p/M_p\right) + V^* \cdot w_s/M_s = 0 \qquad 3.4$$

where M_p and M_s are the polymer and salt molecular weight, respectively, and V^* is the effective excluded volume (*EEV*) of the salt into the polymer aqueous solution. It is important to note that both models have been successfully applied for the correlation of binodal data from polymer/polymer and polymer/salt ATPS [16, 70, 71]. A recent work from Álvarez-Guerra and co-workers [72] has shown that the Merchuk equation can also be used for salt/salt ATPS (which include ionic liquids), but poor results are obtained with the EEV model [73].

The quality of the fitting using these models was assessed with the average arithmetic relative deviation, AARD, calculated as:

$$AARD = \left(\sum |(y^{exp} - y^{calc})/y^{exp}|\right)/N \qquad 3.5$$

where y^{exp} and y^{calc} represent the dependent variable and N the number of data points for a given ATPS.

The fitting parameters, obtained by nonlinear regression, and deviations of the correlation of the binodal curve data for each ATPS and temperature using Merchuk equation are shown in Table 3.22. As expected, this empirical equation provides an excellent performance for the regression of the experimental data. The results of the

correlation using the equation suggested by Guan *et al* [69], *EEV* values and deviations, are presented in Table 3.23. Despite the performance of this model is worse than Merchuk equation, it has a strong theoretical base (statistical geometry) which allows for the evaluation of the salting-out effect of the different salts used.

Table 3.22. Fitting parameters and deviations obtained with the Merchuk Equation

T (K)	a	b	c	r^2	AARD
PEG 4000-Sodium Sulfate-Water					
293.15	0.6277	-4.749	1731	0.9981	0.035
308.15	0.7700	-5.592	2692	0.9997	0.038
PEG 8000-Sodium Sulfate-Water					
293.15	0.6401	-5.701	2139	0.9998	0.005
308.15	0.5459	-4.033	12550	>0.9999	0.005
UCON-Sodium Sulfate-Water					
293.15	1.006	-9.157	4602.6	0.9992	0.340
308.15	1.604	-14.437	13407.9	0.9979	0.285
PEG 1500-Ammonium Sulfate-Water					
298.15	1.443	-6.625	220.1	0.9993	0.107
PEG 4000-Ammonium Sulfate-Water					
278.15	0.6318	-3.036	684.5	0.9987	0.080
293.15	0.6902	-3.388	858.9	0.9979	0.020
308.15	0.8188	-4.486	1118	0.9998	0.010
PEG 8000-Ammonium Sulfate-Water					
278.15	1.170	-6.220	645.1	>0.9999	0.003
293.15	1.020	-5.744	612.4	0.9991	0.008
308.15	0.9599	-5.282	830.7	0.9975	0.015
UCON-Ammonium Sulfate-Water					
278.15	1.259	-7.369	1164.0	0.9999	0.150
293.15	1.642	-9.706	2166.2	0.9994	0.079
308.15	2.510	-15.085	7886.1	0.9991	0.456

Table 3.22. Continuation

T (K)	a	b	c	r^2	AARD
UCON-Potassium Sulfate-Water					
293.15	1.211	-8.995	1829.8	0.9995	0.072
308.15	1.814	-14.304	7637.7	0.9989	0.210
PEG 600-Potassium Tartrate-Water					
278.15	1.344	-3.825	31.14	0.9977	0.033
293.15	1.537	-.312	28.48	0.9996	0.099
308.15	1.688	-4.782	26.54	0.9993	0.143
PEG 1500-Potassium Tartrate-Water					
278.15	1.566	-5.075	68.43	0.9992	0.103
293.15	1.705	-5.567	75.66	0.9994	0.078
308.15	1.808	-6.019	94.68	0.9997	0.289

The correlation of the binodal curves with Merchuck equation allows an easy comparison of the influence of several variables into the size of the heterogeneous regions. Figure 3.21 shows, for all the systems studied, the binodal curves at two different working temperatures. It can be seen that the heterogeneous region increases with the temperature in all the cases (this increase in the case of the ATPS formed with PEG 8000 and ammonium sulfate is very limited). This is in good agreement with results presented in Table 3.23 for *EEV* values that increase with temperature in all the cases except for the system with PEG 600 and potassium tartrate where a slight decrease of *EEV* values with temperature is found. The reason may be due to a poor correlation obtained with this dataset. An increase of the heterogeneous region with temperature implies that lower amounts of the phase-forming components are needed to produce the water splitting into two immiscible phases. Figure 3.21 also allows confirming that the increase of temperature leads to a more negative slope of tie-lines, as it was explained in section 3.3.3.

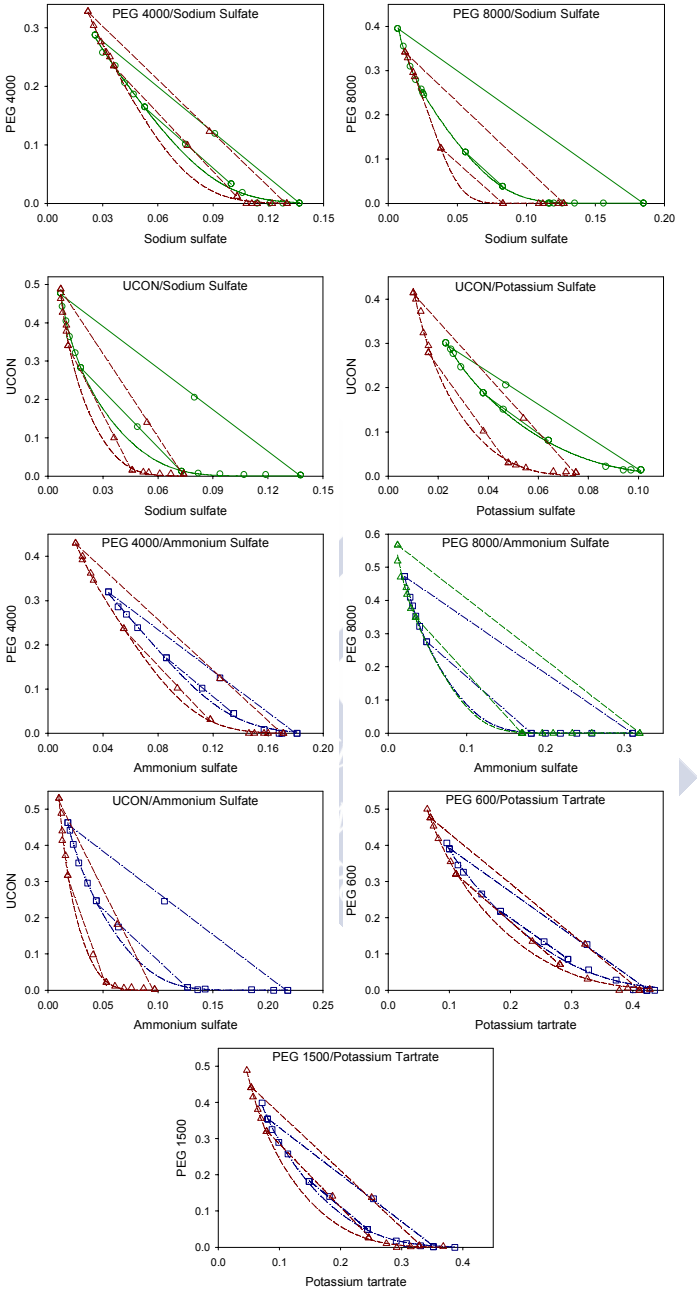

Figure 3.21. Effect of temperature on phase diagrams for all the systems studied. □: 278.15 K, ▯: 293.15 K, Δ: 308.15 K. Lines: tie-lines and binodal curves. -•-• 278.15 K, —293.15 K, --- 308.15 K.

Table 3.23. Effective Excluded Volume parameter correlation

T (K)	EEV (g/mol)	r^2	AARD	T (K)	EEV (g/mol)	r^2	AARD
PEG 4000-Sodium Sulfate-Water				PEG 8000-Sodium Sulfate-Water			
293.15	4961.1	0.9605	0.52	293.15	9357.0	0.8254	0.22
308.15	5136.1	0.9888	0.13	308.15	9304.1	0.9593	0.09
UCON-Sodium Sulfate-Water				UCON-Potassium Sulfate-Water			
293.15	6226.8	0.9984	0.42	293.15	5899.7	0.9958	0.30
308.15	6473.5	0.9740	2.12	308.15	6918.3	0.9608	1.15
PEG 1500-Ammonium Sulfate-Water				PEG 4000-Ammonium Sulfate-Water			
298.15	2417.2	0.9768	0.27	278.15	3473.4	0.9638	0.27
				293.15	3798.1	0.9581	0.19
				308.15	4292.1	0.9667	0.17
PEG 8000-Ammonium Sulfate-Water				UCON-Ammonium Sulfate-Water			
278.15	5674.3	0.9352	0.08	278.15	4384.6	0.9931	0.54
293.15	6452.1	0.9089	0.11	293.15	4685.0	0.9974	0.74
308.15	6727.7	0.9030	0.09	308.15	5364.3	0.9727	2.27
PEG 600-Potassium Tartrate-Water				PEG 1500-Potassium Tartrate-Water			
278.15	1100.8	0.8897	0.35	278.15	2079.9	0.9789	1.08
293.15	1083.2	0.8952	1.86	293.15	2103.2	0.9787	1.20
308.15	1069.7	0.8862	0.38	308.15	2141.5	0.9792	1.96

Figure 3.22 shows phase diagrams (binodal curves and selected tie-lines) at 293.15 K of different ATPS where one of the phase forming agents is PEG (two different molecular weights). It can be seen that an increase of the molecular weight of the polymer means, in all the cases, an increase of the heterogeneous region. Indeed, the values obtained for the Effective Excluded Volume of the salts (Table 3.23) are almost doubled when PEG molecular weight is increased. This effect was expected since it has been previously observed with a wide variety of polymers, including PEG, and salts [15, 74, 75]. The higher molecular weight of the polymer, the lower amounts of the phase-forming components are needed to generate the ATPS. The influence of the PEG molecular weight on STL is much smaller, leading

a decrease of the molecular weight to a more negative slope of tie-lines except in the case of the organic salt where the contrary effect was found. This figure also allows the comparison of ATPS formed with sulfate salts. Sodium cation produces larger immiscibility of the polymer/salt aqueous biphasic system than ammonium, thus proving to be more effective in ATPS formation. The same result has been obtained for a variety of salts and polymers, namely with PEG systems [76]. This effect is related to the ion hydration shell and its Gibbs energy of hydration (ΔG_{hyd}): larger hydration shells (or more negative ΔG_{hyd}) reduce the number of water molecules available for PEG solvation. Thus, ions with larger hydration shells are more effective salting-out agents. The size of hydration shells of ions and their ΔG_{hyd} have been extensively studied by Marcus [77]. Values reported for these cations are: −285 kJ·mol^{-1} for ammonium and −365 kJ·mol^{-1} for sodium at 298.15 K.

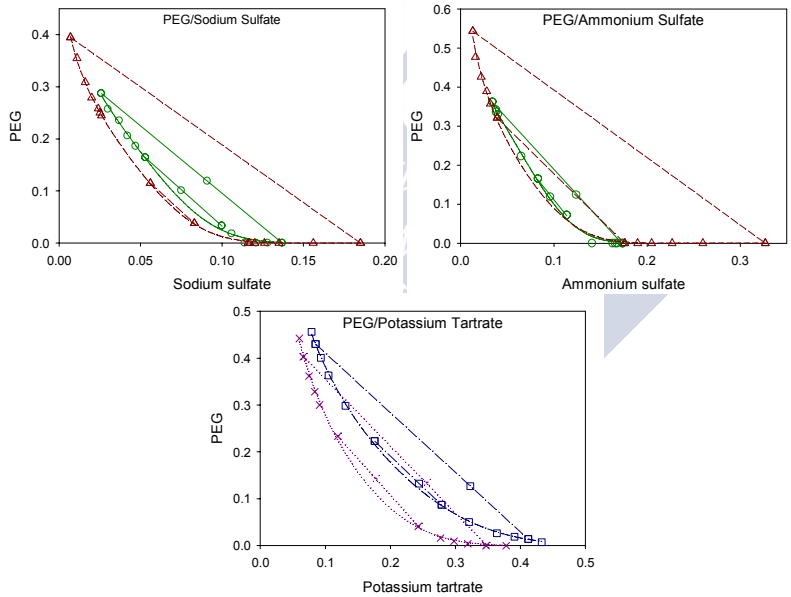

Figure 3.22. Experimental tie-lines and Merchuk correlation for the binodal curves. Compositions in mass fraction. (-··-□-··- PEG 600; ···×··· PEG 1500; —▯— PEG 4000; ---Δ--- PEG 8000)

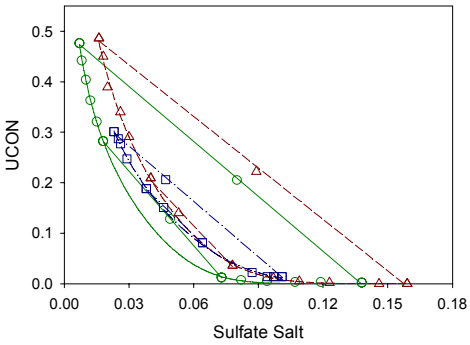

Figure 3.23. Comparison of Merchuk correlation for the systems formed with UCON and different sulfate salts (—□— Sodium Sulfate, ---Δ--- Ammonium Sulfate, -·-□ -·- Potassium Sulfate)

Figure 3.23 shows a comparison of binodal curves and tie-lines for ATPS formed with UCON and different sulfate salts at 293.15 K. The ability of the cation to produce ATPS with UCON follows the series: $Na^+ > K^+ > NH_4^+$, despite potassium and ammonium are close. The effective excluded volumes obtained with Equation 3.4 follow the same series at 293.15 K, but not at 308.15 K. That may be due to the poorer correlations obtained at the highest temperature in the system with potassium salt. As explained above, the series are in agreement with the cation Gibbs energy of hydration at 298.15 K, as published by Marcus [77]: −285 kJ·mol^{-1} for ammonium, −365 kJ·mol^{-1} for sodium and -295kJ·mol^{-1}for the potassium.

3.3.3.2. Tie-line data correlation

The compositions of the liquid-liquid equilibrium data can be correlated using a simple two parameter equation derived from the binodal theory and proposed by Guan and co-workers [69]:

$$Ln\left(w_s^{top}/w_s^{bot}\right) = \beta + k * \left(w_p^{bot} - w_p^{top}\right) \qquad 3.6$$

where β and k are fitting parameters that can be related to "effective" virial (or activity) coefficients and the salting-out coefficient of the salt, w_i are mass fractions of polymer and salt, and superscripts indicate the *top* and bottom (*bot*) phases. The

values for β and k were obtained for all the systems by linear regression and are presented in Table 3.24. The regression statistics also shown in Table 3.24 demonstrate a good representation of the experimental data.

Table 3.24. Fitting parameters for Equation 3.6 and statistics of regression (coefficient of determination, r^2, and AARD)

T (K)	k	B	r^2	AARD
PEG 4000-Sodium Sulfate-Water				
293.15	7.4598	0.4984	0.9774	0.05
308.15	7.7674	0.7691	0.9999	0.0004
PEG 8000-Sodium Sulfate-Water				
293.15	10.0986	0.9904	0.9996	0.007
308.15	11.2956	1.5076	0.9955	0.08
UCON-Sodium Sulfate-Water				
293.15	8.0002	0.8029	0.996	0.57
308.15	5.9618	0.5153	0.989	0.56
UCON-Potassium Sulfate-Water				
293.15	5.1447	0.0409	0.996	0.93
308.15	5.7291	0.3696	0.995	0.55
PEG 1500-Ammonium Sulfate-Water				
298.15	5.8533	0.3780	0.9996	0.07
PEG 4000-Ammonium Sulfate-Water				
278.15	4.8424	0.1855	0.9910	0.03
293.15	6.1163	0.5930	0.9986	0.002
308.15	8.0873	1.3368	0.9927	0.003
PEG 8000-Ammonium Sulfate-Water				
278.15	7.1021	0.6612	0.9995	0.002
263.15	7.7905	0.9967	0.9970	0.003
308.15	8.1960	1.2892	0.9770	0.009
UCON-Ammonium Sulfate-Water				
278.15	6.3167	0.4580	0.999	2.16
293.15	5.2803	0.2692	0.997	0.74
308.15	4.9645	0.4027	0.997	0.11

Table 3.24. Continuation

T (K)	k	B	r^2	AARD
PEG 600-Potassium Tartrate-Water				
278.15	3.7388	0.0194	0.9995	0.29
293.15	4.0012	0.0920	0.9998	0.56
308.15	3.9112	0.0782	0.9942	0.38
PEG 1500-Potassium Tartrate-Water				
278.15	4.4732	0.1149	0.9988	0.04
293.15	4.4928	0.1542	0.9995	0.03
308.15	4.7762	0.2792	0.9967	0.29

The results of the correlations with Equation 3.6 are shown in Figure 3.24 to Figure 3.27 for all ATPS and temperatures. In many cases, the tie-line with lowest concentration (shortest TLL, and closer to the plait point) had to be excluded of the regression (outliers), nonetheless they are also included into the figures.

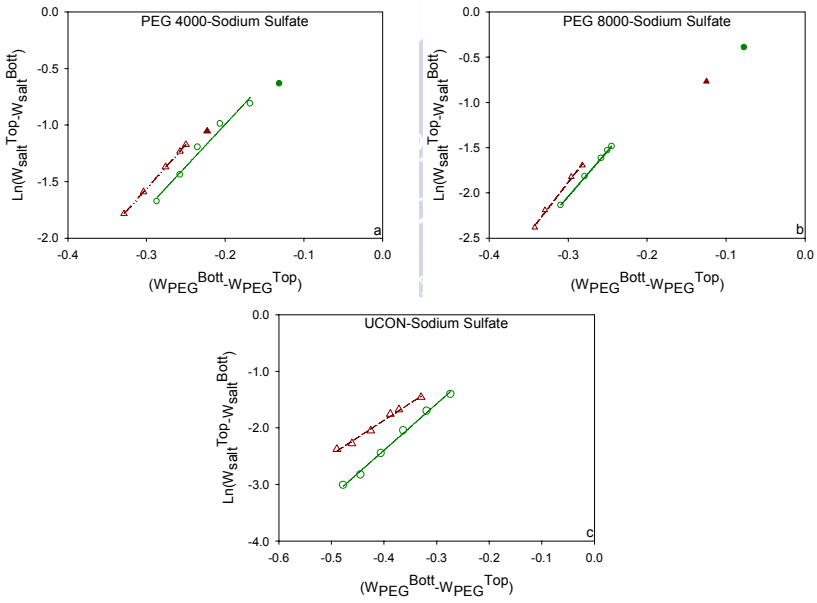

Figure 3.24. Correlations for tie-line data. a) PEG 4000-Sodium Sulfate system. b) PEG 8000-Sodium Sulfate system. c) UCON-Sodium Sulfate system. (—□— 293.15 K, ---Δ--- 308.15 K. Solid symbols: outliers)

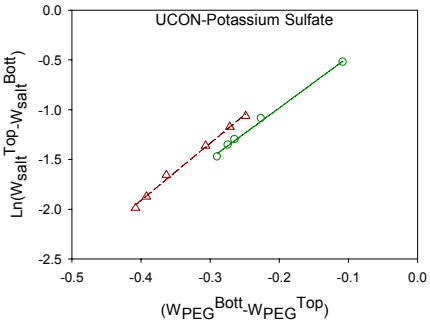

Figure 3.25. Correlations for tie-line data. UCON-Potassium Sulfate system. (—□—293.15 K, ---Δ--- 308.15 K. Solid symbols: outliers)

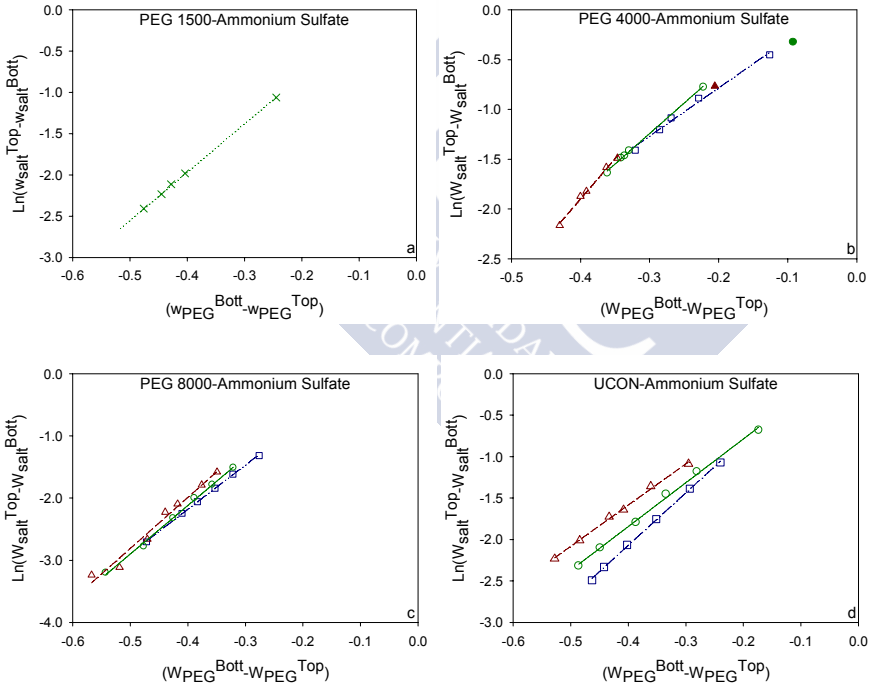

Figure 3.26. Correlations for tie-line data. a) PEG 1500-Ammonium Sulfate system. b) PEG 4000- Ammonium Sulfate system. c) PEG 8000- Ammonium Sulfate system. d) UCON-Ammonium Sulfate system. (-··-□-··- 278.15 K, —□— 293.15 K, ···×··· 298.15 K, ---Δ--- 308.15 K)

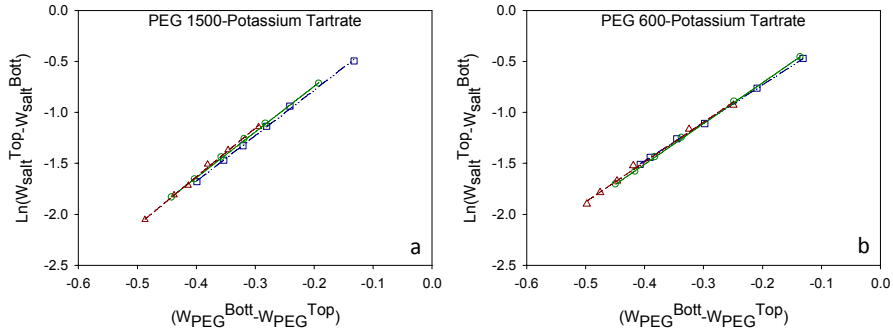

Figure 3.27. Correlations for tie-line data. a) PEG 1500-Potassium Tartrate system. b) PEG 600-Potassium Tartrate system. (-···□-··· 278.15 K, —▯— 293.15 K, ---Δ--- 308.15 K)

The slope of Setschenow-derived equation (3.6) increases with temperature (see Table 3.24). This means that the temperature affects the equilibrium composition: increase the polymer content in the top phase whilst the salt composition in the bottom phase decreases. This is in good agreement with the increasing of the heterogeneous region with temperature found in section 3.3.3.1.

The influence of the polymer molecular weight on the TLL is reflected in the *k* values obtained from Equation 3.6 and shown in Table 3.24. This parameter relates the compositions of the components in the equilibrium phases, and thus depends on the size (TLL) and slope (STL) of the tie-lines within the ATPS. When the phase-forming components are PEG of different molecular weights and a salt (sodium sulfate, ammonium sulfate or potassium tartrate), an increase of the molecular weight of the polymer leads to an increase of *k* what is in agreement with the increase of the heterogeneous region shown in section 3.3.3.1.

The *k* parameter in Equation 3.6 can also be related to the salting-out effect. As explained in the previous section, the ability of the cation to produce ATPS with UCON follows the series: $Na^+ > K^+ > NH_4^+$. This can be seen in the values of *k* presented in Table 3.24. At the studied temperatures, the largest values obtained correspond to Na_2SO_4 followed by potassium and ammonium with close values.

USC
UNIVERSIDADE
DE SANTIAGO
DE COMPOSTELA

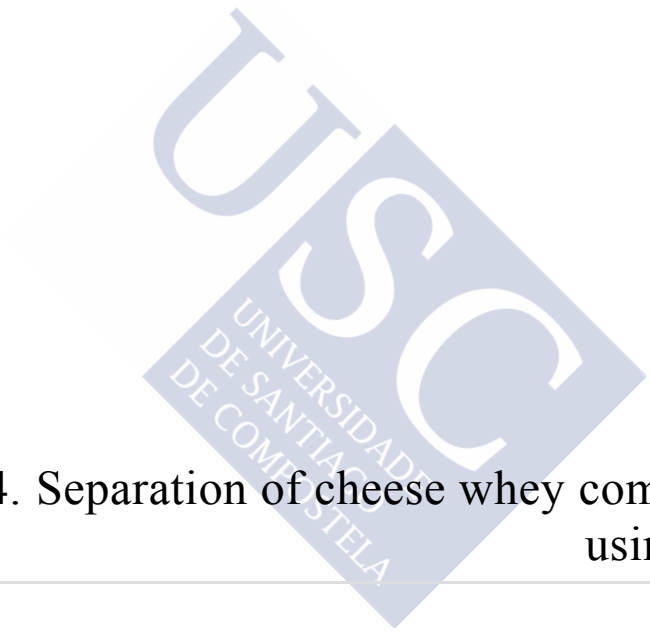

4. Separation of cheese whey components using ATPS

USC
UNIVERSIDADE
DE SANTIAGO
DE COMPOSTELA

4. SEPARATION OF CHEESE WHEY COMPONENTS USING ATPS

4.1. INTRODUCTION

ATPS characterized in chapter 3 will be used for the separation of the main components of cheese whey (lactose, bovine serum albumin, α-lactalbumin and β-lactoglobulin). In order to analyze whether the concentration of the biomolecule affects its distribution between the equilibrium phases, a first study will be performed with lactose as solute. Secondly, the distribution of each of the four biomolecules in different tie-lines of selected ATPS will be determined. The aim is analyzing which is the most adequate concentration of the phase-forming components to carry out the separation. According to the results, adequate phase-forming and solute compositions will be selected and applied to all the systems studied. The partitioning of the key biomolecules in the different ATPS will be measured experimentally, and the effect of different parameters such as polymer molecular weight or pH on the process will be evaluated. Based on these results, different separation strategies will be considered to carry out the valorization of cheese whey. Finally, these strategies will be assessed using first a synthetic whey formulated with the key solutes dissolved in distilled water, and later using a real cheese whey from a local cheese producer (Queizúar S.L.).

4.2. MATERIAL AND METHODS

4.2.1. Chemicals

Polymers and salts used in this work were previously described in section 3.2.1. PEG 200 (BioUltra 200), PEG 300 (BioUltra 300) and PEG 400 (BioUltra 400), obtained from Sigma, were also used. In order to control de pH, buffers were prepared using sodium phosphate dibasic dihydrate ($Na_2HPO_4{\cdot}2H_2O$) and sodium phosphate monobasic monohydrate ($NaH_2PO_4{\cdot}H_2O$) from Panreac Applichem, and citric acid ($C_6H_8O_7$, ACS reagent, >99.5 % wt) from Sigma Aldrich. Also phosphate

buffered saline solution (PBS, 100 TAB) was purchased from Sigma. It was used to re-suspend the proteins precipitated in the ATPS interface.

Other chemicals were used in the preparation of HPLC eluents. Sulfuric acid (H_2SO_4, ACS reagent, 95.0-98.0 % wt) was obtained from Sigma Aldrich. Trifluoroacetic acid ($C_2F_3O_2H$-TFA, synthesis grade) and acetonitrile (CH_3CN-AcN, gradient 240nm/far UV HPLC grade) were obtained from Scharlau.

Bovine serum albumin (lyophilized powder, ≥98 % wt), *β*-lactoglobulin ($C_{37}H_{64}N_{12}O_8S$, lyophilized powder from bovine milk, ≥85 % wt), *α*-lactalbumin (Type I, lyophilized powder from bovine milk, ≥85 % wt), and *α*-lactose monohydrate ($C_{12}H_{22}O_{11}{\cdot}H_2O$, ≥99 % wt), were obtained from Sigma.

Table 4.1. Components of cheese whey

	Synthetic Whey	Real whey
BSA	0.40 mg/mL	0.46 mg/mL
ß-LG	2.52 mg/mL	3.20 mg/mL
α-LA	1.06 mg/mL	1.20 mg/mL
Lactose	50 mg/mL	38 mg/mL

Synthetic cheese whey was prepared in distilled water combining the model solutes. The composition is presented in Table 4.1. Real cheese whey was supplied by Queizúar S.L. It is an acid whey with a pH value of 6.5. The composition of this real, pre-treated cheese whey was analyzed by HPLC and it is also presented in Table 4.1. Figure 4.1 shows the comparison, regarding the three proteins of interest, between synthetic and real whey.

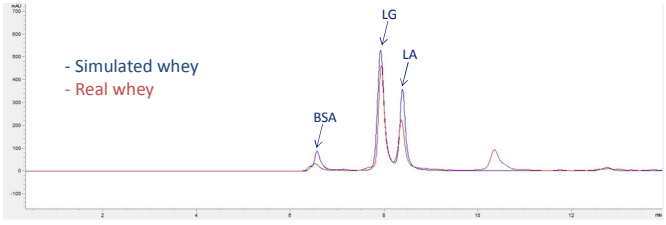

Figure 4.1. Comparison between synthetic and real cheese whey.

4.2.2. Methods

Systems were prepared gravimetrically on a Mettler Toledo balance model XPE205 (Figure 3.1), adding suitable amounts of polymer, salt, solute and water in Eppendorf tubes of 2 mL. Bulk polymer and salt were added while for the different key solutes stock solutions (ca. 2 mg/mL) were used. The systems were vigorously vortex-mixed (Figure 4.2a) for at least one minute and left to rest one hour in a thermostatic bath Julabo F12-EH (Figure 3.4) at the corresponding equilibrium temperature (293.15 or 298.15 K depending on the system). Then, the tubes were centrifuged at 13000 rpm during 5 min using a centrifuge Ortoalresa series Digicen 21 (Figure 4.2b). Samples from top and bottom phases were withdrawn and diluted (1:10) with water for analysis by HPLC, using the methods described below. All the experiments were carried out a minimum of two times, ensuring that the compositions obtained agreed within the expected uncertainty.

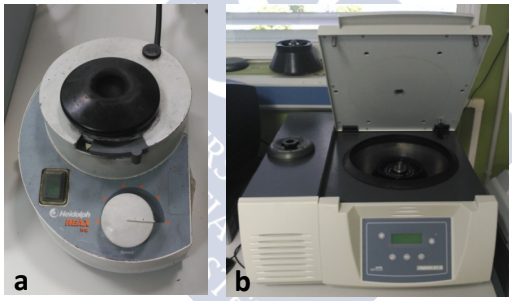

Figure 4.2. a) Vortex-mixer; b) Centrifuge

When the effect of pH in solutes partitioning was analyzed, a buffer solution was used instead of water. The buffer solutions with pH upper than 6 were prepared with sodium phosphate buffer, while the solutions with pH lower than 6 were prepared with a sodium phosphate-citrate buffer. Table 4.2 and Table 4.3 show the volumes employed to prepare different buffer solutions.

Table 4.2. Mixed volumes of 0.1 M solution of citric acid and 0.2 M solution of sodium phosphate dibasic dihydrate to prepare different buffers

pH	x mL $C_6H_8O_7$	y mL Na_2HPO_4
4	61.45	38.55
5	48.50	51.50

Table 4.3. Mixed volumes of 0.2 M solution of sodium phosphate dibasic dihydrate and 0.2 M solution of sodium phosphate monobasic monohydrate to prepare different buffers

pH	x mL Na_2HPO_4	y mL NaH_2PO_4
6	6.15	43.85
7	30.50	19.50
8	47.35	2.65

The pH was measured using a HANNA instruments pH-meter model HI 223 with the refillable double junction pH electrode HI 1131P (Figure 4.3). The precision in the measurement of pH was 0.01.

Figure 4.3. pH-meter

Solute quantification was achieved using the Agilent series 1100 high-performance liquid chromatography (HPLC) shown in Figure 4.4. Lactose quantification was carried out using a refraction index detector (RID) Agilent 1260 infinite series. As for protein quantification, a diode array detector (DAD) Agilent 1100 series was used. These detectors are installed in series in the HPLC, since they

are both non-destructive. Two different columns have been used for lactose: a) Bio-Rad Aminex HPK-87H, 7.8 x 300 mm, particle size 9 μm. This column worked at 323.15 K, with an injection volume of 20 μL. The mobile phase (0.6 mL/min) was 5 mM sulfuric acid in distilled water. b) Phenomenex Yarra SEC 2000, 7.8 x 300 mm and pore size 145 Å. This column worked at 323.15 K, with an injection volume of 25 μL. The mobile phase is a mixture of two solutions: 79.3 % of a solution A (composed by 72.3 % wt distilled water with 0.1 % wt TFA and 27.7 % wt acetonitrile with 0.1 % wt TFA) and 20.7 % wt of a solution B (composed by 0.1 % wt TFA in acetonitrile). This second column and method were used only when samples also contained proteins.

Figure 4.4. HPLC

Also two different columns were used for protein quantification: a) Shodex Protein KW-800, 8 x 300 mm, absorbance measured at a wavelength of 280 nm. b) Phenomenex Yarra SEC 2000, 7.8 x 300 mm and pore size 145 Å, absorbance measured at a wavelength of 214 nm. Both columns worked at 323.15 K with an injection volume of 25 μL. A gradient method is applied: Solution A is composed by 72.3 % wt distilled water with 0.1 % wt TFA and 27.7 % wt acetonitrile with 0.1 % wt TFA, whilst Solution B is acetonitrile with 0.1 % wt TFA. The parameters of this gradient method are summarized in Table 4.4.

Table 4.4. Parameters of the gradient method employed with proteins

Time (min)	Solution A (%)	Solution B (%)	Flow (mL/min)
0	100	0	0.8
20	70	30	0.8
21	50	50	0.8
22	30	70	0.8
23	0	100	0.8
35	100	0	1.0/0.8*
45/55	100	0	1.0/0.8*

* with Shodex column flow set to 1 mL/min and 45 min total time; with Yarra column 0.8 mL/min flow and 55 min total time.

Finally, amicon ultra-0.5 centrifugal filter devices (30 K and 50 K) were used for centrifugation tests. Amicon devices were inserted into micro-centrifuge tubes with 500 µL of sample. The tubes were centrifuged at 12300 rpm during 10 minutes. To recover the concentrate solute, the amicon ultra filter device was placed in a clean micro-centrifuge tube and centrifuged at 3300 rpm during 2 minutes to transfer the concentrated sample from the device to the tube.

4.3. RESULTS AND DISCUSSION

4.3.1. Biomolecules partitioning

4.3.1.1. Influence of solute concentration

In order to analyze whether the concentration of the biomolecule affects its distribution between the equilibrium phases, samples with six different concentrations of lactose (ranging from 0 to 30 mg/mL) were prepared in aqueous solutions of polymer and salt with the components and compositions shown in Table 4.5. Distribution coefficients, *K*, of lactose were determined as the slope of the linear fit of data of solute concentrations in the top versus bottom phases. Values are presented in Table 4.5 with deviations obtained in the fit. Very good fits with R-squared greater than 0.98, intersections very close to the origin, and low deviations

were obtained. As an example, Figure 4.5 shows results obtained with PEG 1500/potassium tartrate ATPS. Distribution coefficients do not depend on the quantity of solute in the system. Moreover, obtained values are less than one, meaning that lactose shows greater affinity for the bottom phase (rich in salt).

Table 4.5. Feed composition, distribution coefficient of Lactose and standard error obtained in the fit

TL	Feed (wt)		K	StdEr*	Feed (wt)		K	StdEr*
	Polymer	Salt			Polymer	Salt		
	PEG 4000 + Sodium sulfate + Water				PEG 8000 + Sodium sulfate + Water			
1	0.099	0.081	0.513	0.013	0.098	0.070	0.491	0.005
2	0.110	0.083	0.382	0.006	0.131	0.114	0.382	0.021
	UCON+ Sodium sulfate + Water				PEG 4000 + Ammonium sulfate + Water			
1	0.125	0.052	0.295	0.010	0.119	0.108	0.376	0.005
2	0.169	0.067	0.298	0.011	0.123	0.128	0.287	0.004
	PEG 8000 + Ammonium sulfate + Water				UCON + Ammonium sulfate + Water			
1	0.157	0.127	0.253	0.009	0.172	0.074	0.144	0.007
2	0.109	0.171	0.223	0.011	0.204	0.088	0.108	0.006
	UCON + Potassium sulfate + Water				PEG 600 + Potassium tartrate + Water			
1	0.152	0.047	0.370	0.021	0.115	0.286	0.366	0.020
2	0.173	0.048	0.303	0.005	0.114	0.302	0.357	0.022
	PEG 1500 + Potassium tartrate + Water							
1	0.129	0.217	0.323	0.005				
2	0.125	0.240	0.271	0.014				
3	0.123	0.254	0.252	0.007				
4	0.123	0.268	0.202	0.004				

$^{*}StdEr = \sqrt{\frac{1}{N-2}\sum_{i=1}^{N}(y_i - \hat{y}_i)^2}$

As for each polymer/salt ATPS, distribution coefficients were determined using two feeds of different polymer and salt concentrations belonging to two different tie-lines (four in the case of the system with PEG 1500 and potassium

tartrate), results obtained in this section can also be used to analyze whether partition coefficients depend on concentration of salt and polymer in the system.

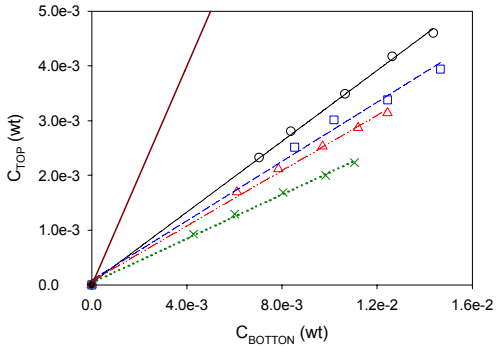

Figure 4.5. Lactose concentration in the top phase versus concentration in the bottom phase for different tie-lines of PEG 1500/Potassium tartrate ATPS. Tie-line 1 (—o—); Tie-line 2 (---□---); Tie-line 3 (···Δ···); Tie-line 4 (···×···)

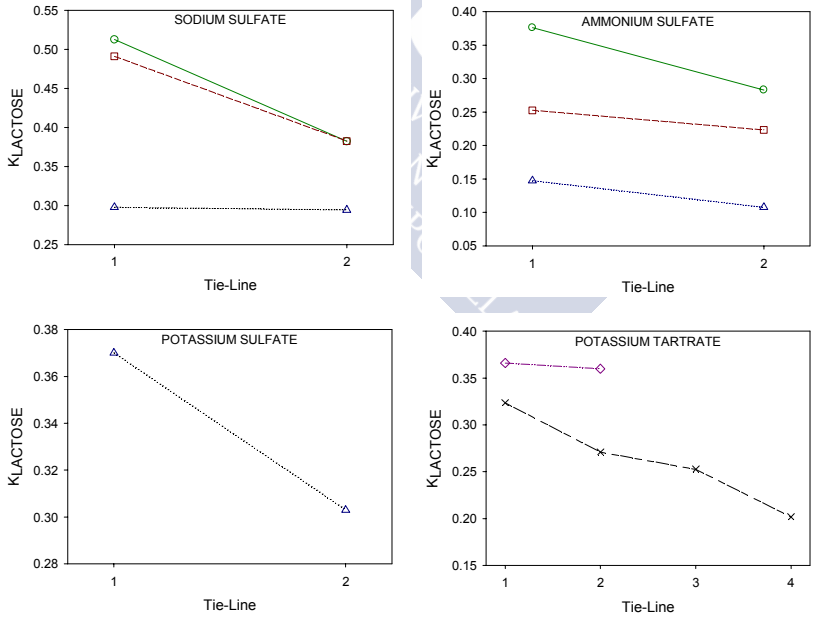

Figure 4.6. Partition coefficient of lactose as a function of used tie-line in different ATPS. (···◇···) PEG 600, (—×-—) PEG 1500, (--□--) PEG 4000, (—o—) PEG 8000 and (···Δ···) UCON

Figure 4.6 presents the distribution coefficient of lactose in different ATPS as a function of the feed to which the sugar was added (used tie-line). This figure shows that, in most of the cases, the concentration of polymer and salt in the system clearly affects the distribution coefficients. The higher concentration of phase-forming agents, the lower the distribution coefficient. As lactose has greater affinity for the phase where salt is concentrated, an increase of its concentration leads to lower distribution coefficients. Low distribution coefficients mean a reduction of the loss of lactose to the top phase. Figure 4.6 also shows that UCON leads to the lowest distribution coefficients. For comparison, Figure 4.7 shows distribution coefficients obtained in ATPS formed with UCON and different sulfate salts. As can be seen, ammonium sulfate has a more extreme partition towards the bottom phase than sodium or potassium. Indeed, the combination of UCON with ammonium sulfate provides the lowest partition coefficient for lactose among all ATPS evaluated.

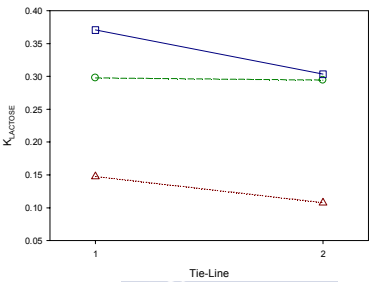

Figure 4.7. Partition coefficient of lactose using UCON/sulfate salt: (--o--) Sodium sulfate, (···Δ···) Ammonium sulfate and (—□—) Potassium sulfate

4.3.1.2. Influence of the concentration of the phase-forming components

In order to further analyze the influence of the concentration of the phase-forming components in the ATPS (or in other words the selected tie-line) on the distribution coefficient of the target biomolecules, new tests were carried out. PEG 600 or 1500/potassium tartrate ATPS at 293.15 K were selected for this study. Table 4.6 presents compositions of salt and polymer used in the feed and the corresponding tie-lines ends. As distribution coefficients do not depend on solute

concentration, a low concentration of the target biomolecules in the feed was used (0.7 mg/mL).

Table 4.6. Feed and tie-lines ends compositions used to evaluate solute partitioning in PEG/potassium tartrate ATPS at 293.15 K

	Feed		Top phase		Bottom phase		
PEG MM	PEG	Salt	PEG	Salt	PEG	Salt	TLL
1500	0.142	0.177	0.233	0.119	0.041	0.243	0.229
	0.139	0.200	0.300	0.091	0.016	0.277	0.338
	0.139	0.212	0.328	0.084	0.009	0.298	0.383
	0.140	0.227	0.362	0.075	0.004	0.319	0.432
600	0.132	0.244	0.233	0.176	0.087	0.279	0.170
	0.132	0.259	0.298	0.131	0.050	0.321	0.312
	0.131	0.285	0.363	0.105	0.026	0.364	0.426
	0.127	0.307	0.401	0.093	0.019	0.391	0.485

Since there was some solute precipitation in most systems (see Figure 4.8), in this case partition coefficients between ATPS phases do not provide the whole picture of solute behavior. For this reason, the solute yield recovered in each phase (values in the precipitated phase were calculated through mass balance) are presented in Tables 4.7 and 4.8. These tables also show partition coefficients when they could be calculated, but these values must be critically analyzed when there is significant precipitation of the biomolecule.

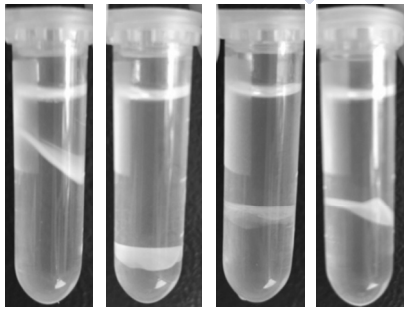

Figure 4.8. Solute precipitation at the interfase

Table 4.7. Recovery yields and partition coefficients for the biomolecules in PEG 1500/potassium tartrate ATPS at 293.15 K

TL	Y_T^{top} (%)	Y_T^{pre} (%)	Y_T^{bot} (%)	K	Y_T^{top} (%)	Y_T^{pre} (%)	Y_T^{bot} (%)	K
	BSA				*a*-Lactalbumin			
1	4	29	66	0.06	58	20	22	2.6
2	10	0	90	0.20	64	26	11	10.42
3	23	8	69	0.45	76	19	5	22.04
4	65	30	5	27.88	71	29	0	-
	B-Lactoglobulin				*a*-Lactose			
1	18	9	73	0.24	30	4	66	0.45
2	13	0	86	0.26	17	0	83	0.18
3	15	17	68	0.29	14	8	79	0.17
4	24	19	57	0.86	7	6	87	0.08

Table 4.8. Recovery yields and partition coefficients for the biomolecules in PEG 600/potassium tartrate ATPS at 293.15 K

TL	Y_T^{top} (%)	Y_T^{pre} (%)	Y_T^{bot} (%)	K	Y_T^{top} (%)	Y_T^{pre} (%)	Y_T^{bot} (%)	K
	BSA				*a*-Lactalbumin			
1	80	16	5	37.72	57	23	20	6.47
2	89	6	4	40.39	75	25	0	-
3	77	19	4	38.16	74	26	0	-
4	79	16	5	39.29	72	28	0	-
	B-Lactoglobulin				*a*-Lactose			
1	51	16	33	3.38	31	14	54	0.57
2	73	9	19	7.47	19	0	86	0.30
3	78	22	0	-	19	9	75	0.26
4	76	24	0	-	8	6	85	0.15

According to Tables 4.7 and 4.8 and, in agreement with results obtained in the previous section, distribution of the biomolecules between equilibrium phases highly depends on the tie-line used as reference, and thus on the concentration of the phase-

forming components. The higher the TLL, the higher concentration of salt and polymer in their respective rich-phases. This increase of concentration promotes a more hydrophobic environment in the polymer-rich phase, and likewise a more hydrophilic environment in the salt-rich phase. Proteins, that preferentially go to the polymer rich phase, increase their distribution coefficient with the increase of TLL. Lactose, which generally goes to the salt rich-phase, decreases their distribution coefficient. So, the selection of high values of TLL favors the separation lactose/proteins.

4.3.1.3. Screening

The main components of cheese whey (lactose, bovine serum albumin, α-lactalbumin and β-lactoglobulin) were separated using the ATPS characterized in Tables 3.12 to 3.21. According to the results obtained in the sections 4.3.1.1 and 4.3.1.2, a low concentration of the biomolecule (0.7 mg/mL for PEG/ammonium sulfate ATPS and 1.3 mg/mL for PEG/sodium sulfate ATPS and UCON/sulfate salts ATPS) and a tie-line involving high concentration of phase-forming components, were selected to carry out the separation of the individual solutes.

Table 4.9. Tie-lines selected for biomolecules separation with PEG/Sodium Sulfate ATPS

		Feed		Top phase		Bottom phase	
PEG MM	T (K)	PEG	Salt	PEG	Salt	PEG	Salt
8000	293.15	0.128	0.084	0.395	0.007	0.000	0.185
4000	293.15	0.119	0.091	0.287	0.026	0.000	0.137
1500[78]	298.15	0.266	0.108	0.463	0.012	0.006	0.236
600[79]	298.15	0.239	0.103	0.577	<0.001	0.037	0.164
400[79]	298.15	0.300	0.096	0.401	0.029	0.013	0.304
300[79]	298.15	0.331	0.098	0.419	0.031	0.004	0.358
200[79]	298.15	0.332	0.092	0.408	0.049	0.065	0.285

The effect of PEG molecular weight on the partition of the target biomolecules was evaluated in PEG/sodium sulfate ATPS. Selected tie-lines are shown in Table

4.9. Data for PEG 8000 and 4000 were obtained from Tables 3.12 and 3.13. In the case of PEG 1500 the tie-line was obtained from literature [78], as in the case of PEG with lower molecular weights [79].

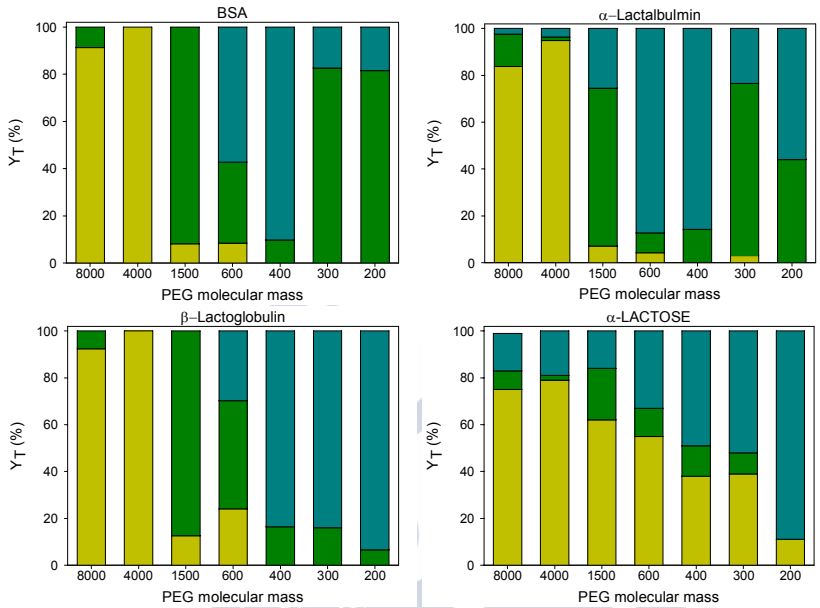

Figure 4.9. Recovery yield with PEG/Sodium sulfate ATPS (bottom: yellow, interface: green and top: blue)

The recovery yield in top, bottom and precipitate phases and distribution coefficients of the studied biomolecules in PEG/sodium sulfate ATPS are shown in Table 4.10 and Figure 4.9. Direct inspection of this figure demonstrates the notable effect of polymer molecular weight on the distribution of the biomolecules. In general, proteins have greater affinity for the top, polymer-rich phase at lower PEG molecular weights, while the affinity moves towards the bottom, salt-rich phase for higher PEG molecular weights. Apolar amino acids confer proteins a certain hydrophobicity [49, 52] while lactose is more hydrophilic. ATPS phases involve a hydrophilic environment but the top phase, rich in polymer, is more hydrophobic, so the more hydrophobic compounds such as proteins show greater affinity for this phase. When the molecular weight of the PEG increases, the ratio of hydrophilic to hydrophobic areas decreases, so a rise in the hydrophobicity is produced, causing

proteins to move to the bottom phase. The resulting protein transfer to the salt rich-phase is also due to a decrease in the free volume available in the top phase as a consequence of the increased PEG molecular weight [18, 49, 52]. Higher molecular weights also favor the concentration of lactose in the more hydrophilic (bottom) phase. In addition, the precipitation of the solutes at the interface is due to the scarcity of free water present in the system [51].

Table 4.10. Recovery yield and partition coefficient for PEG/Sodium sulfate ATPS

PEG MM	Y_T^{top} (%)	Y_T^{pre} (%)	Y_T^{bot} (%)	K	Y_T^{top} (%)	Y_T^{pre} (%)	Y_T^{bot} (%)	K
	BSA				α-Lactalbumin			
8000	0	9	91	-	2	14	84	0.04
4000	0	0	100	-	4	1	95	0.06
1500	0	92	8	-	25	67	7	2.43
600	57	34	8	3.93	87	9	4	11.80
400	90	10	0	-	86	14	0	-
300	17	83	0	-	23	74	3	2.54
200	18	82	0	-	56	44	0	6.17
	ß-Lactoglobulin				α-Lactose			
8000	0	8	92	-	16	8	75	0.28
4000	0	0	100	-	19	2	79	0.35
1500	0	87	13	-	16	22	62	0.18
600	30	46	24	0.75	33	12	55	0.34
400	84	16	0	-	49	13	38	0.43
300	84	16	0	-	52	9	39	0.42
200	94	6	0	-	89	0	11	0.83

A similar study can be carried out using ammonium sulfate as salt. Selected tie-lines of PEG/ammonium sulfate ATPS are shown in Table 4.11. Data for PEG 1500, 4000 and 8000 were obtained from Tables 3.15 to 3.17, in the case of PEG 400 and 600 the tie-lines were obtained from literature [80, 81], and data for PEG 300 were

determined according to the method presented in section 3.2.2.3 to complete the study.

Table 4.11. Tie-lines selected for biomolecules separation with PEG/Ammonium Sulfate ATPS

		Feed		Top phase		Bottom phase	
PEG MM	T (K)	PEG	Salt	PEG	Salt	PEG	Salt
8000	293.15	0.141	0.242	0.543	0.013	0.000	0.327
4000	293.15	0.124	0.124	0.362	0.003	0.000	0.174
1500	298.15	0.138	0.260	0.518	0.024	0.000	0.348
600[80]	298.15	0.396	0.084	0.177	0.200	0.098	0.259
400[81]	298.15	0.323	0.184	0.514	0.044	0.014	0.376
300	298.15	0.300	0.200	0.516	0.046	0.005	0.397

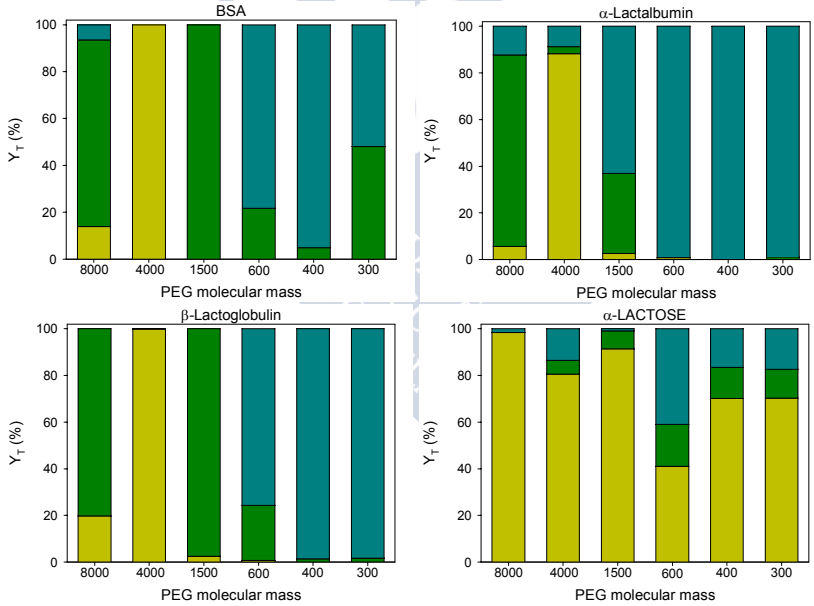

Figure 4.10. Recovery yield with PEG/Ammonium sulfate ATPS (bottom: yellow, interface: green and top: blue)

The recovery yield in top, bottom and precipitate phases and distribution coefficients of the studied biomolecules in PEG/ammonium sulfate ATPS are shown in Table 4.12 and Figure 4.10. Similar results to those obtained with sodium sulfate

were found. PEG with molecular weights lower than 1500 favor the concentration of the proteins in the top phase (polymer-rich phase) while the affinity moves towards the interface or bottom (salt-rich phase) for higher molecular weights. In this case, lactose is always found preferentially in the bottom phase, but again higher polymer molecular weights favor its concentration in this phase.

Table 4.12. Recovery yield and partition coefficient for PEG/Ammonium sulfate ATPS

PEG MM	Y_T^{top} (%)	Y_T^{pre} (%)	Y_T^{bot} (%)	K	Y_T^{top} (%)	Y_T^{pre} (%)	Y_T^{bot} (%)	K
	BSA				α-Lactalbumin			
8000	6	80	14	1.43	12	82	6	6.48
4000	0	0	100	-	9	3	88	0.17
1500	0	100	0	-	63	34	3	66.42
600	78	22	0	-	99	1	0	-
400	95	5	0	-	100	0	0	-
300	52	48	0	-	99	1	0	-
	ß-Lactoglobulin				α-Lactose			
8000	0	80	20	-	2	0	98	0.05
4000	0	0	100	-	14	6	81	0.29
1500	0	97	3	-	1	8	91	0.03
600	76	24	1	11.37	41	18	41	0.22
400	99	1	0	-	17	13	70	0.15
300	98	2	0	-	17	12	70	0.19

Tables 4.10 and 4.12 also present some information in terms of separation of the solutes. In the case of ammonium sulfate, lactose always has greater affinity for the bottom phase, independently of the PEG molecular weight. In the case of sodium sulfate, this is also true, except for PEG with the lowest molecular weights. Moreover, the quantity of lactose precipitated is less than 20 % in all cases. Thus, separation of the proteins may be possible if they are recovered in the top phase or precipitate at the interface. As a consequence, PEG 8000 and 4000 can be discarded for all ATPS because all proteins and lactose are mostly found in the salt-rich phase.

In the sodium sulfate ATPS, low molecular weight PEG (200-400) ATPS can be discarded due to the large affinity of all solutes for the top phase, while at intermediate molecular weight (600-1500) lactose cross-contaminates all phases, in contrast to the proteins which are split among the top and precipitate. Nevertheless, ammonium sulfate ATPS provide promising results at low and intermediate molecular weight (300-1500): Lactose concentrates preferentially in the bottom, salt-rich phase, while proteins concentrate in the top phase and precipitate. Among these results, the system formulated with PEG 1500 provides a very reduced protein loss to the bottom, and a high concentration of lactose in this phase. On the other hand, sodium sulfate ATPS do not show potential for separating lactose from the proteins. Even so, some degree of protein fractionation may be possible at low PEG molecular weight, since BSA mostly precipitates and β-LG concentrates in the top phase. α-LA splits between the top and the precipitate.

To obtain a better comparison among cations, ATPS were produced with UCON and several sulfate salts. Selected tie-lines of PEG/sulfate ATPS are shown in Table 4.13. Data were obtained from Tables 3.14, 3.18 and 3.19.

Table 4.13. Tie-lines selected for biomolecules separation with UCON/Sulfate ATPS at 293.15 K

	Feed		Top phase		Bottom phase	
Sulfate Salts	UCON	Salt	UCON	Salt	UCON	Salt
Sodium	0.205	0.080	0.476	0.007	0.002	0.138
Ammonium	0.222	0.089	0.486	0.016	<0.001	0.159
Potassium	0.206	0.047	0.301	0.023	0.014	0.101

The recovery yield in top, bottom and precipitate phases of the studied biomolecules in UCON/sulfate ATPS are shown in Table 4.14 and Figure 4.11. UCON has a molecular weight of 3900 g/mol, so recovery yields should be very similar to PEG with a molecular weight of 4000 g/mol. The behavior is indeed similar (see Tables 4.10 and 4.12), in the case of α-LA precipitate yields are higher with UCON than with PEG 4000 (with both sodium and ammonium cations).

UCON is more hydrophobic than PEG due to the presence of an additional methyl group [82]. The salting out effect in the bottom phase associated in this case to an increase of the hydrophobicity of the top phase may be the justification for this increase of the precipitate phase. The systems with sodium also present a significant precipitation of BSA at the interface. Comparing cations, sodium has the largest hydration shell and consequently is the most effective salting-out agent.

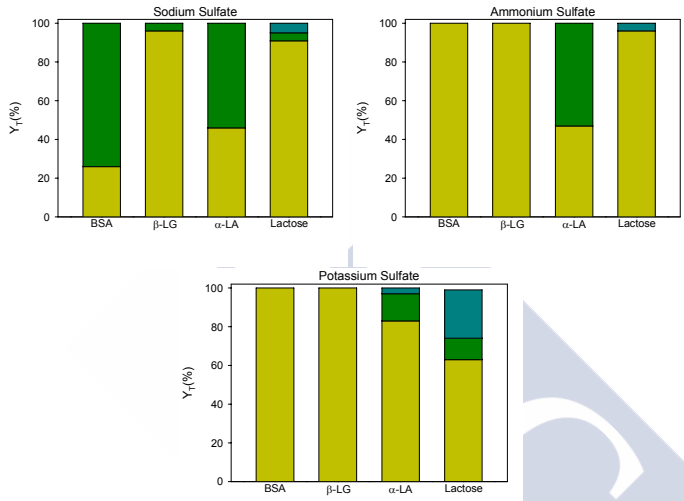

Figure 4.11. Recovery yield with UCON/Sulfate ATPS. Bottom phase: yellow; Interface: green; top phase: blue

Table 4.14. Recovery yield with PEG/Sulfate ATPS

Sulfate	Y_T^{top} (%)	Y_T^{pre} (%)	Y_T^{bot} (%)	Y_T^{top} (%)	Y_T^{pre} (%)	Y_T^{bot} (%)
	BSA			α-Lactalbumin		
Sodium	0	78	22	0	54	46
Ammonium	0	0	100	0	53	47
Potassium	0	0	100	3	14	83
	ß-Lactoglobulin			α-Lactose		
Sodium	0	4	96	3	2	91
Ammonium	0	0	100	4	0	96
Potassium	0	0	100	25	12	63

ATPS with UCON can be discarded for the application because all the biomolecules concentrate fundamentally in the bottom phase and so separation is not possible.

According to results shown in Tables 4.10 and 4.12, PEG with intermediate molecular weights seem to be the best option to separate the biomolecules of interest from cheese whey. A new test was then carried out with ATPS constituted by PEG 1500 and 600 and potassium tartrate as salt. Selected tie-lines of PEG/potassium tartrate ATPS are shown in Table 4.15. Data were obtained from Tables 3.20 and 3.21.

Table 4.15. Tie-lines selected for biomolecules separation with PEG/Potassium Tartrate ATPS at 293.15 K

	Feed		Top phase		Bottom phase	
PEG MM	PEG	Salt	PEG	Salt	PEG	Salt
1500	0.129	0.287	0.442	0.060	0.000	0.738
600	0.126	0.341	0.456	0.079	0.007	0.433

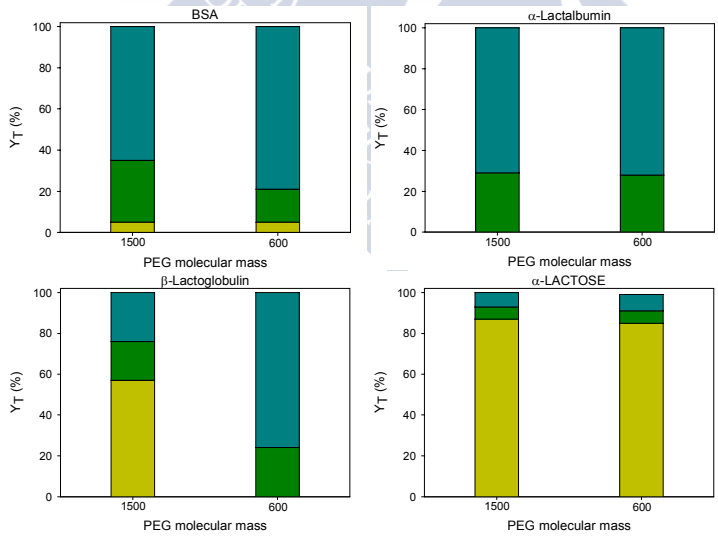

Figure 4.12. Recovery yield with PEG/Potassium tartrate ATPS (bottom: yellow, interface: green and top: blue)

Table 4.16. Recovery yield and partition coefficient with PEG/Potassium tartrate systems

PEG MM	Y_T top (%)	Y_T pre (%)	Y_T bot (%)	K	Y_T top (%)	Y_T pre (%)	Y_T bot (%)	K
	BSA				*a*-Lactalbumin			
1500	65	30	5	27.88	71	29	0	-
600	79	16	5	39.29	72	28	0	-
	B-Lactoglobulin				*a*-Lactose			
1500	24	19	57	0.86	7	6	87	0.08
600	76	24	0	-	8	6	85	0.15

The recovery yield in top, bottom and precipitate phases and distribution coefficients of the studied biomolecules in PEG/potassium tartrate ATPS are shown in Table 4.16 and Figure 4.12. As in the case of sodium or ammonium sulfate salts, the selected molecular weight favor the concentration of the proteins in the top phase and lactose in the bottom phase. Results with PEG 600 are most promising due to the high concentration of β-LG found in the bottom phase in the case of PEG 1500.

According to the results obtained, the most promising ATPS to carry out the proteins and sugar separation would be PEG 1500/ammonium sulfate, only 10 % of the proteins are lost, and PEG 600/potassium tartrate, proteins are only contaminated with less than 10 % of lactose. Furthermore, to carry out the protein partitioning the PEG 300/sodium sulfate ATPS is an interesting alternative.

4.3.1.4. The influence of pH

Considering the significant effect that pH plays on protein behavior, especially when the pI is crossed, the effect of pH on the partitioning behavior was evaluated. The ATPS selected were PEG 1500/ammonium sulfate, PEG 600/potassium tartrate, and PEG 300/sodium sulfate, since previous studies in this section showed their possible application in the valorization of cheese whey. In those studies, the pH was not fixed and values about 7.5 in the top and 8.2 in the bottom phases were found for systems with PEG and potassium tartrate, while the pH value in systems with PEG

and sulfate salts varied between 3.5 and 5.8 in both equilibrium phases. In this investigation, pH was changed in the range from 4 to 8. As the proteins have isoelectric points about 4.5-5, the screening crosses the pI of all of them.

The recovery yield in top, bottom and precipitate phases and distribution coefficients of the studied biomolecules in PEG 1500/ammonium sulfate ATPS at different pH are shown in Table 4.17 and Figure 4.13. The affinity of all proteins for the top, polymer-rich phase increases with the pH, which is in agreement with other results from the literature [49]. BSA and *β*-LG in all cases appear as a precipitate in the interface, while *α*-LA increases its affinity for the upper phase as pH reaches 7-8. About 70 % of the lactose was recovered in the bottom phase at all pH values. Even though 30 % of lactose precipitate, the best pH value to carry out the separation is 4, because 70 % of the lactose is recovered in the bottom phase while more than 95 % of proteins are precipitated.

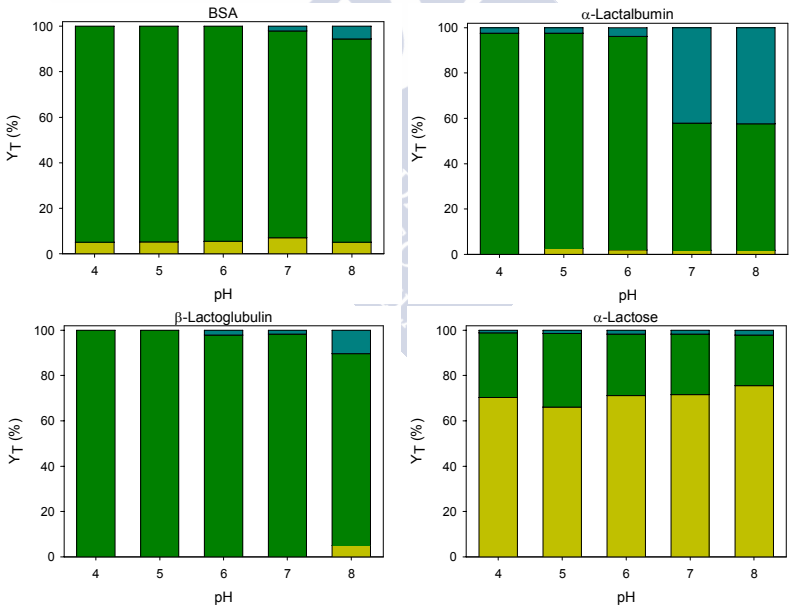

Figure 4.13. Recovery yield for PEG 1500/Ammonium sulfate systems as a function of pH (bottom: yellow, interface: green and top: blue)

Table 4.17. Recovery yield and partition coefficient for PEG 1500/Ammonium sulfate systems at different pH

pH	YT top (%)	YT pre (%)	YT bot (%)	K	YT top (%)	YT pre (%)	YT bot (%)	K
	BSA				α-Lactalbumin			
4	0	95	5	-	2	98	0	-
5	0	95	5	-	2	95	3	1.25
6	0	95	5	-	4	94	2	2.63
7	2	91	7	0.85	42	56	2	31.71
8	6	89	5	2.92	42	56	2	31.06
	ß-Lactoglobulin				α-Lactose			
4	0	100	0	-	1	29	70	0.04
5	0	100	0	-	1	33	66	0.06
6	0	98	2	-	2	27	71	0.06
7	0	98	2	-	2	27	72	0.07
8	5	85	10	1.31	2	22	76	0.07

Yield data corresponding to the PEG 600/potassium tartrate ATPS at different pH are shown in Table 4.18 and Figure 4.14. In this case, little influence of pH in biomolecules separation is found. This is likely due to the addition of the buffer solution to fix the pH produced in all the cases a white precipitate. An ion exchange was produced between sodium cation of the buffer solution and potassium cation of the ATPS salt. As a result, sodium tartrate (with much lower solubility than potassium tartrate) precipitated.

Yields presented in Table 4.18 and Table 4.8 for natural pH (tie-line 4), are very similar (see also Figure 4.14). Independently of the pH employed more than 85 % of lactose was recovered in the bottom phase, and more than 93 % of BSA and all *β*-LG and *α*-LA were recovered in top and precipitate phases. There is no reason to change the natural pH of this ATPS.

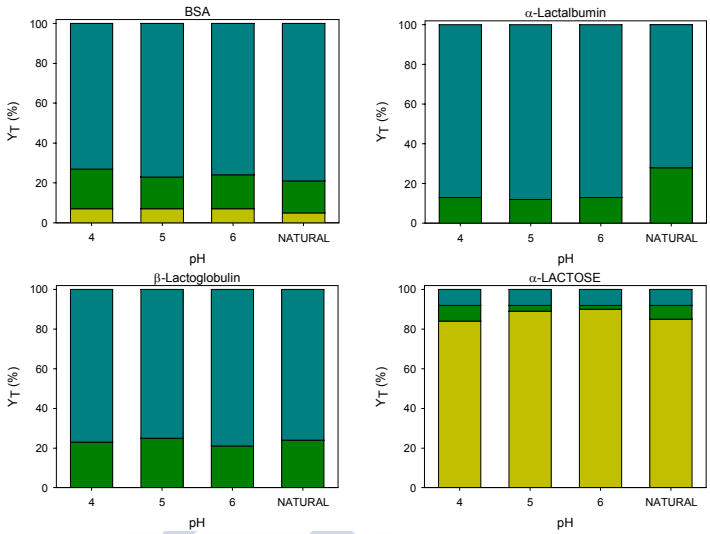

Figure 4.14. Recovery yield for PEG 600/potassium tartrate systems as a function of pH (bottom: yellow, interface: green and top: blue)

Table 4.18. Recovery yield and partition coefficient for PEG 600/Potassium tartrate systems at different pH

pH	YT top (%)	YT pre (%)	YT bot (%)	K	YT top (%)	YT pre (%)	YT bot (%)	K
	BSA				α-Lactalbumin			
4	73	20	7	25.61	87	13	0	-
5	77	16	7	25.76	88	12	0	-
6	76	17	7	26.73	87	13	0	-
	ß-Lactoglobulin				α-Lactose			
4	77	23	0	-	8	9	84	0.21
5	75	25	0	-	8	3	89	0.21
6	79	21	0	-	8	2	90	0.20

The influence of pH on the proteins separation using PEG 300/sodium sulfate ATPS was also studied. Previous results showed that there is no influence of pH on lactose separation, which is why this study was not carried out. The recovery yield in top, bottom and precipitate phases and distribution coefficients of the proteins in PEG 300/sodium sulfate ATPS at different pH are shown in Table 4.19 and Figure 4.15. In this ATPS, protein affinity for the polymer phase also increases with pH.

Besides, *β*-LG shows affinity for the top phase rich in polymer at all pH evaluated but BSA and *α*-LA precipitate at low pH. Thus, pH may be manipulated to provide some fractionation of the whey proteins. Considering these results, a partial separation could be obtained at pH 4-5.

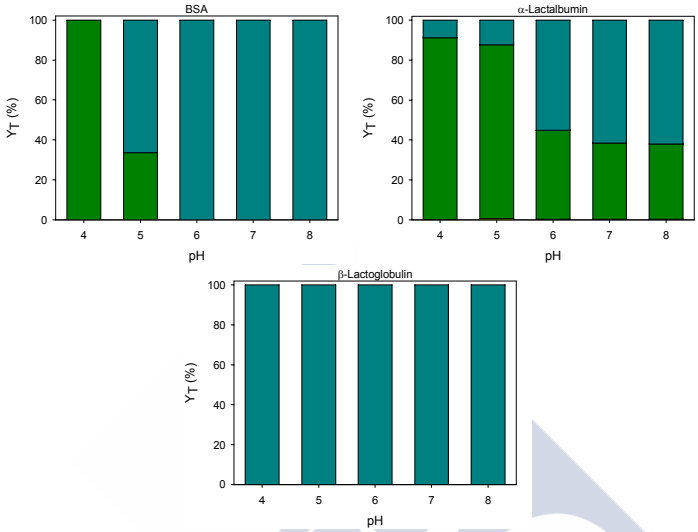

Figure 4.15. Recovery yield for PEG 300/sodium sulfate ATPS as a function of pH (bottom: yellow, interface: green and top: blue)

Table 4.19. Recovery yield and partition coefficient for PEG 300/Sodium sulfate systems at different pH.

pH	YT top (%)	YT pre (%)	YT bot (%)	K	YT top (%)	YT pre (%)	YT bot (%)	K
	BSA				α-Lactalbumin			
4	0	100	0	-	9	91	0	-
5	66	34	0	-	12	87	1	9.70
6	100	0	0	-	55	45	0	-
7	100	0	0	-	61	39	0	-
8	100	0	0	-	62	38	0	-
	ß-Lactoglobulin							
4	100	0	0	-				
5	100	0	0	-				
6	100	0	0	-				
7	100	0	0	-				
8	100	0	0	-				

4.3.2. Separation Strategies

The results obtained in the previous section were used to depict different strategies in order to carry out the recovery of added-value compounds in cheese whey using ATPS. These strategies were assessed using first a synthetic whey formulated with the key solutes dissolved in distilled water, and later using a real cheese whey from a local cheese producer. Comparisons with a most traditional method (UF) were also carried out. According to results obtained in section 4.3.1, an initial separation of proteins and sugar was considered, followed by a proteins fractionation stage.

4.3.2.1. Proteins/sugar separation

PEG 1500/Ammonium Sulfate ATPS

PEG 1500/ammonium sulfate at 298.15 K and pH=4 may provide a way of recovering most proteins on the top phase or precipitate, and thus separated from lactose which is recovered mostly on the bottom phase. Some limited BSA loss to the bottom phase and some cross-contamination of lactose in the precipitate could be expected (see Table 4.17, Figure 4.13). This strategy is presented in Figure 4.16.

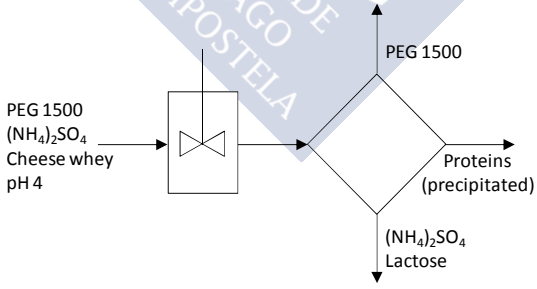

Figure 4.16. Flow diagram with the strategy to separate lactose and proteins with PEG 1500/ammonium sulfate ATPS at pH=4.

The results of the application of this strategy of separation to simulated and real cheese whey are summarized in Table 4.20 and Figure 4.17. It is clear that the outcome for real cheese whey just confirms the behavior of the simulated whey. The

results mimic what was found for the individual solutes at pH 4 (see Figure 4.13). For both simulated and real whey 100 % of BSA and β-LG and >96 % of α-LA were recovered as a precipitate in the interface. This precipitate also contained 15 % (simulated)-20 % (real) of lactose, that was recovered preferentially in the bottom phase. Thus, the separation of these compounds is feasible using one step extraction.

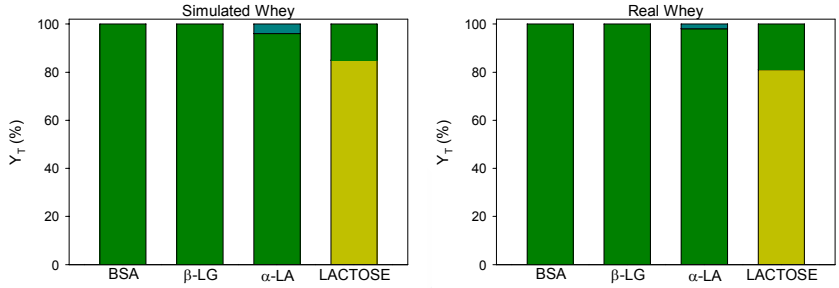

Figure 4.17. Recovery yields results of the application of PEG 1500/ammonium sulfate ATPS to simulated and real cheese whey (Bottom: yellow, interface: green and top: blue)

Table 4.20. Recovery yield results of the application of PEG 1500/ammonium sulfate ATPS to simulated and real cheese whey at 298.15 K and pH=4

Target	Simulated Whey			Real Whey		
	YT top (%)	YT pre (%)	YT bot (%)	YT top (%)	YT pre (%)	YT bot (%)
BSA	0	100	0	0	100	0
ß-LG	0	100	0	0	100	0
α-LA	4	96	0	2	98	0
α-Lactose	0	15	85	0	19	81

PEG 600/Potassium tartrate ATPS

Another interesting alternative to be considered in proteins and sugar separation is formulated combing PEG 600 and potassium tartrate at 293.15 K and the natural pH of the system. According to Table 4.18 and Figure 4.14, about 85 % of lactose should be recovered in the bottom phase with a little contamination of

BSA, and most of the proteins should be recovered in the top and precipitate phases. This strategy of separation is presented in Figure 4.18.

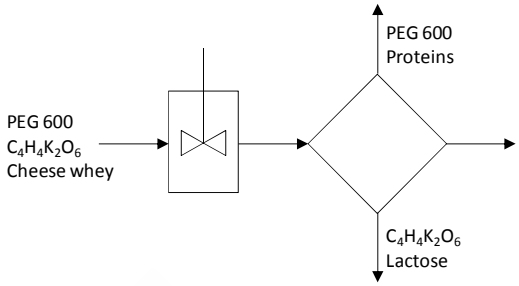

Figure 4.18. Flow diagram with the strategy to separate lactose and proteins with PEG 600/potassium tartrate ATPS

The results of the proteins and sugar separation with this strategy are summarized in Table 4.21 and Figure 4.19. Again, results obtained with simulated and real cheese whey are very similar. However, results are more promising than expected. All the lactose was obtained in the bottom phase without contamination of any protein. Those could be recovered from top and precipitate phases. Pure lactose and a whey protein concentrate were obtained with this strategy.

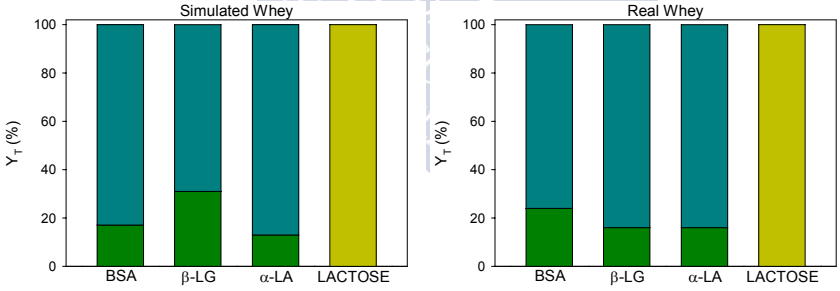

Figure 4.19. Recovery yields results of the application of PEG 600/potassium tartrate ATPS to simulated and real cheese whey (Bottom: yellow, interface: green and top: blue)

Table 4.21. Recovery yield results of the application of PEG 600/potassium tartrate ATPS to simulated and real cheese whey a 293.15 K and natural pH

Target	Simulated Whey			Real Whey		
	YT top (%)	YT pre (%)	YT bot (%)	YT top (%)	YT pre (%)	YT bot (%)
BSA	83	17	0	76	24	0
ß-LG	69	31	0	84	16	0
α-LA	87	13	0	84	16	0
α-Lactose	0	0	100	0	0	100

Ultrafiltration

The last strategy of proteins/lactose separation tested was UF. To that aim, Amicon Ultra-0.5 Centrifugal Filter Devices ultracel 30 K were used. Recovery yields in retentate (ret) and permeate (per) are summarized in Table 4.22 and Figure 4.20. Mass balance was used to calculate the biomolecules retained inside the filter (fil). As expected, and with similar numbers for simulate and real cheese whey, lactose was mainly recovered in the permeate and the proteins in retentate. However, significant quantities of β-LG and α-LA were lost inside the filter. This fact prevents the use of UF in just one step of separation.

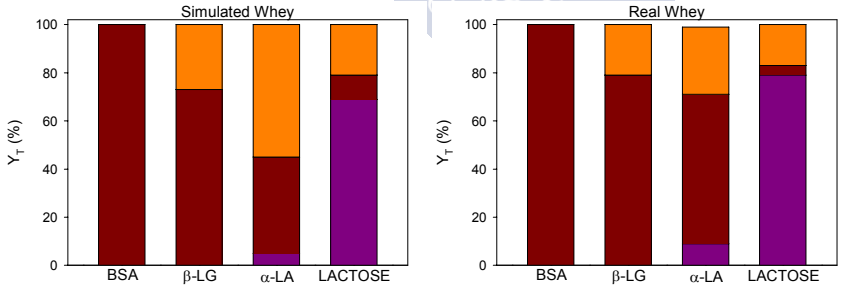

Figure 4.20. Recovery yields results of the application of UF to simulated and real cheese whey (Retentate: red, permeate: purple and lost in the filter: orange).

Table 4.22. Recovery yield results of the application of UF to simulated and real cheese whey at room conditions.

Target	Simulated Whey			Real Whey		
	YT ret (%)	YT per (%)	YT filt (%)	YT ret (%)	YT per (%)	YT filt (%)
BSA	100	0	0	100	0	0
β-LG	73	0	27	79	0	21
α-LA	40	5	55	63	9	28
α-Lactose	10	68	21	4	79	17

4.3.2.2. Proteins' fractionation

PEG 300/sodium sulfate ATPS

This strategy involves the use of two aqueous biphasic systems in series. First step at pH 4 separates the β-LG in the top phase contaminated with ~9 % of the *α*-LA, whilst most *α*-LA and BSA are precipitated in the interface (Table 4.19, Figure 4.15). Then BSA and *α*-LA are separated using the same phase-forming compounds at pH 5, which yields BSA in the top phase and *α*-LA in the precipitate (see Figure 4.21).

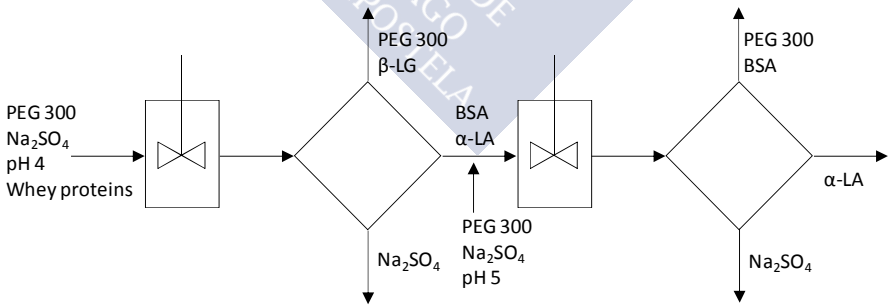

Figure 4.21. Flow diagram with the strategy for whey proteins' fractionation using two ATPS in series

When the precipitate, obtained from the treatment of simulated and real cheese whey with PEG 1500/Ammonium Sulfate ATPS, was re-suspended (either in

distilled water or phosphate buffer solution), all proteins precipitated in the first step of this strategy and no separation was obtained. The same problem was found working with the precipitate obtained with PEG 600/potassium tartrate. Protein co-precipitation or the presence of components from the previous ATPS may be the reasons for this behavior, different from what would be expected from the single solutes. But that was not further investigated. Instead, a simulated whey without lactose was prepared and this strategy was tested again. The results obtained are presented in Table 23 and Figure 22. In the first step with the simulated whey, the expected recovery of β-LG in the top phase was not obtained: 18 % β-LG was lost in the precipitate, and 44 % of the α-LA was also present in the top phase. The second step (applied to the precipitated proteins) also did not reproduce the behavior of single solutes. Most of the proteins again precipitated, and no further fractionation was obtained. When the real cheese whey was used, the mass of BSA recovered as a precipitate in the interface of the ATPS was significantly lower, while β-LG and α-LA behave similarly to the simulated whey. In the second step, it was again impossible to obtain the separation of the proteins. It is clear that in these ATPS the behavior of the proteins changes with the presence of other proteins (mixture), avoiding a proper fractionation of the key proteins.

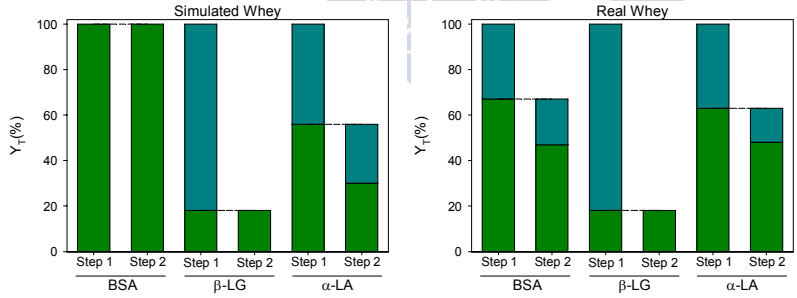

Figure 4.22. Recovery yield for key solutes. (Interface: green and top: blue)

Table 4.23. Recovery yield (%) for proteins using two ATPS in series

	Step 1 (ATPS)			Step 2 (ATPS)		
	Bottom	Precipitate	Top	Bottom	Precipitate	Top
Protein	Simulated whey					
BSA	0	100	0	0	100	0
β-LG	0	18	82	0	18	0
α-LA	0	56	44	0	30	26
	Real whey					
BSA	0	67	33	0	47	20
β-LG	0	18	82	0	18	0
α-LA	0	63	37	0	48	15

PEG 300/sodium sulfate ATPS + UF

This strategy involves the use of one ATPS followed by ultrafiltration. The first part of the whey treatment would be the same that in the previous strategy. Then in a second step the precipitated is re-suspended using PBS and UF is used to separate BSA and *α*-LA (see Figure 4.23).

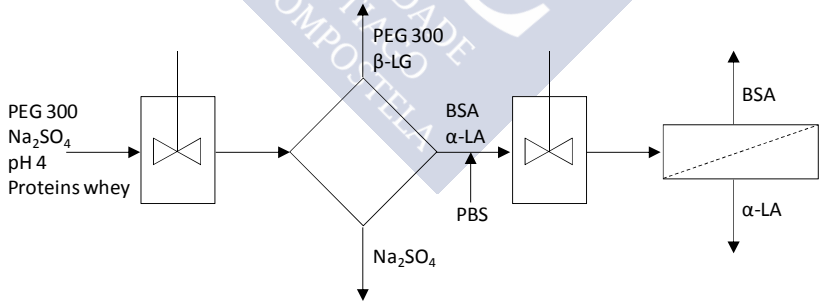

Figure 4.23. Flow diagram with the strategy for whey proteins' fractionation using an ATPS followed by UF

The results obtained are presented in Table 4.24 and Figure 4.24. Obviously, the results of the first step were coincident with the previous strategy: with simulated whey 82 % *β*-LG was separated in the first step (contaminated with the other

proteins). The second step also did not reproduce the expected behavior. A very low quantity of α-LA was obtained in the permeate, a mixture of proteins was found in the retentate and significant losses (inside the filter) were detected. The behavior with the real whey was very similar.

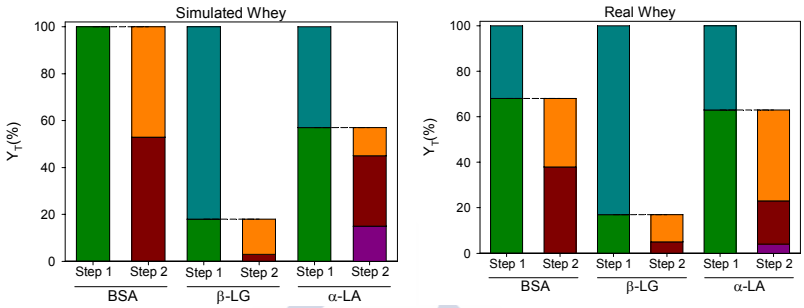

Figure 4.24. Recovery yield for key solutes. (ATPS: Precipitate: green, top phase: blue; UF: Retentate: red, permeate: purple, lost in the filter: orange)

Table 4.24. Recovery yield (%) for proteins using ATPS followed by UF

	Step 1 (ATPS)			Step 2 (UF)		
	Bottom	Precipitate	Top	Permeate	Retentate	Filter
Protein	Simulated whey					
BSA	0	100	0	0	53	47
ß-LG	0	18	82	0	3	15
α-LA	0	57	43	15	20	12
	Real whey					
BSA	0	68	32	0	38	30
ß-LG	0	17	83	0	5	12
α-LA	0	63	37	4	19	40

UF + PEG 300/sodium sulfate ATPS

A last attempt to recover proteins is proposed according the strategy shown in Figure 4.25. Whey is first filtered to separate BSA and then PEG 300 and sodium sulfate are used at pH=4 to form an ATPS for the separation of β-LG and α-LA.

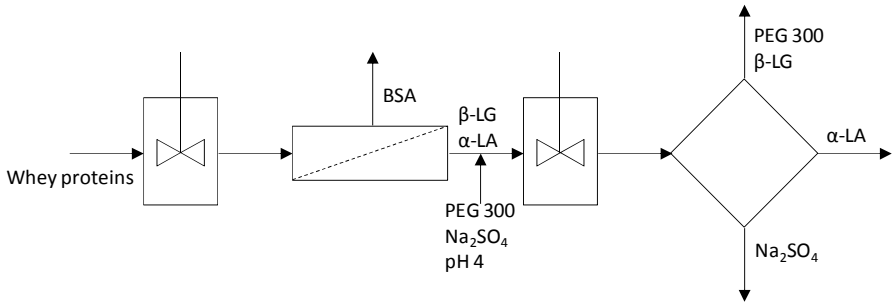

Figure 4.25. Flow diagram with the strategy for whey proteins' fractionation using UF followed by ATPS

The results obtained with simulated whey (without lactose) are presented in Table 4.25 and Figure 4.26. About 74 % of BSA was recovered in the retentate with a significant contamination of the other proteins. In addition more than 20 % of the proteins was lost inside the filter. In the second step, 29 % of the original quantity of α-LA was obtained pure in the top phase of the ATPS, the rest of the proteins from the permeate phase were found mixed at the interface of the ATPS as a precipitate. Due to the bad results, tests were not carried out with real cheese whey.

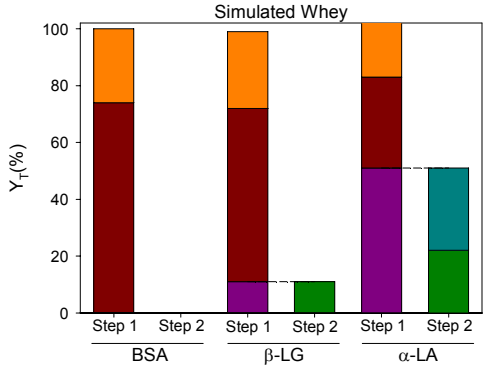

Figure 4.26. Recovery yield for key solutes. (ATPS: Precipitate: green, top phase: blue; UF: Retentate: red, permeate: purple, lost in the filter: orange)

Table 4.25. Recovery yield (%) for proteins using UF followed by ATPS

	Step 1 (phase)			Step 2 (phase)		
Protein	Permeate	Retentate	Filter	Bottom	Precipitate	Top
BSA	0	74	26	0	0	0
β-LG	11	61	27	0	11	0
α-LA	51	32	18	0	22	29

5. Conclusions

USC
UNIVERSIDADE
DE SANTIAGO
DE COMPOSTELA

5. CONCLUSIONS

In order to evaluate whether ATPS can be used for the recovery of high added-value components from cheese whey, polymers and salts were selected as phase-forming agents due to their low toxicity and biocompatibility with the biomolecules to be extracted.

The pairs PEG 4000, PEG 8000 or UCON with sodium sulfate, UCON with potassium sulfate, PEG 1500, PEG 4000, PEG 8000 or UCON with ammonium sulfate, and PEG 600 or PEG 1500 with potassium tartrate are able to form two equilibrium phases with high proportion of water at temperatures from 278.15 K to 308.15 K. In the case of sodium sulfate, its low solubility in water at 278.15K prevents the formation of ATPS at this temperature due to problems of salt precipitation. In contrast, the high solubility of potassium tartrate in water, even at low temperatures, makes this salt a promising phase-forming ingredient for ATPS formulations, and thus of interest for the application of extraction processes in biotechnology.

The use of density in the case of binary mixtures (water and salt), and density and refractive index in the case of ternary mixtures (water, salt and polymer) is a suitable analytical tool to determine compositions. The determination of tie-lines' ends with this method leads to more accurate data than other methods frequently used in literature that are based on visual inspection.

Regarding the phase diagrams obtained, the heterogeneous region for each system increases with temperature. Although increasing the temperature produces an increase of the immiscible region and consequently the requirement of lower amounts of the phase-forming agents, this also leads to a higher energy demand. Temperatures closer to ambient would be considered preferable for industrial applications. In all the systems studied, the top phase is polymer-rich, and the bottom phase is salt-rich. However, in the case of systems with UCON, a phase

inversion occurs at the highest temperature (308.15 K), a fact that should be considered in processes with these systems.

In the case of sulfate salts, the sodium ion (with a larger hydration shell than potassium and ammonium and thus a better salting-out agent) leads to larger heterogeneous regions. In the case of PEG, an increase of the polymer molecular weight also increases the immiscible region. However, the appropriate salt and polymer for the separation of cheese whey components, or any other application, can only be defined through study of the partitioning of the solutes of interest.

The Merchuk equation provides an excellent correlation of binodal curve data. This empirical equation leads to better results than the effective excluded volume model of Guan and co-workers. However, the latter provides some thermodynamic insight and the obtained *EEV* in general confirm the influence of temperature, salt and polymer on the heterogeneous region of the phase diagrams. Also the model of Guan and co-workers satisfactorily correlates tie-lines' data except in the region closer to the plait point.

Partitioning of the main components of cheese whey (lactose, BSA, β-LG and α-LA) in the characterized ATPS was studied. The work at different concentrations of lactose indicates that the concentration of solute does not affect the distribution coefficients obtained. The work with all the solutes, using ATPS with different PEG and potassium tartrate concentrations, shows that high values of *TLL* led to higher protein and lower lactose distribution coefficients, so favor the desired separation.

For systems formulated with sodium or ammonium salts, all the biomolecules concentrate in the top phase in the case of PEG of higher molecular weights. Lactose, which is more hydrophilic, preferentially goes to the bottom phase with a decrease of the polymer molecular weight. According to this study with the individual solutes, ammonium sulfate with PEG 1500 at 293.15 K would be an appropriate system to obtain lactose in the bottom phase and proteins in the top or precipitate phase. This separation is favored at low pH (4). PEG 600 and potassium tartrate at 293.15 K could also be used to separate lactose and proteins at the natural

pH of the system (the introduction of buffers to modify the pH causes problems of precipitation). With all the systems studied, a high percentage of precipitate was found at the interface, making yields more useful parameters to analyze biomolecule separation than distribution coefficients or selectivities. ATPS formulated with UCON and sulfate salts at 293.15 K are not useful for the target application because all the biomolecules concentrate in the bottom phase (with higher precipitation at the interface with the sodium cation due to its higher salting-out effect). Systems with PEG 300 and sodium sulfate at 298.15 K were found to be able to fractionate proteins. pH values of 4-5 could be used to optimize the process.

According to these conclusions, different separation strategies were designed to carry out the lactose/protein separation and then fractionation of the proteins. These separation strategies were evaluated experimentally using first a simulated cheese whey (aqueous solution of the biomolecules of interest) and then a real cheese whey from a local producer (Queizúar S.L.).

Results obtained with the real cheese whey confirmed the behavior obtained with the synthetic mixture. As expected, PEG 1500/ammonium sulfate and PEG 600/potassium tartrate ATPS are useful tools to separate lactose and a protein concentrate from cheese whey. The system with the organic salt is more promising because a perfect separation was reached with total absence of cross-contamination. Unfortunately, protein fractionation was not possible using PEG 300/ sodium sulfate ATPS. In spite of having obtained better results than those using UF in just one stage, the separation of the individual proteins from the concentrate was not achieved. Future studies need to be carried out first to separate lactose and proteins from the aqueous solutions with the phase-forming agents, and then focusing on the fractionation of the concentrate with ATPS or different technologies.

USC
UNIVERSIDADE
DE SANTIAGO
DE COMPOSTELA

REFERENCES

USC
UNIVERSIDADE
DE SANTIAGO
DE COMPOSTELA

REFERENCES

[1] H. Sainz, A. Sanz, J. Agudo, V.J. Martín Cerdeño, Alimentación en España 2016, 19th ed., Madrid (Spain), 2016/2017.

[2] A.R. Prazeres, F. Carvalho, J. Rivas, Cheese whey management: A review, *J. Environ. Manage.*, 110 (2012) 48-68.

[3] Estadísticas agrarias, Online resource, avaliable at: https://www.mapa.gob.es/es/estadistica/temas/estadisticas-agrarias/ganaderia/estadistica-industrias-lacteas/, (last accessed: January 2019) (2005-2017).

[4] M.I.G. Siso, The biotechnological utilization of cheese whey: A review, *Bioresource Technol.*, 57 (1996) 1-11.

[5] C. Mollea, L. Marmo, F. Bosco, Valorisation of Cheese Whey, a By-Product from the Dairy Industry, in: I. Muzzalupo (Ed.) Food Industry, 2013, pp. 549-588.

[6] L.M. Huffman, L. de Barros Ferreira, Whey-Based Ingredients, in: A.K. Ramesh C. Chandan (Ed.) Dairy Ingredients for Food Processing, Wiley-Blackwell, Iowa (USA), 2011, pp. 179-198.

[7] M.R. Etzel, Manufacture and use of dairy protein fractions, *J. Nutr.*, 134 (2004) 996-1002.

[8] A.R. Madureira, C.I. Pereira, A.M.P. Gomes, M.E. Pintado, F. Xavier Malcata, Bovine whey proteins – Overview on their main biological properties, *Food Res. Int.*, 40 (2007) 1197-1211.

[9] G. Johansson, Partitioning of Proteins in: D.E. Brooks, D. Fisher (Eds.) Partitioning in Aqueous Two-Phase System, Academic Press, Orlando (USA), 1985, pp. 161-226.

[10] P. Kumar, N. Sharma, R. Ranjan, S. Kumar, Z. Bhat, D.K. Jeong, Perspective of membrane technology in dairy industry: A review, *Asian Austral. J. Anim*, 26 (2013) 1347-1358.

[11] M.M.H. El-Sayed, H.A. Chase, Trends in whey protein fractionation, *Biotechnol. Lett.*, 33 (2011) 1501-1511.

[12] P.G. Mazzola, A.M. Lopes, F.A. Hasmann, A.F. Jozala, T.C. Penna, P.O. Magalhaes, C.O. Rangel-Yagui, A. Pessoa Jr, Liquid–

liquid extraction of biomolecules: an overview and update of the main techniques, *J. Chem. Technol. Biot.*, 83 (2008) 143-157.

[13] A. Dobry, F. Boyer-Kawenoki, Phase separation in polymer solution, *J. Polym. Sci.*, 2 (1947) 90-100.

[14] P.Å. Albertsson, Partition of Cell Particles and Macromolecules, 3rd ed., J. Wiley, New York (USA), 1985.

[15] B.Y. Zaslavsky, Aqueous two-phase partitioning: physical chemistry and bioanalytical applications, CRC Press, New York (USA), 1994.

[16] S.C. Silvério, O. Rodríguez, J.A. Teixeira, E.A. Macedo, The Effect of Salts on the Liquid–Liquid Phase Equilibria of PEG600 + Salt Aqueous Two-Phase Systems, *J. Chem. Eng. Data*, 58 (2013) 3528-3535.

[17] Y. Liu, Y. Yu, M. Chen, X. Xiao, Advances in aqueous two-phase systems and applications in protein separation and purification, *Can. J. Chem. Eng. Technol.*, 2 (2011) 1-7.

[18] M. Rito-Palomares, J. Benavides, Aqueous Two-Phase Systems for Bioprocess Development for the Recovery of Biological Products, Springer, Whashinton State University (USA), 2017.

[19] H.O. Johansson, M. Svensson, J. Persson, F. Tjerneld, Aqueous two-phase systems with smart polymers, in: Igor Y. Galaev, B. Mattiasson (Eds.) Smart Polymers, Taylor & Francis, 2002.

[20] M. Pereira, Y.-T. Wu, A. Venâncio, J. Teixeira, Aqueous two-phase extraction using thermoseparating polymer: a new system for the separation of endo-polygalacturonase, *Biochem. Eng. J.*, 15 (2003) 131-138.

[21] M. Pereira, Y.-T. Wu, P. Madeira, A. Venâncio, E. Macedo, J. Teixeira, Liquid−Liquid Equilibrium Phase Diagrams of New Aqueous Two-Phase Systems: Ucon 50-HB5100 + Ammonium Sulfate + Water, Ucon 50-HB5100 + Poly(vinyl alcohol) + Water, Ucon 50-HB5100 + Hydroxypropyl Starch + Water, and Poly(ethylene glycol) 8000 + Poly(vinyl alcohol) + Water, *J. Chem. Eng. Data*, 49 (2004) 43-47.

[22] G. Tubio, B.B. Nerli, G.A. Picó, A. Venâncio, J. Teixeira, Liquid–liquid equilibrium of the Ucon 50-HB5100/sodium citrate aqueous two-phase systems, *Sep. Purif. Technol.*, 65 (2009) 3-8.

[23] S.C. Silvério, O. Rodríguez, J.A. Teixeira, E.A. Macedo, Liquid−Liquid Equilibria of UCON + (Sodium or Potassium) Phosphate Salt Aqueous Two-Phase Systems at 23 °C, *J. Chem. Eng. Data*, 55 (2010) 1285-1288.

[24] E. Lladosa, S.C. Silvério, O. Rodríguez, J.A. Teixeira, E.A. Macedo, (Liquid + liquid) equilibria of polymer-salt aqueous two-phase systems for laccase partitioning: UCON 50-HB-5100 with potassium citrate and (sodium or potassium) formate at 23 °C, *J. Chem. Thermodyn.*, 55 (2012) 166-171.

[25] K.S. Nascimento, S. Yelo, B.S. Cavada, A.M. Azevedo, M.R. Aires-Barros, Liquid− liquid equilibrium data for aqueous two-phase systems composed of ethylene oxide propylene oxide copolymers, *J. Chem. Eng. Data*, 56 (2011) 190-194.

[26] A.D. Diamond, J.T. Hsu, Aqueous two-phase systems for biomolecule separation, in: G.T. Tsao (Ed.) Bioseparation, Springer Berlin Heidelberg, 1992, pp. 89-135.

[27] J. Benavides, M. Rito-Palomares, Practical experiences from the development of aqueous two-phase processes for the recovery of high value biological products, *J. Chem. Technol. Biot.*, 83 (2008) 133-142.

[28] M.G. Freire, A.F.M. Claudio, J.M. Araujo, J.A. Coutinho, I.M. Marrucho, J.N.C. Lopes, L.P.N. Rebelo, Aqueous biphasic systems: a boost brought about by using ionic liquids, *Chem. Soc. Rev.*, 41 (2012) 4966-4995.

[29] Y. Wang, Y. Yan, S. Hu, J. Han, X. Xu, Phase Diagrams of Ammonium Sulfate + Ethanol/1-Propanol/2-Propanol + Water Aqueous Two-Phase Systems at 298.15 K and Correlation, *J. Chem. Eng. Data*, 55 (2010) 876-881.

[30] C.W. Ooi, B.T. Tey, S.L. Hii, S.M.M. Kamal, J.C.W. Lan, A. Ariff, T.C. Ling, Purification of lipase derived from Burkholderia pseudomallei with alcohol/salt-based aqueous two-phase systems, *Process Biochem.*, 44 (2009) 1083-1087.

[31] A. Salabat, M.R. Far, S.T. Moghadam, Partitioning of Amino Acids in Surfactant Based Aqueous Two-Phase Systems Containing the Nonionic Surfactant (Triton X-100) and Salts, *J. Solution Chem.*, 40 (2011) 61-66.

[32] M. Amid, F.S. Murshid, M.Y. Manap, M. Hussin, A Novel Aqueous Micellar Two-Phase System Composed of Surfactant and Sorbitol for Purification of Pectinase Enzyme from Psidium guajava and Recycling Phase Components, *Biomed. Res. Int.*, 2015 (2015) 8.

[33] F.A. Vicente, L.P. Malpiedi, F.A. e Silva, A. Pessoa, J.A.P. Coutinho, S.P.M. Ventura, Design of novel aqueous micellar two-phase systems using ionic liquids as co-surfactants for the selective extraction of (bio)molecules, *Sep. Purif. Technol.*, 135 (2014) 259-267.

[34] G. Pico, D. Romanini, B. Nerli, B. Farruggia, Polyethyleneglycol molecular mass and polydispersivity effect on protein partitioning in aqueous two-phase systems, *J. Chromatogr. B* 830 (2006) 286-292.

[35] C.-l. Liu, D.T. Kamei, J.A. King, D.I.C. Wang, D. Blankschtein, Separation of proteins and viruses using two-phase aqueous micellar systems, *J. Chromatogr. B*, 711 (1998) 127-138.

[36] S.P. Duarte, A.G. Fortes, D.M. Prazeres, J.C. Marcos, Preparation of plasmid DNA polyplexes from alkaline lysates by a two-step aqueous two-phase extraction process, *J. Chromatogr. A*, 1164 (2007) 105-112.

[37] C. Kepka, R. Lemmens, J. Vasi, T. Nyhammar, P.-E. Gustavsson, Integrated process for purification of plasmid DNA using aqueous two-phase systems combined with membrane filtration and lid bead chromatography, *J. Chromatogr. A*, 1057 (2004) 115-124.

[38] E. Esmanhoto, B.V. Kilikian, ATPS applied to extraction of small molecules - polycetides - and simultaneous clarification of culture media with filamentous microorganisms, *J. Chromatogr. B* 807 (2004) 139-143.

[39] K.-H. Nam, W.-J. Chang, H. Hong, S.-M. Lim, D.-I. Kim, Y.-M. Koo, Continuous-Flow Fractionation of Animal Cells in Microfluidic Device Using Aqueous Two-Phase Extraction, *Biomed. Microdevices*, 7 (2005) 189-195.

[40] D.M. Morré, D.J. Morre, Aqueous two-phase partition applied to the isolation of plasma membranes and Golgi apparatus from cultured mammalian cells, *J. Chromatogr. B*, 743 (2000) 377-387.

[41] R. Hatti-Kaul, Aqueous two-phase systems: methods and protocols, Humana Press, Inc., New Jersey (USA), 2000.

[42] O. Rodríguez, S.C. Silvério, P.P. Madeira, J.A. Teixeira, E.A. Macedo, Physicochemical Characterization of the PEG8000-Na2SO4Aqueous Two-Phase System, *Ind. Eng. Chem. Res.*, 46 (2007) 8199-8204.

[43] J. Benavides, O. Aguilar, B.H. Lapizco-Encinas, M. Rito-Palomares, Extraction and Purification of Bioproducts and Nanoparticles using Aqueous Two-Phase Systems Strategies, *Chem. Eng. Technol.*, 31 (2008) 838-845.

[44] J.A. Asenjo, B.A. Andrews, Aqueous two-phase systems for protein separation: a perspective, *J. Chromatogr. A*, 1218 (2011) 8826-8835.

[45] B.A. Andrews, A.S. Schmidt, J.A. Asenjo, Correlation for the partition behavior of proteins in aqueous two-phase systems: Effect of surface hydrophobicity and charge, *Biotechnol. Bioeng.*, 90 (2005) 380-390.

[46] J. Huddleston, A. Veide, K. Köhler, J. Flanagan, S.-O. Enfors, A. Lyddiatt, The molecular basis of partitioning in aqueous two-phase systems, *Trends Biotechnol.*, 9 (1991) 381-388.

[47] L.R. Rodrigues, A. Venâncio, J.A. Teixeira, Partitioning and separation of α-lactalbumin and β-lactoglobulin in polyethylene glycol/ammonium sulphate aqueous two-phase systems, *Biotechnol. Lett.*, 23 (2001) 1893-1897.

[48] J.G.L.F. Alves, L.D.A. Chumpitaz, L.H.M. da Silva, T.T. Franco, A.J.A. Meirelles, Partitioning of whey proteins, bovine serum albumin and porcine insulin in aqueous two-phase systems, *J. Chromatogr. B*, 743 (2000) 235-239.

[49] J.P. Chen, Partitioning and separation of α-lactalbumin and β-lactoglobulin in PEG/potassium phosphate aqueous two-phase systems, *J. Ferment. Bioeng.*, 73 (1992) 140-147.

[50] L. Capezio, D. Romanini, G.A. Pico, B. Nerli, Partition of whey milk proteins in aqueous two-phase systems of polyethylene glycol-phosphate as a starting point to isolate proteins expressed in transgenic milk, *J. Chromatogr. B* 819 (2005) 25-31.

[51] H. Zhang, B. Jiang, Z.B. Feng, Y.X. Qu, X. Li, Separation of alpha-Lactalbumin and beta-Lactoglobulin in Whey Protein Isolate by Aqueous Two-phase System of Polymer/Phosphate, *Chinese J. Anal. Chem.*, 44 (2016) 754-759.

[52] A. Boaglio, G. Bassani, G. Picó, B. Nerli, Features of the milk whey protein partitioning in polyethyleneglycol-sodium citrate aqueous two-phase systems with the goal of isolating human alpha-1 antitrypsin expressed in bovine milk, *J. Chromatogr. B*, 837 (2006) 18-23.

[53] L.A.P. Alcântara, L.A. Minim, V.P.R. Minim, R.C.F. Bonomo, L.H.M. da Silva, M.d.C.H. da Silva, Application of the response surface methodology for optimization of whey protein partitioning in PEG/phosphate aqueous two-phase system, *J. Chromatogr. B*, 879 (2011) 1881-1885.

[54] K. Sivakumar, R. Iyyaswami, Recovery and Partial Purification of Bovine α-Lactalbumin from Whey Using PEG 1000–Trisdoium Citrate Systems, *Sep. Purif. Technol.*, 50 (2015) 833-840.

[55] R. Domínguez-Puerto, S. Valle-Guadarrama, D. Guerra-Ramírez, F. Hahn-Schlam, Purification and concentration of cheese whey proteins through aqueous two phase extraction, *CyTA - Journal of Food*, 16 (2018) 452-459.

[56] C. Anandharamakrishnan, S.N. Raghavendra, R.S. Barhate, U. Hanumesh, K.S.M.S. Raghavarao, Aqueous Two-Phase Extraction For Recovery Of Proteins From Cheese Whey, *Food Bioprod. Process.*, 83 (2005) 191-197.

[57] N.R. Council, International Critical Tables of Numerical Data, Physics, Chemistry and Technology, The National Academies Press, Washington, DC, 1930.

[58] M.T. Zafarani-Moattar, B. Asadzadeh, Vapor–Liquid Equilibria, Density, Speed of Sound, and Viscosity of Aqueous Dipotassium

Tartrate Solutions at T = (298.15, 308.15, and 318.15) K, *J. Chem. Eng. Data*, 53 (2008) 1000-1006.

[59] E.W. Washburn, C.J. West, International critical tables of numerical data, physics, chemistry and technology, National Academies, 1928.

[60] D.K. Brenner, E.W. Anderson, S. Lynn, J.M. Prausnitz, Liquid-liquid equilibria for saturated aqueous solutions of sodium sulfate + 1-propanol, 2-propanol, or 2-methylpropan-2-ol, *J. Chem. Eng. Data*, 37 (1992) 419-422.

[61] O.C. Okorafor, Solubility and Density Isotherms for the Sodium Sulfate−Water−Methanol System, *J. Chem. Eng. Data*, 44 (1999) 488-490.

[62] H. von Plessen, Sodium Sulfates, in: Ullmann's Encyclopedia of Industrial Chemistry, Wiley-VCH Verlag GmbH & Co. KGaA, 2000.

[63] S.M. Snyder, K.D. Cole, D.C. Szlag, Phase compositions, viscosities, and densities for aqueous two-phase systems composed of polyethylene glycol and various salts at 25 .degree.C, *J. Chem. Eng. Data*, 37 (1992) 268-274.

[64] M.E. Taboada, O.A. Rocha, T.A. Graber, B.A. Andrews, Liquid−Liquid and Solid−Liquid Equilibria of the Poly(ethylene glycol) + Sodium Sulfate + Water System at 298.15 K, *J. Chem. Eng. Data*, 46 (2001) 308-311.

[65] C.P. Carvalho, J.S.R. Coimbra, I.A.F. Costa, L.A. Minim, L.H.M. Silva, M.C. Maffia, Equilibrium Data for PEG 4000 + Salt + Water Systems from (278.15 to 318.15) K, *J. Chem. Eng. Data*, 52 (2007) 351-356.

[66] S.C. Silvério, P.P. Madeira, O. Rodríguez, J.A. Teixeira, E.A. Macedo, ΔG(CH2) in PEG−Salt and Ucon−Salt Aqueous Two-Phase Systems, *J. Chem. Eng. Data*, 53 (2008) 1622-1625.

[67] Y.-L. Gao, Q.-H. Peng, Z.-C. Li, Y.-G. Li, Thermodynamics of ammonium sulfate—polyethylene glycol aqueous two-phase systems. Part1. Experiment and correlation using extended uniquac equation, *Fluid Phase Equilibr.*, 63 (1991) 157-171.

[68] J.C. Merchuk, B.A. Andrews, J.A. Asenjo, Aqueous two-phase systems for protein separation: Studies on phase inversion, *J. Chromatogr. B*, 711 (1998) 285-293.

[69] Y. Guan, T.H. Lilley, T.E. Treffry, A new excluded volume theory and its application to the coexistence curves of aqueous polymer two-phase systems, *Macromolecules*, 26 (1993) 3971-3979.

[70] M.T. Zafarani-Moattar, S. Hamzehzadeh, Liquid–liquid equilibria of aqueous two-phase systems containing polyethylene glycol and sodium succinate or sodium formate, *Calphad*, 29 (2005) 1-6.

[71] J.G. Huddleston, H.D. Willauer, R.D. Rogers, Phase Diagram Data for Several PEG + Salt Aqueous Biphasic Systems at 25 °C, *J. Chem. Eng. Data*, 48 (2003) 1230-1236.

[72] E. Alvarez-Guerra, S.P.M. Ventura, M. Alvarez-Guerra, J.A.P. Coutinho, A. Irabien, Modeling of the binodal curve of ionic liquid/salt aqueous systems, *Fluid Phase Equilibr.*, (2016).

[73] S. Hamzehzadeh, M.T. Zafarani-Moattar, Phase separation in aqueous solutions of polypropylene glycol and sodium citrate: Effects of temperature and pH, *Fluid Phase Equilibr.*, 385 (2015) 37-47.

[74] K. Wysoczanska, E.A. Macedo, Influence of the Molecular Weight of PEG on the Polymer/Salt Phase Diagrams of Aqueous Two-Phase Systems, *J. Chem. Eng. Data*, 61 (2016) 4229-4235.

[75] R. Ghahremani, F. Rahimpour, Equilibrium Phase Behavior of Aqueous Two-Phase Systems Containing Ethylene Oxide–Propylene Oxide of Different Molecular Weight (2500, 12000) and Sodium Citrate Salt at Various Temperatures and pH, *J. Chem. Eng. Data*, 59 (2014) 218-224.

[76] S.C. Silvério, A. Wegrzyn, E. Lladosa, O. Rodríguez, E.A. Macedo, Effect of Aqueous Two-Phase System Constituents in Different Poly(ethylene glycol)–Salt Phase Diagrams, *J. Chem. Eng. Data*, 57 (2012) 1203-1208.

[77] Y. Marcus, Thermodynamics of solvation of ions. Part 5.-Gibbs free energy of hydration at 298.15 K, *J. Chem. Soc. Faraday T.*, 87 (1991) 2995-2999.

[78] J.P. Martins, C.d.P. Carvalho, L.H.M.d. Silva, J.S.d.R. Coimbra, M.d.C.H.d. Silva, G.D. Rodrigues, L.A. Minim, Liquid–Liquid Equilibria of an Aqueous Two-Phase System Containing Poly(ethylene) Glycol 1500 and Sulfate Salts at Different Temperatures, *J. Chem. Eng. Data*, 53 (2008) 238-241.

[79] M.R. Almeida, H. Passos, M.M. Pereira, Á.S. Lima, J.A.P. Coutinho, M.G. Freire, Ionic liquids as additives to enhance the extraction of antioxidants in aqueous two-phase systems, *Sep. Purif. Technol.*, 128 (2014) 1-10.

[80] D. Baskaran, K. Chinnappan, R. Manivasagan, R. Selvaraj, Liquid–Liquid Equilibrium of Polymer–Inorganic Salt Aqueous Two-Phase Systems: Experimental Determination and Correlation, *J. Chem. Eng. Data*, 62 (2017) 738-743.

[81] G.F. Murari, J.A. Penido, P.A.L. Machado, L.R.d. Lemos, N.H.T. Lemes, L.S. Virtuoso, G.D. Rodrigues, A.B. Mageste, Phase diagrams of aqueous two-phase systems formed by polyethylene glycol+ammonium sulfate+water: equilibrium data and thermodynamic modeling, *Fluid Phase Equilibr.*, 406 (2015) 61-69.

[82] L. Breydo, A.E. Sales, T. Frege, M.C. Howell, B.Y. Zaslavsky, V.N. Uversky, Effects of Polymer Hydrophobicity on Protein Structure and Aggregation Kinetics in Crowded Milieu, *Biochemistry-US*, 54 (2015) 2957-2966.

USC
UNIVERSIDADE
DE SANTIAGO
DE COMPOSTELA

List of Symbols

USC
UNIVERSIDADE
DE SANTIAGO
DE COMPOSTELA

LIST OF SYMBOLS

a,b,c,…f	fitting parameters in Equations 3.1, 3.2 and 3.3
C	solute concentration
Calc	calculated value
EEV	effective excluded volume
Exptl	experimental value
K	partition coefficient
M	molecular weight
N	number of data points
S	selectivity
V	volume
V*	effective excluded volume
w	mass fraction
X	concentration for component 1 in Equations 2.1 and 2.2
y	dependent variable in Equation 3.5
Y	concentration for component 2 in Equations 2.1 and 2.2
Y_T	recovery yield
z	density in Equation 3.1
z	physical property in Equation 3.2

Subscripts

B	bottom phase
biosp	biospecific
conf	conformational contributions
elec	electrochemical
hyfob	hydrophobic
i	solute in stock solution in Equation 2.7
p	polymer
s	salt
S1	solute 1 in Equation 2.6
S2	solute 2 in Equation 2.6
t	solute in partitioned phase in Equation 2.7
T	top phase

Superscripts

bot	bottom phase
calc	calculated
exp	experimental
o	reference
top	top phase

Greek letters

β	fitting parameter in Equation 3.6
ρ	density
κ	fitting parameter in Equation 3.6

ACRONYMES

AARD	average arithmetic relative deviation
ATPS	aqueous two phase system
BSA	bovine serum albumin
EOPO	random ethylene glycol and propylene glycol copolymers
α-LA	α-lactalbumin
β-LG	β-lactoglobulin
LCST	lower critical solution temperature
MF	microfiltration
NF	nanofiltration
PEG	polyethyleneglycol
RO	reverse osmosis
STL	tie-line slope
TLL	tie-line length
UCON	poly(ethylene glycol-ran-propylene-glycol) monobutyl ether
UF	ultrafiltration
WPC	whey protein concentrate
WPI	whey protein isolate

Appendix A: Resumen (Summary, in Spanish)

USC
UNIVERSIDADE
DE SANTIAGO
DE COMPOSTELA

El sector lácteo tiene una gran importancia en Galicia no sólo desde un punto de vista económico sino también social, puesto que fomenta la continuidad y desarrollo del medio rural, al ser las explotaciones ganaderas la base del sustento de la mayor parte de las familias que habitan en estos lugares. Este sector engloba no sólo la producción de leche sino también su tratamiento industrial y el de sus derivados, siendo algunos ejemplos de éstos: los yogures, la mantequilla o el queso. Teniendo en cuenta la materia prima y los productos derivados, se puede generalizar que las corrientes residuales producidas en esta industria van a poseer una alta carga de contaminantes orgánicos, si bien la composición de los efluentes va a variar en función del producto obtenido. En ningún caso las corrientes de proceso pueden ser vertidas directamente al medio ambiente debido al alto impacto medioambiental que esto conlleva. Sin embargo estas corrientes también contienen una gran carga de nutrientes, muchos de los cuales pueden ser extraídos como productos de alto valor añadido. Un ejemplo son las proteínas que se encuentran en el suero producido durante la fabricación del queso. Este hecho hace posible pensar en estas corrientes no como un residuo, sino más bien como una fuente de obtención de productos de gran interés. El aprovechamiento de estas corrientes permitiría aumentar la competitividad de las empresas lácteas al valorizar una corriente residual.

Esta tesis tiene como objetivo la valorización del suero de queso mediante la recuperación de compuestos de alto valor añadido (lactosa y proteínas) empleando para ello una novedosa técnica de separación, los sistemas de dos fases acuosas. Dada su naturaleza, estos sistemas proporcionan un medio adecuado para la recuperación de proteínas y otras biomoléculas.

Los sistemas de dos fases acuosas (ATPS, de las siglas en inglés: *Aqueous Two Phase Systems*) se obtienen al mezclar dos disoluciones acuosas de ciertos compuestos bajo determinadas condiciones de temperatura y concentración. Una vez alcanzado el equilibrio, el sistema se separa en dos fases coexistentes, inmiscibles y con un alto contenido en agua. Una de las fases estará enriquecida en uno de los compuestos mientras que la otra fase tendrá una composición mayoritaria en el otro compuesto. Tradicionalmente estos sistemas se forman con dos polímeros o un

polímero y una sal. Sin embargo en los últimos años se han desarrollado sistemas basados en la combinación de un líquido iónico y una sal (dando lugar a sistemas sal-sal), la combinación de un alcohol con una sal o el empleo de surfactantes.

La representación habitual de estos sistemas consiste en una gráfica XY con la composición de cada uno de los compuestos que generan el ATPS en los ejes. La región homogénea (en la que ambos compuestos son totalmente miscibles y por tanto el sistema sólo muestra una única fase) se separa de la región heterogénea (que es aquella en la que dos fases están presentes) mediante una curva denominada binodal. Una mezcla de composición conocida situada en la región heterogénea se separará en dos fases, cada una enriquecida en uno de los compuestos, de forma que si se unen con una línea los puntos correspondientes a la alimentación, la composición de la fase superior y la composición de la fase inferior se obtienen las rectas de reparto. Cualquier mezcla cuya composición se encuentre en una recta de reparto, dará lugar a la misma composición de las fases en equilibrio.

Los ATPS fueron descubiertos por Beijerinck en 1896, sin embargo sus aplicaciones en biotecnología no se produjeron hasta 1950 cuando Albertsson propuso su uso para la separación de biomoléculas. Estas aplicaciones son posibles debido a que gracias al elevado contenido en agua presente en ambas fases en equilibrio, los solutos encuentran un medio apropiado que, por ejemplo, en el caso de las proteínas mantiene su estructura evitando la desnaturalización de las mismas.

Hasta el momento de la presentación de este trabajo, los estudios encontrados en la bibliografía sobre la recuperación de los principales componentes de valor añadido del suero de queso en la bibliografía es muy escasa. Existe un número muy limitado de trabajos que se centran en la separación de proteínas pero sin un estudio riguroso del equilibrio implicado. Por otra parte sólo se encontró un estudio reciente sobre la separación de la lactosa y proteínas. Esto corroboró la necesidad de investigar este tema.

La experimentación presentada en esta tesis se divide en dos partes principales, en la primera de ellas se realizó la caracterización de una serie de ATPS. En la

segunda parte se llevó a cabo un estudio del reparto de los solutos presentes en el suero del queso (proteínas y lactosa) en esos sistemas previamente caracterizados. A partir del estudio de la distribución de los solutos individuales, se definieron diferentes estrategias de separación que fueron probadas para llevar a cabo el objetivo de la tesis.

Caracterización de sistemas de dos fases acuosas

Los ATPS empleados combinan un polímero y una sal. Los polímeros seleccionados fueron polietilenglicoles (PEG) de diferentes pesos moleculares y éter monobutílico de poli(etilenglicol-ran-propilenglicol), conocido con el nombre comercial UCON, un copolímero aleatorio compuesto al 50 % glicol de polietileno y 50 % glicol de polipropileno. Se seleccionaron sales de dos tipos, inorgánicas (sulfatos) con tres cationes diferentes (sodio, amonio y potasio), y una orgánica (tartrato de potasio). Se eligieron estos componentes para la formación de ATPS debido a su relativamente bajo coste y carácter verde, además de su compatibilidad con los componentes del suero del queso.

Con el objetivo de comprobar qué rango de composiciones de la sal se podrían usar para la formación de los ATPS, se estudió la solubilidad a diferentes temperaturas del sulfato de sodio y del tartrato de potasio. Para ello se empleó una celda de vidrio termostatizada donde se añadió sal en exceso al agua. La disolución se mezcló con un agitador magnético durante cinco horas y se dejó reposar durante un día. El exceso de sal se depositó en el fondo de la celda y se tomó una muestra del sobrenadante para su análisis mediante la medida de la densidad. Esto implicó la determinación de curvas de calibrado previas. Los resultados mostraron que la solubilidad del sulfato de sodio disminuye drásticamente con la temperatura, lo que impide la formación de ATPS a bajas temperaturas ya que se produciría la precipitación de la sal. En el caso del tartrato de potasio, la solubilidad aumenta con la temperatura, siendo más pronunciado este efecto a las temperaturas más altas. Al contrario que en el caso anterior, con esta sal se encontró una alta solubilidad incluso

a las temperaturas más bajas, haciendo que esta sal sea prometedora para la formulación de ATPS.

Los sistemas objeto de estudio fueron los ATPS formados con PEG 4000, PEG 8000 o UCON y sulfato de sodio, UCON con sulfato de potasio, PEG 1500, PEG 4000, PEG 8000 o UCON con sulfato de amonio, y PEG 600 o PEG 1500 con tartrato potásico. Se determinaron los datos de equilibrio líquido-líquido de los sistemas implicados (polímero + sal + agua) a diferentes temperaturas (desde 278 hasta 308 K) y presión atmosférica. Para la determinación de las líneas de reparto se empleó una celda de equilibrio líquido-líquido fabricada con vidrio. Esta celda se conectó a un baño termostático para mantener controlada la temperatura del sistema en todo momento. Se introdujeron en la celda cantidades conocidas de polímero, sal y agua para obtener mezclas en la región heterogénea del diagrama. Se utilizó agitación magnética durante treinta minutos para obtener una buena mezcla de los componentes y a continuación se dejó reposar la mezcla durante veinticuatro horas para obtener dos fases totalmente claras y separadas. Estudios previos llevaron a la definición de los tiempos de operación necesarios en cada etapa. Una vez que las dos fases estaban completamente separadas, se extrajeron muestras de cada una de ellas para ser analizadas mediante la determinación de sus propiedades físicas. En el caso de sistemas binarios se utilizó la densidad y en el caso de ternarios densidad e índice de refracción. Para la realización de los calibrados se determinaron las propiedades físicas para estos sistemas en un rango de mezclas miscibles, obteniendo así datos de interés (especialmente la densidad) para el diseño, simulación u operación de procesos con estos componentes.

Los diagramas de fases obtenidos permitieron evaluar el efecto de diferentes variables (temperatura, peso molecular del polímero y catión de la sal) en la región heterogénea. Al evaluar el efecto de la temperatura en las rectas de reparto se observó, para todos los sistemas, que la región heterogénea aumenta con la temperatura. Al aumentar la temperatura aumenta la composición de polímero en la fase superior, mientras que se produce una disminución de la composición de sal en la fase inferior. Este aumento de la región inmiscible implica una disminución de la

cantidad necesaria de los compuestos utilizados para generar el ATPS. Aunque en todos los sistemas estudiados la fase superior era rica en polímero y la inferior en sal, en el caso de los sistemas con UCON a la temperatura más alta (308 K) se produjo una inversión de fases que debe ser considerada en la operación con estos sistemas. En el caso de los sulfatos, a una temperatura determinada, el sodio (con mayor capa de hidratación) da lugar a una mayor región de inmiscibilidad que el potasio o el amonio. En el caso del PEG, un aumento del peso molecular del polímero también incrementa la región heterogénea.

Los datos de equilibrio obtenidos se correlacionaron para facilitar así su manejo y la comparación entre sistemas. Los datos de las curvas binodales fueron correlacionados mediante la ecuación empírica de Merchuk y la ecuación de Guan que posee una fuerte base teórica. Esta última permite obtener el valor del volumen excluido efectivo (EEV, de las siglas en inglés) para la evaluación del efecto de diferentes parámetros sobre la región heterogénea de los sistemas. Las rectas de reparto también fueron correlacionadas mediante una ecuación derivada de esta teoría de Guan. Como era de esperar, la ecuación de Merchuk proporcionó una excelente correlación de los datos de las curvas binodales. Esta ecuación proporcionó mejores resultados que la de Guan, sin embargo el EEV obtenido con este modelo permitió confirmar la influencia de la temperatura, la sal y el peso molecular del polímero en la región heterogénea de los diagramas de fase. El modelo de Guan también correlacionó de forma satisfactoria los datos de las líneas de reparto, excepto en la región más cercana al punto crítico (misma composición para ambas fases en equilibrio).

Separación de los compuestos del suero del queso usando ATPS

Se estudió el reparto de los principales componentes del suero de queso (α-lactosa, albúmina de suero bovino, α-lactalbúmina y β-lactoglobulina) en los ATPS previamente caracterizados. Los sistemas fueron preparados por pesada añadiendo las cantidades apropiadas de polímero, sal, soluto y agua en un tubo Eppendorf y agitados en un agitador *vortex* durante un minuto. Posteriormente las muestras se

dejaron reposar una hora a temperatura controlada mediante un baño termostático. Finalmente se procedió a la centrifugación y separación de las fases que fueron analizadas mediante HPLC. El control de pH, en los casos requeridos, se realizó utilizando un tampón de fosfato de sodio para los valores básicos y un buffer de fosfato de sodio-citrato para los valores ácidos.

Para evaluar la eficiencia de separación de los solutos de interés en cada ATPS se emplearon dos parámetros diferentes: el coeficiente de distribución y el rendimiento de recuperación. El coeficiente de reparto es el cociente entre las concentraciones de soluto de interés en la fase superior e inferior del ATPS. El rendimiento de recuperación es el cociente entre la cantidad de soluto que está presente en la fase donde se recupera con respecto a la cantidad inicial en la alimentación.

Se inició el estudio analizando la influencia de la concentración de soluto en los coeficientes de reparto obtenidos con los diferentes ATPS estudiados. Para ello se eligió lactosa como soluto. Se encontró que dicha concentración (siempre en los valores bajos estudiados) no afecta al coeficiente de reparto obtenido. Además se observó que, debido a su carácter hidrofílico, en todos los casos la lactosa mostró una mayor afinidad por la fase inferior rica en sal. Un aumento en la concentración de los compuestos que forman el sistema, produjo una disminución en el coeficiente de reparto de este azúcar.

Posteriormente se estudió la influencia de la concentración de los compuestos que forman el ATPS (o lo que es lo mismo, la recta de reparto elegida) en el reparto de los cuatro solutos de interés (lactosa, albúmina de suero bovino, α-lactalbúmina y β-lactoglobulina). Para ello se seleccionaron los sistemas formados por tartrato de potasio con PEG 600 y 1500. En este caso se encontró que los mayores valores de la longitud de la recta de reparto seleccionada en el sistema, permiten simultáneamente un mayor coeficiente de reparto para las proteínas y una disminución del coeficiente para la lactosa. Esto implica que las proteínas tienen una mayor afinidad por la fase superior rica en polímero (estando poco presentes en la fase inferior), mientras que

para la lactosa ocurre todo lo contario. Altas concentraciones de los componentes utilizados para formar el ATPS favorecen por tanto la separación.

Seleccionando rectas de reparto de la parte superior de los diagrama de fases (alta concentración de polímero y sal), se realizó un barrido con todos los ATPS estudiados para analizar el reparto de los solutos de interés entre las dos fases en equilibrio. En la mayoría de los sistemas apareció un precipitado en la interfase, por lo que la eficacia de la separación tuvo que analizarse fundamentalmente a través del rendimiento de recuperación, resultando inadecuado el uso de coeficientes de distribución o selectividades. En los sistemas con PEG y sulfato de sodio o sulfato de amonio se comprobó que cuando el peso molecular del polímero aumenta se produce un aumento de la hidrofobicidad en la fase polimérica, causando el desplazamiento de las proteínas hacia la fase salina. Por lo tanto, PEG de pesos moleculares intermedios condujeron a las mejores separaciones. Los ATPS formulados con UCON y sulfato no permitieron separación alguna ya que todos los solutos se concentraron en la fase inferior, produciéndose una gran precipitación en la interfase. A partir de este estudio se concluyó que los ATPS más prometedores para llevar a cabo la separación de lactosa y proteínas son los formados por PEG 600 y tartrato de potasio a 293 K o PEG 1500 a y sulfato de amonio a 298 K. Para el fraccionamiento de proteínas el sistema más adecuado es el formado por PEG 300 y sulfato de sodio a 298 K.

Dado el gran efecto del pH sobre la distribución de biomoléculas en un ATPS, se evaluó el efecto de esta variable sobre el reparto de los solutos en los sistemas considerados de interés. Este parámetro afecta a la distribución de las proteínas, especialmente cuando se cruza el punto isoeléctrico de las mismas. Se comprobó que el pH no afectó a la distribución de la lactosa pero, como era de esperar, sí tuvo una gran influencia sobre las proteínas que se concentraron en la fase superior al aumentar el pH. El único sistema que no se vio afectado por el pH fue el constituido por PEG 600 y tartrato potásico, debido a un problema de interacción entre las sales utilizadas para fijar el pH y las del sistema, que daba lugar a precipitación. Para el sistema con PEG 1500 y sulfato de amonio, se encontró que el pH 4 es el más

adecuado para la separación ya que produce la precipitación de las proteínas en la interfase mientras que la lactosa se recupera entorno al 70 % en la fase inferior. En el caso del PEG 600 y tartrato de potasio a pH natural, más de un 85 % de la lactosa se recupera en la fase inferior, mientras que la mayor parte de las proteínas se recuperan en la fase superior o como precipitado en la interfase. Para el sistema con PEG 300 y sulfato de sodio, se encontró que con una variación de pH entre 4 y 5 se podría llevar a cabo un fraccionamiento de las proteínas.

De acuerdo a estos estudios, se diseñaron diferentes estrategias para la separación de los principales componentes del suero de la leche, combinado el uso de ATPS y ultrafiltración. Para mostrar la eficacia de las mismas se utilizó un suero simulado y uno proporcionado por un proveedor local (Queizúar S.L.). El suero simulado se preparó mezclando los solutos puros (lactosa, albúmina de suero bovino, α-lactalbúmina y β-lactoglobulina) en agua con una composición similar al suero real.

Para la separación de las proteínas y la lactosa se estudiaron tres estrategias diferentes: a) ATPS con PEG 1500 y sulfato de amonio a pH 4 y 298 K, b) ATPS con PEG 600 + tartrato de potasio a pH natural y 293 K y c) ultrafiltración. El uso de ATPS pretendía recuperar la lactosa en la fase inferior y las proteínas como precipitado en la interfase. Ambos sistemas estudiados presentaron buenos resultados pero en el caso del PEG 600 con tartrato potásico, la separación fue perfecta. Los resultados obtenidos con el suero real, en todos los casos, confirmaron lo encontrado con el suero simulado. En el caso de la ultrafiltración, la separación no fue eficaz con gran pérdida de proteínas y lactosa en el interior del filtro.

Para el fraccionamiento de proteínas también se estudiaron tres estrategias diferentes. a) ATPS con PEG 300 y sulfato de sodio a 298 K a pH 4 seguido del mismo ATPS a pH 5, b) ATPS con PEG 300 y sulfato de sodio a 298 K y pH 4 seguido de una etapa de ultrafiltración, y c) ultrafiltración seguida de ATPS con PEG 300 y sulfato de sodio a 298 K a pH 4. Ninguna de las estrategias dio resultado cuando se utilizó el suero proveniente de la separación lactosa/proteínas,

probablemente debido a la presencia de compuestos provenientes de la anterior estrategia. Trabajando con un suero simulado sin lactosa, las dos primeras estrategias (primera parte común) consiguieron extraer toda la albúmina de suero bovino que se recuperó como precipitado. La segunda etapa, con cualquiera de las dos estrategias, no permitió una buena separación de las dos proteínas restantes. Aún más, en la operación con el suero real no se consiguió una separación eficaz de la albúmina de suero bovino que ya en la primera etapa apareció mezclada con las otras proteínas en el precipitado. La tercera estrategia propuesta fue ineficaz desde el principio debido al alto contenido de proteínas que quedó retenido en el filtro.

La investigación en este tema de tanto interés para la industria láctea debe continuar. El estudio de la separación de la lactosa y el concentrado de proteínas de los componentes utilizados para la formación de los ATPS es fundamental. Por otra parte, para el fraccionamiento de las diferentes proteínas, es necesario acudir a nuevos ATPS formados con diferentes compuestos o incluso cambiar la tecnología.

USC
UNIVERSIDADE
DE SANTIAGO
DE COMPOSTELA

Appendix B: List of publications

USC
UNIVERSIDADE
DE SANTIAGO
DE COMPOSTELA

M. González-Amado, E. Rodil, A. Arce, A. Soto, O. Rodríguez, The effect of temperature on polyethylene glycol (4000 or 8000)-(sodium or ammonium sulfate) Aqueous Two Phase Systems, *Fluid Phase Equlibr.*, 428 (2016) 95-101.

X. Rico-Castro, M. González-Amado, A. Soto, O. Rodríguez, Aqueous two-phase systems with thermo-sensitive EOPO co-polymer (UCON) and sulfate salts: Effect of temperature and cation, *J. Chem. Thermodyn*., 108 (2017) 136-142.

M. González-Amado, E. Rodil, A. Arce, A. Soto, O. Rodríguez, Polyethylene glycol (1500 or 600)-potassium tartrate aqueous two phase systems, *Fluid Phase Equlibr*., 470 (2018) 120-125.

M. González-Amado, A. P. M. Tavares, M. G. Freire, J. A. P. Coutinho, A. Soto, O. Rodríguez, Cheese Whey valorization with PEG/sulfate Aqueous Two Phase Systems: Recovery of lactose and proteins, *Bioresource Technol*. Sent for publication.

USC
UNIVERSIDADE
DE SANTIAGO
DE COMPOSTELA